Title
Serotonergic modulation of visual neurons in Drosophila melanogaster

Author
Sampson, Maureen M

Publication Date
2020

Peer reviewed|Thesis/dissertation

UNIVERSITY OF CALIFORNIA

Los Angeles

Serotonergic modulation of visual neurons in *Drosophila melanogaster*

A dissertation submitted in partial satisfaction of the

requirements for the degree Doctor of Philosophy

in Molecular Toxicology

by

Maureen McGuirk Sampson

2020

ABSTRACT OF THE DISSERTATION

Serotonergic modulation of visual neurons in *Drosophila melanogaster*

by

Maureen McGuirk Sampson

Doctor of Philosophy in Molecular Toxicology

University of California, Los Angeles, 2020

Professor David Krantz, Chair

Sensory systems rely on neuromodulators, such as serotonin, to provide flexibility for information processing in the face of a highly variable stimulus space. Serotonergic neurons broadly innervate the optic ganglia of *Drosophila melanogaster*, a widely used model for studying vision. The role for serotonergic signaling in the *Drosophila* optic lobe and the mechanisms by which serotonin regulates visual neurons remain unclear. Here we map the expression patterns of serotonin receptors in the visual system, focusing on a subset of cells with processes in the first optic ganglion, the lamina, and show that serotonin can modulate visual responses. Serotonin receptors are expressed in several types of columnar cells in the lamina including 5-HT2B in lamina monopolar cell L2, required for the initial steps of visual processing, and both 5-HT1A and 5-HT1B in T1 cells, whose function is unknown. Subcellular mapping with GFP-tagged 5-HT2B and 5-HT1A constructs indicates that these receptors localize to layer M2 of the medulla, proximal to serotonergic boutons, suggesting that the medulla is the primary site of serotonergic regulation for these neurons. Serotonin increases intracellular calcium in L2 terminals in layer M2 and alters the kinetics of visually induced calcium transients in L2 neurons following dark flashes. These effects were not observed in flies without functional 5-HT2B, which displayed severe differences

in the amplitude and kinetics of their calcium response to both dark and light flashes. While we did not detect serotonin receptor expression in L1 neurons, they also undergo serotonin-induced calcium changes, presumably via cell non-autonomous signaling pathways. We provide the first functional data showing a role for serotonergic neuromodulation of neurons required for initiating visual processing in *Drosophila*. These findings demonstrate that tracing the molecular mechanisms of serotonergic modulation require a combination of receptor mapping to individual cells and subcellular compartments with complementary functional assays. We have identified a testable model system for these studies and developed new tools for studying the serotonin transporter.

The dissertation of Maureen McGuirk Sampson is approved.

Anne Andrews

Jeff Bronstein

Stephen Zipursky

David Krantz, Committee Chair

University of California, Los Angeles

2020

Table of Contents

List of Figures

List of Tables

Acknowledgments

Science is never driven by a single person. It is a community-based enterprise that requires sharing expertise and knowledge within a team to create something new. I have been blessed with the most extraordinary team of scientists and friends who made this journey possible.

Dr. David Krantz might be the best human I have ever met. As a scientist, David is creative and open to new ideas—he thinks without limits. Most people envision the scientific enterprise as a "eureka" moment, but David has taught me to find joy in the process of discovery rather than to chase a hypothesis. As a person, David is kind and assumes the best in people, always. He encourages people to be fully human—he believes we should feel as free to cry as we do to laugh. He has supported and guided me through both personal and scientific crises, for which I am forever grateful. David is a loving father and caring psychiatrist, both of which seem to spill over into his role as a mentor.

There was a time when I thought about leaving graduate school, but David offered me a home and a place to grow. It felt serendipitous that David was starting a project involving serotonin at the same time that I was searching for a lab. Joining David's lab just felt right and this was enormously comforting to me during this time of uncertainly. He, working in close collaboration with Kathy, gave me exactly what I needed to find my strength and a renewed interest in science. I am so thankful for everything I learned from David about being a good scientist and a good person. Mine is just one of the many lives that David has touched. The world is innumerably better because he is here with us. Thank you, David.

Dr. Anne Andrews was my first mentor at UCLA and one of the most impactful. I rotated in Anne's lab because I was interested in studying the biology underlying depression and anxiety. Anne introduced me to serotonin biology and neuroscience. She taught me the history of the field and introduced me to her vast network of colleagues from Monitoring Molecules in Neuroscience and Serotonin Club. I am so thankful for the foundational knowledge I received from my time in the Andrews lab and for Anne's continued guidance as I pursued my research in the Krantz lab. Thank you, Anne, for your generosity and honesty though it all.

Thank you to **Dr. Jeff Bronstein**, who has been part of my journey at UCLA from the beginning. I really appreciate your thoughtful feedback, support and mentorship. It has been an honor to work with **Dr. Larry Zipursky**, who also trained David Krantz! I am so grateful for your insights and constructive feedback. I am so lucky to work with the vision extraordinaire, **Dr. Mark Frye**, who has shared tremendous expertise in visual behavior, and also granted me access to his fancy 2-photon system! Mark, I am so thankful to have you as a co-sponsor on my F99 and for our collaboration on the serotonin vision project.

Dr. Kathy Myers Gschweng taught me everything I know about flies, IHC, and confocal microscopy. She was generous with her expertise and time, and was kind when I made mistakes. She was the first postdoc I interacted with at UCLA and one of the best examples of how to be an effective mentor. When I am a postdoc, I will try to be like you, Kathy!

I am so grateful to **Dr. Ben Hardcastle** who taught me how to perform the 2-photon live imaging experiments in Chapter 2! He also introduced me to Matlab and analyzed the live imaging data sets. Ben, I am so grateful for your support and contribution to the serotonin vision project. Cheers to the fun happy hours!

I am grateful for the entire Krantz lab, who together cultivated a supportive, rigorous environment for our studies. **Dr. Shivan Bonanno** is an amazing postdoc mentor and molecular bio extraordinaire. He held my hand through cloning and western blots and also designed the CRISPR constructs from Chapter 4. He is an advocate for mental health and work life balance. Shivan, I learned so much from you and also had a lot of fun. I will miss our massive dissection/FACS days because I really enjoyed our time together. **Rebecca Arnold** and **Nikoo Dalili,** you were the highlight of my time in the Krantz Lab. You are both amazing scientists and leaders. I can't wait to see where your journey takes you! **Aditya Eamani** cloned most of the HA-SerT construct in Chapter 4. Thank you, Aditya, for keeping the lab running smoothly and being the best lab bench neighbor. I am so grateful for the time I had getting to know you. It was also a joy to know your sweet daughter, Tanmaya. It's been fantastic to work with **Ethan Rohrbach**, who has infectious enthusiasm and energy for science. Thanks for making lab fun and inspiring me with your tireless work ethic! Thank you to **Dr. Sonali Deshpande** for your leadership in lab and being a shining example of a strong woman in STEM. Thank you to Sonali, Ethan, Shivan, Aditya, Kathy, **Jenna Harrigan** and **Dr. James Asuncion** for your valuable insights and suggestions in lab meetings.

Thank you to my fellow Molecular Toxicology grads, **Dr. Dawoud Sulaiman, Dr. Julie Castañeda**, **Dr. Jess Camacho,** and **(Dr. to be) Ellen O'Connor** for guiding me when I was lost and making sure I took the time to explore Los Angeles. Julie and Jess took me out for a drink (Hello Kitty) the very first day we met and the rest is history. Special thank you to Dawoud who was my ride or die from Day 1. We were the only two students in the 2014 class and I honestly could not imagine this journey without him. Thank you, Dawoud, for all the long study sessions, pep talks in the botanical garden, happy hours and CHS lunches.

I am so grateful for my friendship with fellow *Drosophila* neuroscientist **(Dr. to be) Karen Cheng**. Thanks for being my sounding board and entertaining my random science questions. I am so grateful for all of our adventures outside of lab, especially chasing waterfalls and superblooms! Thank you to **Dr. Nako Nakatsuka** for showing me how to balance life and science. I've been so lucky to witness your amazing journey. You are a role model for me, Nako. Research is a rollercoaster, with ups and downs. Everyone struggles in graduate school, but in particular **Dr. Emma Karey** and I could write a solid movie script based on our experiences. Thank you for all the pep talks, Emma!

I met **Dr. Tim Sampson** in 2006 at the end of my first year of college. I was 19 years old. Our lives were just beginning, and we were finding our path and porpoise in life together. One thing that immediately connected us was our shared love for science. I was majoring in biochemistry and Tim was majoring in microbiology. Tim, being in his second year of college, had already started research in Graham Hatfull's lab. One of my first memories of Tim was him proudly showing me his TEM image of a phage he discovered, BPS. I think we were bound for life after I baked him a phage sugar cookie... When I met Tim, it was unclear whether research was my path. After seeing Tim so happy and engaged with his research, I became involved with research at Chatham. I would absolutely not be here, on the cusp of getting my PhD, without Tim Sampson. Thank you, Tim, for always encouraging me to aim higher.

Thank you for the support from my entire family: **Mom**, **Dad**, **Pat, Tricia, Max, Patrick, Maggie, Sean,** and **Elysha.**

There is no one on this planet that I love more than **Max McGuirk**, to whom I dedicate this work.

Biographical Sketch

Chatham University, Pittsburgh, PA	BS	2005 – 2009	Biochemistry
UCLA, Los Angeles, CA	PhD Candidate in Molecular Toxicology		

Through my undergraduate and professional research experiences, I developed a strong interest in toxicology rooted in analytical and environmental chemistries. As an undergraduate, I worked in the laboratory of Dr. Larry Viehland, where I employed computational methods to examine interactions between Ba^{n+} and noble gases. Understanding these interactions has relevance for ion traps and ion mobility spectrometry. In addition to this theoretical research, I worked with Dr. Renee Falconer quantifying 14 organochlorine pesticides (e.g., DDT) in commercial potting soils using GC/MS. We found that potting soils contained similar pesticide concentrations as agricultural soils, with correlations to specific soil components (e.g., sphagnum peat moss).

Following graduation, I joined the Volatile Organic Compounds (VOC) Laboratory at the Centers for Disease Control where I quantified VOCs in biological and environmental matrices to support national and regional exposure investigations. I was responsible for quantifying 54 compounds in whole human blood for longitudinal biomonitoring of the United States population. In addition, I adapted these methods to quantify VOCs in rat tissues for studies modeling solvent exposures and developed an automated quantification assay for 22 VOCs in cigarette smoke. I greatly enjoyed this analytical work, but I felt increasingly compelled to address the toxicological consequence of the chemical exposures that I reported. For this reason, I joined the Molecular Toxicology PhD program at UCLA.

I was drawn to cellular and molecular neuroscience as I progressed through my graduate program. I first rotated in the laboratory of Dr. Anne Andrews where I used LC/ECD to measure neurotransmitters in brain tissue homogenate and perform *in vivo* brain microdialysis in behaving mice. I later joined the laboratory of Dr. David Krantz where I have applied genetic approaches to understand basic principles of neuromodulation using *Drosophila melanogaster*. For my dissertation work, I mapped serotonin receptor expression in the fly optic lobe, identifying neuromodulation points in specific neurons and visual processing pathways. These neurons respond to serotonin with an increase in baseline calcium and serotonin enhances the calcium transients that occur in response to visual stimuli. We have examined the connectivity of these cells and performed RNA-Seq to better understand this circuit. After obtaining my PhD in the summer of 2020, I will begin a postdoctoral training position in the Sloan Lab at Emory University in Atlanta, GA. The Sloan Lab is interested in the role of glia in neural circuit development and how abnormal glial development might contribute to neurodevelopmental disorders. I will approach this question from a toxicological perspective, asking how exposure to developmental lead disrupts neuron-glia interactions, neuroprotection by glia, and neural stem cell differentiation.

SELECTED AWARDS

- NIH NINDS F99 NS113454 (2019 – 2020)
  "Serotonin Signaling in Visual Processing Circuitry over Multiple Timescales"
- NIH NIEHS K00 NS113454 (2020 – 2024)
  "Neuron-Astrocyte Interactions in Developmental Lead Exposure"
- International Society for Serotonin Research "Young Investigator" (2020)
- National Science Foundation Graduate Research Fellowship (2015 – 2019)
- SFN Scholars' Program Associate (2018 – 2019)
- SFN Professional Development Award (2019)

PUBLICATIONS (ORCID: 3-1536-3229)

[8] *__Sampson, M.__; *Gschweng, K.; Hardcastle, B.; Frye, M.; Krantz, D. "Serotonergic modulation of a visual microcircuit in *Drosophila melanogaster.*" *Plos Genetics*. Accepted Aug **2020** *Equal contribution

[7] __Sampson, M.__; Yang, H.; Andrews, A. "Advanced microdialysis approaches reveal differences in serotonin homeostasis and signaling." *Compendium of In-Vivo Monitoring in Real-Time Molecular Neuroscience - Volume 2 : Microdialysis And Sensing Of Neural Tissues*. World Scientific Publishing. June 28, **2016**.

[6] Pazo, D.; Chambers, D.; __Sampson, M.__; Moliere, F.; Blount, B.; Watson, C. "Mainstream Smoke Levels of Volatile Organic Compounds in 50 US Domestic Cigarette Brands Smoked with the ISO and Intense Regimens." *Nicotine and Tobacco Research*. April 25, **2016**.

[5] Yang, H.; __Sampson, M.__; Senturk, D.; Andrews, A. "Sex- and SERT-Mediated Differences in Stimulated Serotonin Revealed by Fast Microdialysis." *ACS Chemical Neuroscience*. 6. July 13, **2015**.

[4] __Sampson, M.;__ Chambers, D.; Pazo, D.; Moliere, F.; Blount, B.; Watson, C. "Simultaneous Analysis of 22 VOCs in Mainstream Cigarette Smoke by Gas Phase SPME GC/MS." *Analytical Chemistry*. 86:14. July 16, **2014**.

[3] MacNeil, J.; Gess, S.; Gray, M.; __McGuirk, M.__ "Mushroom Magic: A Student-Developed Laboratory for the Analysis of Metals in a Familiar Food." *Journal of Chemical Education.* 89:1. Nov 9, **2011**.

[2] Chambers, D.; Ocariz, J.; __McGuirk, M.__; Blount, B. "Impact of cigarette smoking on Volatile Organic Compound (VOC) blood levels in the U.S. Population: NHANES 2003-2004." *Environment International*. 37:B. May 25, **2011**.

[1] __McGuirk, M.__; Viehland, L.; Lee, E.; Breckenridge,W.; Withers, C.; Gardner, A.; Plowright, R.; Wright, T. "Theoretical Study of Ba^{n+}-RG complexes and Transport of Ba^{n+} through RG (n=1,2; RG=He-Rn)." *Journal of Chemical Physics*. 130:19. May 19, **2009**.

SELECTED PRESENTATIONS

__Sampson, M.__; Gschweng, K.;Hardcastle, B.; Bonanno, S.; Frye, M.; Krantz, D. "Serotonergic neuromodulation in the *Drosophila* visual system." International Society for Serotonin Research. Cancun, Mx. Rescheduled due to COVID-19. (Oral Presentation, "Featured Young Investigator")

__Sampson, M.__; Gschweng, K.; Hardcastle, B.; Bonanno, S.; Frye, M.; Krantz, D. "Serotonergic neuromodulation in the *Drosophila* visual system." Society for Neuroscience. Chicago, CA, USA. October, 2019. (Poster)

__Sampson, M.__; Gschweng, K.; Hardcastle, B.;Frye, M.; Krantz, D. "A Novel Serotonergic Microcircuit in the *Drosophila* Visual System." Society for Neuroscience. San Diego, CA, USA. November, 2018. (Poster)

__Sampson, M.__; Gschweng, K.; Hardcastle, B.;Frye, M.; Krantz, D. "Serotonin Modulates a Novel Microcircuit in the *Drosophila* Visual System." International Society for Serotonin Research. Cork, Ireland. July, 2018. (Poster)

Gschweng, K., __Sampson, M.__; Sadaf, S.; Sizemore, T.; Dacks, A.; Frye, M.; Krantz, D. "Mapping serotonergic circuits in the optic lobe of Drosophila melanogaster." Neurobiology of *Drosophila*. Cold Spring Harbor, NY, USA. October, 2017. (Poster)

__Sampson, M.__; Chambers, D.; Moliere, F.; Blount, B. "Appropriate Implementation and New Applications for the Quantification of 56 VOCs in Blood and Other Matrices by SPME/ GC/MS." The Pittsburgh Conference. Philadelphia, PA, USA. March, 2013. (Oral Presentation)

Introduction: Basic Principles of Serotonin Biology and Neuromodulation

Serotonin Neuromodulation

Serotonin is a phylogenetically ancient signaling molecule that is used for cell-to-cell communication in animals. In the brain, chemical neurotransmitters such as serotonin encode information passed between neurons. Neurotransmitters activate receptors on postsynaptic neurons before being removed from the extracellular space by presynaptic reuptake transporters, metabolism, or diffusion. Serotonin receptors induce second messenger cascades that alter the biophysical properties of individual neurons within a circuit, ultimately adjusting circuit computations and output to best meet the animal's changing needs [1-5]. The molecular mechanisms underlying serotonin signaling are critical for understanding the role of serotonin in health and disease.

Serotonin binds to a large class of diverse receptors. There are 14 genetically distinct serotonin receptors in mammals, 13 of which are G-Protein Coupled Receptors (GPCRS) [6-10]. GPCRs induce different intracellular signaling cascades by coupling to specific G-protein α subunit families: $G_{\alpha s}$, $G_{\alpha q}$, and $G_{\alpha i}$ [11, 12]. The second messenger cascades associated with each G_{α} subtype are distinct, but target overlapping second messengers and ions. These include cAMP and Ca^{2+}, which both broadly modulate cell "state" by influencing voltage-dependent channels, kinases, phospholipases, and transcription factors [11, 12]. In general, the effects of GPCR signaling are thought to be slower and more enduring than those of ligand-gated ion channels, but do not typically induce neuron depolarization events. For this reason, neurotransmitters that activate GPCRs are often called neuromodulators.

Serotonin receptors can traffic to different compartments of a neuron, such as the cell body, dendrites or axons. Acute increases in local Ca^{2+} will lead to different outcomes in different subcellular compartments. For example, local increases in axonal Ca^{2+} could increase SNARE activity and modulate vesicle fusion, possibly leading to more neurotransmitter release

onto post-synaptic circuitry. In contrast, increases in dendritic Ca^{2+} will modulate the neurons response to pre-synaptic inputs.

The flexibility and diversity of the serotonin system is such that there is not a common cellular response to serotonin. Serotonin signaling is enriched by the heterogeneous expression of many different serotonin receptor subtypes with differing affinities, kinetics, and signaling cascades. In some cases, serotonin receptors can heterodimerize with other GPCRs, leading to bias in signaling cascades, and adding another layer of flexibility [13, 14]. However, there exists a relatively limited number of second messenger cascades associated with GPCRs and the flexibility of the brain is only achieved by combinatorial signaling from many different modulators. Thus, the intracellular physiology—or "state"—of a given neuron is a dynamic compilation of input from many GPCRs and cross-talk between signaling cascades. Upon serotonin receptor activation, intracellular cascade components interact with the existing proteome and physiological conditions of the cell, leading to diverse outcomes. Thus, serotonin receptor effectors interact with current cell "state" and serotonin input to the same cell could lead to different effects when intracellular and extracellular conditions change.

The term neuromodulation is typically used to describe signaling that activates GPCRs and occurs outside of a typical synapse. Neuromodulator GPCR activation is not thought to induce large changes in membrane potentials that lead to depolarization. Rather, neuromodulators change the cell "state" and influence how neurons respond to and propagate to synaptic input. Neuromodulators typically target many cells across a circuit, leading to emergent modulation features that are challenging to predict.

Serotonin modulation targets cells within larger networks and the effect of serotonin signaling on an individual cell is not controlled exclusively by the expression of serotonin receptors. In many cases, serotonin can modulate cell activity by non-cell autonomous means. For example, a neuron lacking serotonin receptors may be synaptically or electrically coupled to

other cells expressing serotonin receptors. Through these mechanisms, the effects of serotonin modulation potentially travel across multiple synapses and can affect entire circuits. Neuromodulators shape the relationship between components (e.g., synaptic strength) and can therefore “reconfigure” circuits [2] so that quantifying synaptic connections, such as has been done in EM-based connectome projects [15-20], does not comprehensively describe the range of possible circuit activities.

Serotonergic Neurons

Extracellular serotonin concentrations are controlled by neurons that release and re-uptake serotonin from the extracellular space. These neurons synthesize serotonin from the amino acid tryptophan, which is hydrolyzed by the rate-limiting enzyme tryptophan hydroxylase (TRH or TPH) and then decarboxylated by L-amino-acid decarboxylase (AADC). Serotonin is transported from the cytoplasm into vesicles by the vesicular monoamine transporter (VMAT). When these vesicles fuse with the cell membrane serotonin is released into the extracellular space. Serotonin molecules can then diffuse away from the serotonergic neuron to signal to other cells or be transported back into the neuron by the serotonin transporter (SERT). When serotonin signaling occurs outside of a typical synapse and relies on diffusion of serotonin away from the presynaptic release site it is called volume transmission. Serotonin signaling can also occur at “hard-wired,” synaptic connections between neurons, but this is less common in the mammalian brain [21-23].

Serotonergic neurons use autoreceptors to sense extracellular serotonin concentrations and inform their regulation of serotonin synthesis, release and re-uptake. The serotonin transporter (SERT) is a membrane-bound transporter protein that relies on the Na^+/Cl^- concentration gradients to drive serotonin re-uptake. Importantly, SERT activity mediates the magnitude and duration of serotonin signal in the extracellular space. In general, short-term

increases in SERT activity decrease serotonin signaling at post-synaptic receptors, whereas decreases in SERT activity increase the maximal concentration and endurance of serotonin in the extracellular space. Because serotonin signaling can occur outside of a typical synapse and often depends on diffusion to post-synaptic neurons, SERT-controlled concentration gradients are important variables in serotonin signaling.

SERT in human health

Serotonin has demonstrated tractability as a target for the treatment of mood disorders. The most commonly prescribed drugs for depression are serotonin-selective reuptake inhibitors (SSRIs) [24], which inhibit the serotonin transporter (SERT). A significant unanswered question in this field is why major depressive disorder requires weeks to months of SSRI treatment [25], despite almost immediate action at the protein target. Further complicating this line of questioning, premenstrual dysphoric disorder patients are largely responsive to the same SSRIs within days [26-28] and some studies have reported temporary increases in anxiety immediately after beginning SSRI treatment [29, 30]. In rodent models of depression, some behavior paradigms are immediately responsive to SSRIs (e.g., forced-swim), while others require chronic SSRI treatment (e.g., chronic defeat [31]). Together, these data demonstrate that changes in serotonin signaling over longer or shorter timeframes differentially modulates behavior circuits.

Contributions of this work to field of serotonin biology

Serotonin is a neuromodulator [1-5] in many sensory systems [32-43]. In *Drosophila melanogaster*, serotonin neurons densely innervate all neuropils of the visual system [44-48], yet the role of serotonin signaling is unknown. The *Drosophila* visual system provides a powerful genetic model to study the mechanisms underlying visual circuit activity as well as their

regulation [49, 50]. Significant progress has been made in mapping hard-wired, synaptic circuitry within the *Drosophila* visual system, enabling the generation of a 'connectome' atlas of visual-processing neurons and their associated circuits [15-20]. In contrast, little work has examined the integration of neuromodulatory signaling in these circuits.

The *Drosophila* eye has rich cell diversity [51, 52] and the discrete flow of visual information from photoreceptors to downstream circuits has enabled the characterization of many cells' stereotyped responses to visual stimuli for functional studies [53-56]. I therefore leveraged these well-described neurons to investigate how serotonin receptor activation modulates individual neurons within the context of the larger computational circuitry of the fly visual system.

Five serotonin receptors have been identified in *Drosophila melanogaster*, all of which are metabotropic GPCRs. In Chapter 1, I mapped novel targets of serotonin modulation in the *Drosophila* visual system and identified neuromodulation sites in prominent visual processing pathways. Calcium imaging demonstrated a response to bath applied serotonin (Chapter 1) and this enhanced the response to visual stimuli (Chapter 2). In Chapter 2, I closely examined the role of 5-HT2B in L2 neurons and its response to visual inputs. In Chapter 3, I mapped connections between visual neurons (GRASP) and identified serotonergic autoreceptors in the optic lobe. Finally, Chapter 4 describes molecular genetic tools I have generated for the study of the serotonin transporter, SERT. The findings, experimental framework, and new tools described here will be useful for future studies of serotonin biology in flies and other model systems.

Chapter 1: Serotonin Receptors in the *Drosophila* Optic Lobe

Introduction

Serotonin acts a neuromodulator [1-5] in a variety of networks including the sensory systems required for olfaction, hearing, and vision [32-43]. The visual system of *Drosophila melanogaster* provides a powerful genetic model to study the mechanisms underlying visual circuit activity as well as their regulation [49, 50]. In *Drosophila,* visual processing begins in the lamina where intrinsic monopolar neurons receive direct input from photoreceptors [20]. Significant progress has been made in mapping the synaptic connectivity and function of visual processing neurons in the lamina and medulla, including those required for motion detection [15-20, 57]. Despite a nearly complete map of the synaptic connections in the fly visual system, there is little information about non-synaptic neuromodulatory pathways.

Standard methods for connectivity mapping such as serial EM or GRASP are not possible for most neuromodulatory pathways as signaling often occurs outside of a typical synapse. The presence neuromodulators throughout the visual system is well documented [50, 58] and additional studies have shown that aminergic neuromodulators signal to visual information processing neurons in flies and other insects [50, 59-64]. Octopamine, the invertebrate equivalent of noradrenaline, is present in processes innervating the medulla and lobula in *Drosophila*, where it regulates state-dependent modulation of visual interneurons [60, 64] including the saliency of objects during flight [61]. Serotonergic neurons also innervate the optic ganglia [45, 65-69] and previous studies indicate that serotonin has an impact on both cellular activity and visual behavior in insects [62, 63, 70, 71]. Although there is evidence that serotonin modulates the insect visual system, the molecular mechanisms responsible for these effects and the potential contributions of specific subtypes of serotonin receptors are unknown.

Serotonin receptor signaling occurs via diverse secondary messenger cascades [7, 9] and receptors can induce both immediate and long-term changes in cell physiology. Serotonin

receptors may act individually or combinatorally within a single cell [13, 72] or circuit [73] and can have different functions in different cellular compartments. For this reason, it is important to map serotonin receptors to specific cell types and functionally assay the role of these receptors. In Chapter 1, I focus on mapping serotonin receptors to individual cells in the visual system and test for an acute functional response to serotonin using calcium and voltage sensors.

Results

Serotonin receptors in the optic lobe

Five genes encoding serotonin receptors have been identified in the *Drosophila* genome: 5-HT1A, 5-HT1B, 5-HT2A, 5-HT2B and 5-HT7 [74-78]. To identify specific optic lobe neurons expressing each receptor, we expressed the marker mCD8::GFP under the control of a recently characterized panel of T2A-GAL4 insertions in Minos-Mediated Integration Cassettes (MiMICs) located in serotonin receptor gene introns [79]. The GAL4 sequence was inserted into receptor-encoding genes where it acts as an artificial exon and is expected to "mimic" the endogenous gene expression patterns [80]. Ribosome skipping via T2A allows GAL4 to be expressed as a separate protein, rather than a fusion protein with the serotonin receptor, in cases where the MiMIC site is 5' of the first exon [79, 81].

We observed distinct expression patterns for each receptor including projections into the optic lobes neuropils: the lamina (la), medulla (me), lobula (lo) and lobula plate (lp) (Fig 1A-F). We initially focused on receptor subtypes expressed in the lamina because of the ease of identifying cells based on their morphology [51] as well as prominent role of this structure in the earliest stages of visual processing [52, 53, 82]. Receptors 5-HT1A, 5-HT1B and 5-HT2B showed robust labeling of dense projections in the lamina neuropil (Fig 1B, C, E, arrows). Neuronal cell bodies in the lamina cortex are limited to the 5 subtypes of lamina monopolar cells (L1-5) [51, 52]. We did not detect GFP expression representing cells expressing either 5-HT1A

or 5-HT1B in cell bodies in the lamina cortex (Fig 1B-C). However, we observed somata in the medulla cortex, where cell bodies of neurons that project into both the lamina and medulla—T1, C2, and C3—are located (Fig 1B-C). 5-HT2B driven expression was prominent in the lamina and medulla neuropils as well as in cell bodies in the lamina cortex, suggesting that it might be expressed in one or more subtypes of lamina monopolar cells, the only neurons with cell bodies in this area (Fig 1E). We also observed prominent expression of 5-HT7 in cell bodies within the lamina cortex and extending into the neuropil also consistent with expression in at least one subtype of lamina monopolar cell (Fig 1F). For 5-HT1B and 5-HT2A, additional pleomorphic labeling was observed in the lamina cortex (arrowheads in Fig 1C-D) in a pattern that appeared similar to that of optic lobe glia [83]. Based on their location and morphology these cells are likely either fenestrated or pseudocartridge glia [83].

As shown previously, immunolabeling for serotonin can be observed within the neuropil of all optic ganglia (Fig 1G) [44-48]. We also observed a cluster of 8-10 cell bodies in the cortical layer of the accessory medulla (Fig 1G-H). These cell bodies correspond to cluster LP2 (or Cb1), previously shown to project into the medulla [44-48]. Serotonergic boutons in medulla appeared to be organized in layers corresponding to those previously defined [51]. This included strong labeling at the junction between M1 and M2, as well as additional labeling in M4 and the inner medulla (iM) as previously reported [45, 47, 84, 85]. Many of the neuronal processes from cells expressing serotonin receptor MiMIC-T2A-GAL4 driven GFP showed close apposition to serotonergic boutons. For example, terminals from 5-HT1B-expressing cells in the outer medulla were surrounded by a honeycomb pattern of serotonergic immunolabeling (Fig 1H").

Fig 1. Serotonin receptors and serotonergic projections in the optic lobe. Serotonin receptor MiMIC-GAL4 lines were crossed to UAS-mCD8::GFP to identify patterns of expression in the optic lobe. (**A**) A schematic of the optic lobe neuropils including the lamina (la), medulla (me), lobula (lo) and lobula plate (lp) with the neuropil in brown and the cortex containing neuronal cell bodies in beige. (**B-F**) GFP-labeled cells representing the 5-HT1A (**B**), 5-HT1B (**C**), 5-HT2A (**D**), 5-HT2B (**E**), and 5-HT7 (**F**). MiMIC-GAL4 lines were visible in all optic lobe neuropils including the lamina neuropil (arrows, B, C, E). The arrowheads in (C, D) mark pleomorphic 5-HT1B and 5-HT2A labeling in the lamina cortex, possibly representing glial expression. (**G**) Anti-serotonin labeled boutons were observed throughout the optic lobe, including medulla layer M2 (asterisk) and the indicated LP2 cluster of cells. (**G-G”**). Serotonin receptor 5-HT1B>GFP was in proximity to serotonin immunoreactive boutons in M2 and co-labeled at least one serotonergic cell in LP2 (arrowhead). (**H-H”**) In a frontal view, serotonin boutons surround each column containing 5-HT1B>GFP projections in the medulla. N=6-13 brains per condition. Scale bars are 20 μm.

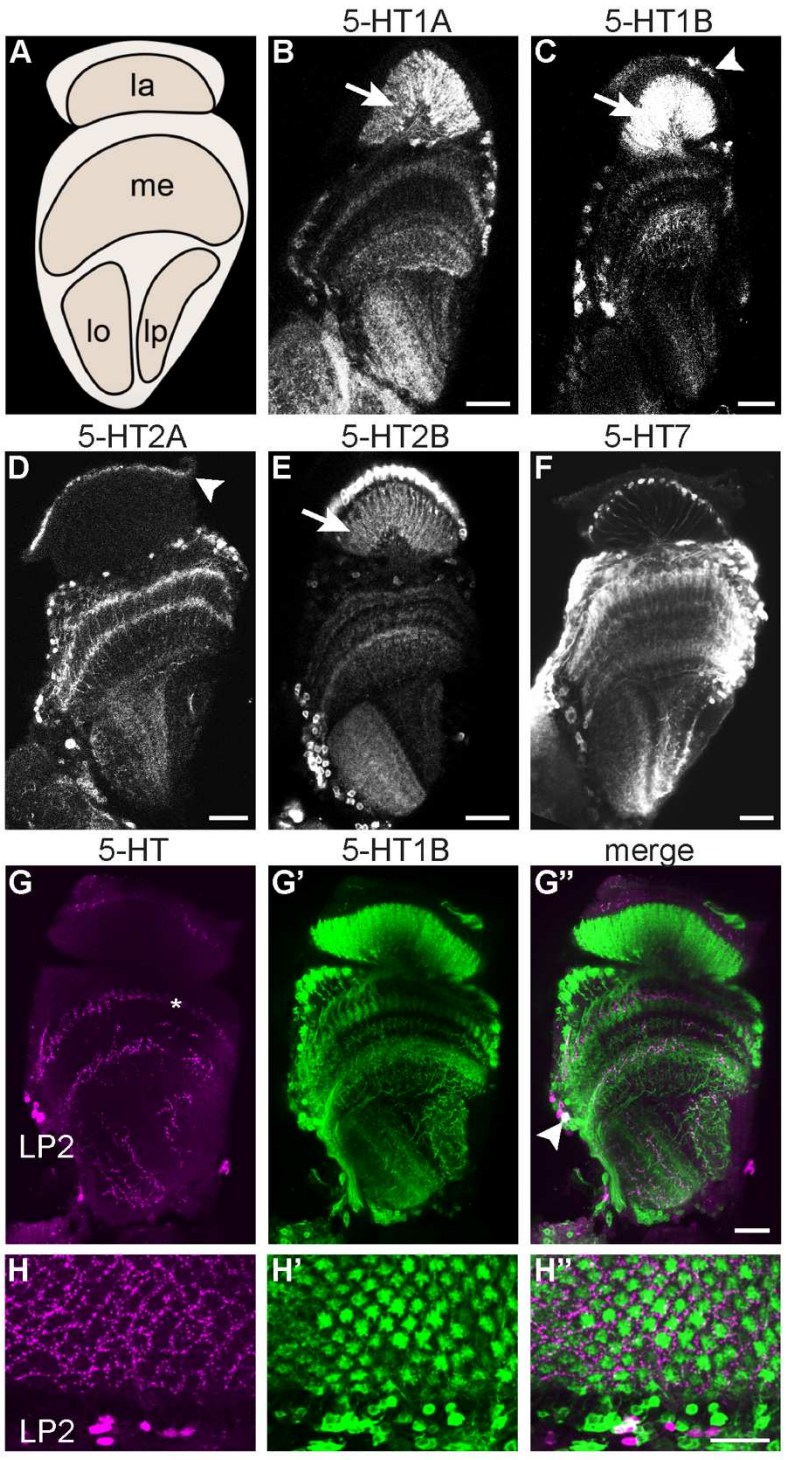
A
la
me
lo
lp
5-HT1A
B
5-HT1B
C
5-HT2A
D
5-HT2B
E
5-HT7
F
5-HT
G
LP2
5-HT1B
G'
merge
G''
H
LP2
H'
H''

Distinct lamina neurons express different serotonin receptors

To identify the cell types that express each serotonin receptor, we used the receptor MiMIC-T2A-GAL4 lines described above in combination with the sparse labeling technique MultiColor FlpOut 1 (MCFO) [86]. Importantly, in contrast to most neurons in the central brain, the stereotyped position and morphology of all neurons in the lamina as well as their organization into repetitive arrays allow them to be unambiguously identified on the basis on their shape and location alone. Although MCFO can be used for lineage tracing [86], we induced MCFO in adult flies, when visual system neurons are post-mitotic, and under these conditions MCFO labeling does not represent clonal events.

Using 5-HT1A and 5-HT1B MiMIC-T2A-GAL4 lines with MCFO we observed a subtype of cells with a soma in the medulla cortex, a long basket-like projection in the lamina, and a smaller projection in the medulla (Fig 2A-B). This morphology is identical to that of T1 cells and distinct from other cell types in the lamina (Fig 2C) [51]. T1 cells were identified in 23 of 31 brains (71%) for 5-HT1A and in 10 of 11 brains (91%) for 5-HT1B. On average, we observed thirteen MCFO-labeled T1 cells per individual optic lobe for 5-HT1A and nine T1 cells per optic lobe for 5-HT1B. These data are consistent with the results of recently published studies that used TAPIN-Seq or FACS-SMART-Seq to analyze expression in T1 as well as other cells in the visual system [58, 87] (see Fig 7 for comparison).

We found that 5-HT1A>MCFO labeled lamina wide-field neurons (Lawf) in 14 of 31 brains (Fig 2D). In some cases, the proximity of other 5-HT1A+ processes made it difficult to determine the precise number of Lawf neurons per brain. It also remains unclear whether labeled cells represent Lawf1 [51] (shown in Fig 2C) or Lawf2, which was identified more recently and is not shown in 2C [54, 88].

Using the 5-HT2B MiMIC-T2A-GAL4 driver with MCFO, we observed labeled cells with a soma in the lamina cortex, dense projections extending into the lamina neuropil, and a single

bushy terminal in the medulla (Fig 2E), a morphology identical to lamina monopolar neuron L2 and no other lamina cell types (Fig 2C) [51]. We observed L2 cells in 9 of 9 (100%) 5-HT2B>MCFO brains, observing an average of eleven L2 neurons per optic lobe. A previous TAPIN-Seq study [58] reported a high probability of 5-HT2B expression in L2 cells, consistent with these findings.

For 5-HT7>MCFO, we observed lamina monopolar cells in 7 of 13 brains (54%) (Fig 2F), with an average of 20 cells per optic lobe. Over 99% of the lamina monopolar cells labeled with 5-HT7>MCFO lacked the dense processes in the neuropil that are characteristic of L1-L3, and also lacked the vertically oriented collaterals in the inner (proximal) lamina seen in L4 neurons (Fig 2C, F). We therefore suggest that 5-HT7 is expressed in the one remaining subtype, L5 cells, which was also reported in recent study [58]. Consistent with our observations using 5-HT2A MiMIC-T2A-GAL4>GFP, all (18/18, 100%) 5-HT2A>MFCO brains labeled cells with a morphology and location possibly consistent with the fenestrated or pseudocartridge glia in the lamina cortex (Fig 2G, see Fig 3) [83].

As noted above, in some cases, multiple cells of each subtype were labeled in each brain. However, we also detected less frequent events for other columnar cells in the lamina. These include observations of multiple centrifugal C2 cells in 3 of 31 5-HT1A>MCFO brains (Fig 2H) consistent with two previous reports of 5-HT1A in C2 [58, 87]. We also observed a single lamina monopolar cell with arborizations in the lamina neuropil similar to L1-L3 in one 5-HT7>MCFO brain, compared to 152 presumptive L5 cells counted in the thirteen 5-HT7>MCFO brains.

Medulla neurons, glia and serotonergic neurons express serotonin receptors

The results of other more comprehensive studies of RNA expression in visual system neurons prompted us to look beyond our primary focus of lamina neurons [58, 87]. In addition to

the columnar neurons that express serotonin receptors and extend projections into the lamina [51], we have tentatively identified cells with projections that are either confined to the medulla, or include both medulla and lobula complex, and may also express serotonin receptors Although further work will be needed for more precise identification, their morphology strongly suggest that they represent subtypes of distal medulla (Dm) amacrine neurons, medulla intrinsic (Mi) neurons, and transmedullary Y neurons (TmY). Dm neurons have cell bodies in the medulla cortex but, unlike other medullar neurons, project into the distal medulla [51].

For 5-HT1B, we observed a single Dm-like cell (Fig 2I). Using 5-HT7>MCFO we observed medulla intrinsic cells, which are confined to the medulla, that are morphologically similar to Mi1 labeled in 6 of 13 brains (Fig 2J). TmY cell bodies are located in the medulla cortex and send projections through the medulla; their processes terminate in both the lobula and lobula plate, thus uniquely identifying this cell class [51]. We observed potential TmY3 cells labeled in five 5-HT1A>MCFO brains (Fig 2K) and four 5-HT7>MCFO brains (Fig 2L). We observed TmY cells labeled in all 18 5-HT2A>MCFO brains, with an average of 18 TmY cells per optic lobe (Fig 2M). We anticipate that these data may be useful for comparisons with genomic studies of the optic lobe [58] and generate hypotheses about the potential serotonergic regulation of these cells.

Fig 2. Lamina neurons including T1 and L2 express serotonin receptors. (**A-B, D-M**) Serotonin receptor MiMIC-GAL4 lines were crossed to UAS-MCFO-1 to sparsely label individual cells in the lamina. Cells are indicated by an arrowhead. 5-HT1A (**A,**) and 5-HT1B (**B**) MCFO crosses revealed cells with morphologies identical to T1 neurons. (**C**) A diagram showing lamina neurons adapted from [51] highlights L1 (blue), L2 (green), L5 (orange), T1 (purple), C2 (pink), and Lawf (dark purple) cells. (**D**) 5-HT1A>MCFO also labeled Lawf-like cells. (**E**) 5-HT2B>MCFO labeled cells are morphologically identical to L2 neurons. (**F**) 5-HT7>MCFO-1 labeled neurons most likely representing L5 lamina monopolar cells. (**G**) 5-HT2A>MCFO-1 cells in the lamina cortex with a location and morphology consistent with glia. (**H**) 5-HT1A>MCFO labeled cells with morphology similar to C2 cells. (**I**) 5-HT1B>MCFO labeled a distal medulla neuron (Dm). (**J**) 5-HT7>MCFO a medulla intrinsic neuron that resembled Mi1. (**K-M**) 5-HT1A, 5-HT7 and 5-HT2A>MCFO labeled TmY cells. Scale bars are 20 μm and N=10-31 brains imaged per receptor subtype. Cell types shown were observed in a subset of brains: 22/31 (**A**), 10/11 (**B**), 14/31, 14/31 (**D**), 10/10 (**E**), 7/13 (**F**), 18/18 (**G**), 3/31 (**H**), 1/11 (**I**), 7/13 (**J**), 5/31 (**K**), 4/13 (**L**), 18/18 (**M**).

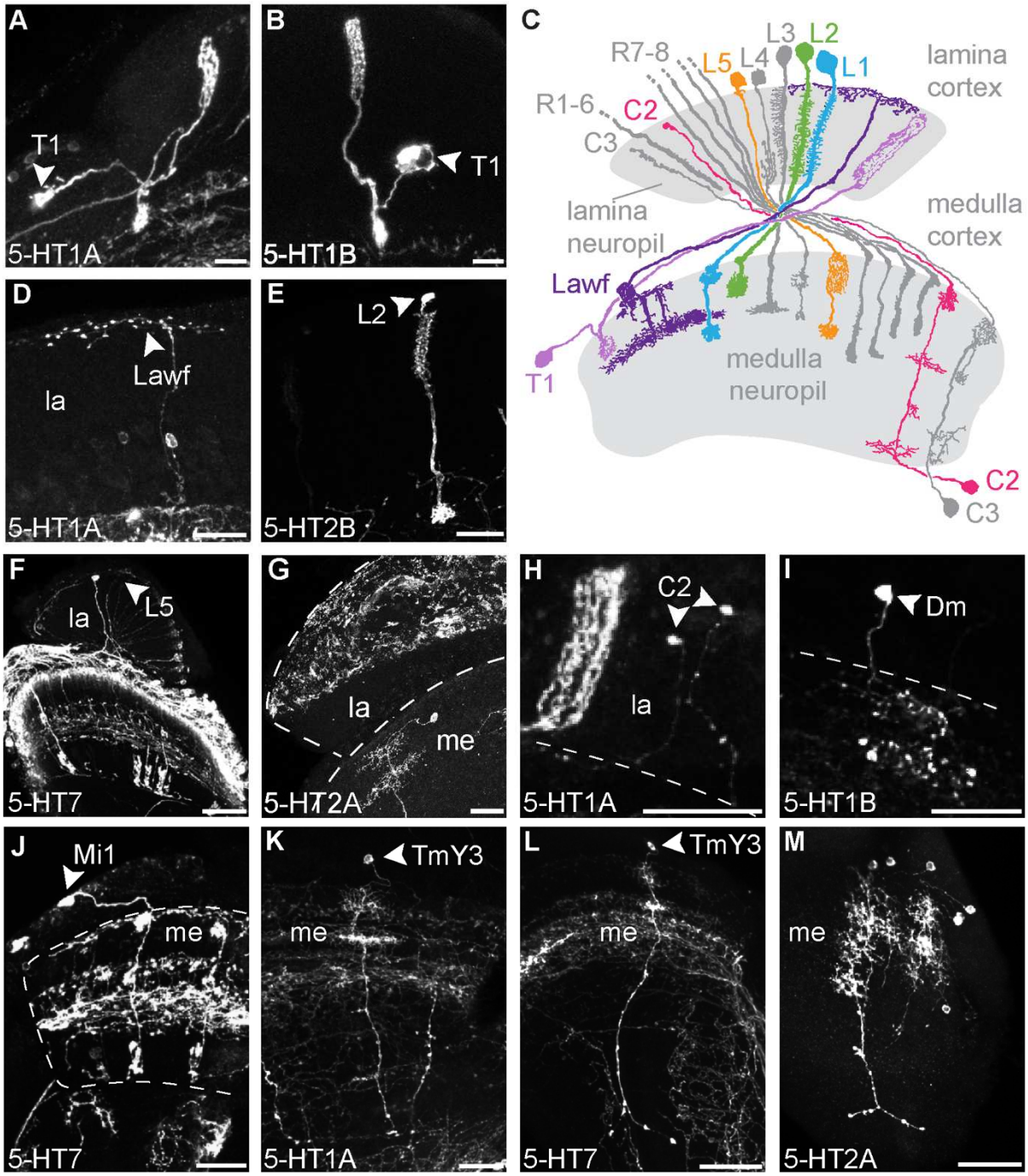
A
T1
5-HT1A
B
T1
5-HT1B
C
R7-8
L3
L2
L5
L4
L1
lamina cortex
R1-6
C2
C3
lamina neuropil
medulla cortex
Lawf
T1
medulla neuropil
C2
C3
D
Lawf
la
5-HT1A
E
L2
5-HT2B
F
la
L5
5-HT7
G
la
me
5-HT2A
H
C2
la
5-HT1A
I
Dm
5-HT1B
J
Mi1
me
5-HT7
K
TmY3
me
5-HT1A
L
TmY3
me
5-HT7
M
me
5-HT2A

For 5-HT2A MCFO, we observed irregularly shaped cells in the distal lamina cortex (Fig 3A). Anti-repo labeled nuclei showed close proximity to many 5-HT2A labeled cells (Fig 3B), but one-to-one matching was not possible due to irregular cell morphology. Therefore, further experiments are necessary to identify the specific cell type expressing 5-HT2A in the lamina cortex. A previous microarray study of glia suggested that 5-HT1A and 5-HT7 are enriched in repo-GAL4 specified glia, while 5-HT1B was enriched in surface glia (personal communication, Roland Bainton, UCSF, and [89]). Additionally, a previous study [58] reported expression of 5-HT7 in three types of lamina glia—epithelial glia, proximal satellite glia and marginal glia.

Fig 3. 5-HT2A labeling in lamina cortex may represent glial cells. (**A**) Sparse labeling with 5-HT2A-GAL4>MCFO V5 (green) and HA (magenta) marked unidentified cells confined the distal lamina cortex. (**B**) 5-HT2A-T2A-GAL4>UAS-mCD8::GFP (green) labeled cells in the lamina cortex in close proximity to nuclei labeled with repo antibody (magenta) N=18 brains for (A) and N=4 brains for (B). Scale bars are 20 μm.

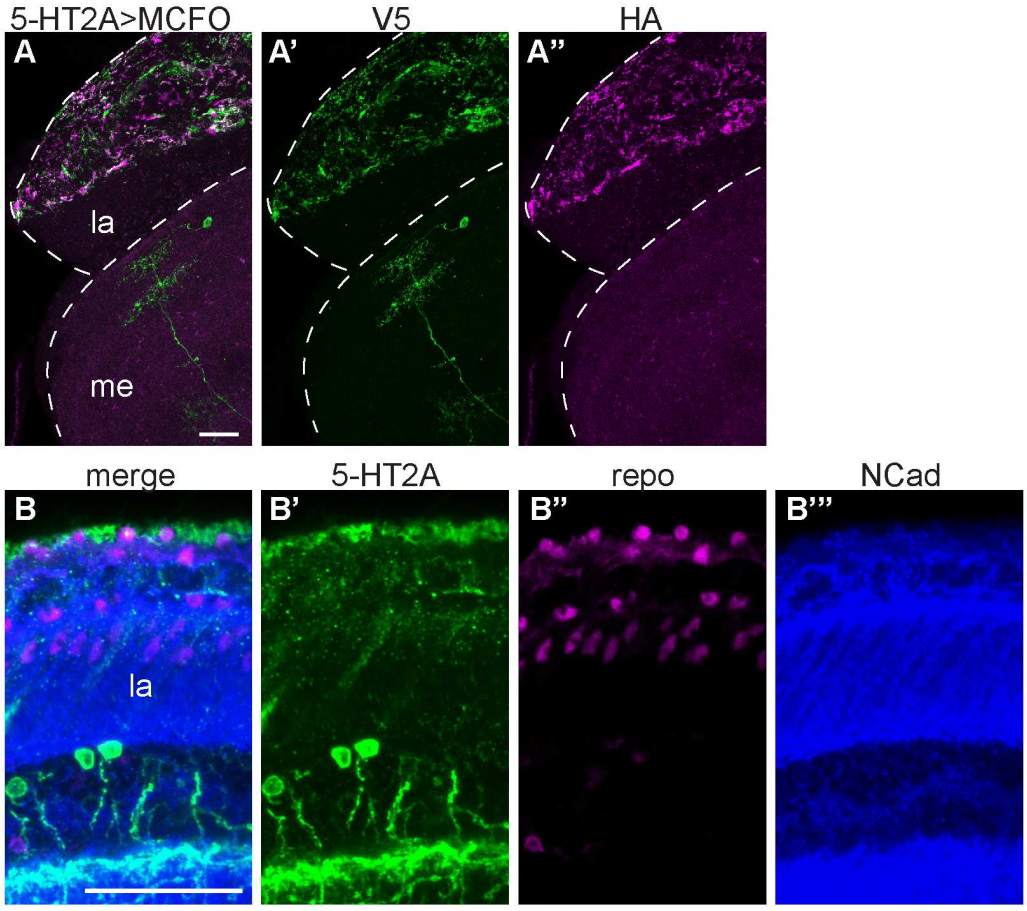

L2 neurons express 5-HT2B and T1 neurons express 5-HT1A and 5HT1B

Comprehensive genomic studies of optic lobe neurons were recently reported [58, 87]. Before embarking on functional studies of specific neurons in the lamina, we sought to confirm the expression of serotonin receptors independently of both previous studies [58, 87] and the data we obtained using MiMIC-T2A-GAL4 lines. To this end, we used a separate set of split-GAL4 [54] or LexA drivers previously shown to be specific for particular cell types and focused on a small subset of lamina neurons: T1, L1 and L2. Drivers representing each cell were used to express GFP, and the GFP-labeled cells were isolated via Fluorescence Activated Cell Sorting (FACS). RNA was then extracted from T1, L1 and L2 FACS isolates as well as the unlabeled cells. To probe for serotonin receptor expression in each cell type, we used both RT-qPCR and RNA-Seq. Consistent with our MCFO data, RT-qPCR from GFP-labeled T1 isolates (N=6) showed enrichment of both 5-HT1A and 5-HT1B transcripts, but no other serotonin receptors (Fig 4A and Table 1). Using RNA-Seq, we compared the relative abundance for each receptor by calculating Transcripts Per Million (TPMs). We found that 5-HT1A (182±43 TPM±stdev) and 5-HT1B (278±25 TPM±stdev) were more abundant than other serotonin receptors (range 0.1±0.1 to 2.5±4 TPM±stdev) in T1 samples (N=3, Fig 4B and Table 2).

Using RT-qPCR, L2 isolates showed consistent enrichment for 5-HT2B, but not 5-HT1A or 5-HT1B transcripts (Fig 4C and Table 1) and higher TPMs for 5-HT2B (130±75 TPM±stdev) compared to other serotonin receptors (range 6±6 to 31±9 TPM±stdev) (Fig 4D and Table 2). In addition, 5-HT7 was amplified by RT-qPCR in 3/5 L2 samples and 5-HT2A in 1/5 L2 samples (Fig 4C and Table 1). By contrast, using RNA-Seq we did not detect high abundance of either 5-HT2A or 5-HT7 transcripts in L2 neuron isolates. It is possible that the amplification of 5-HT2A in a single L2 sample was a result of contamination as this was not observed in the other four RT-qPCR samples nor any of the RNA-Seq samples. Although we cannot rule out the presence

of 5-HT2A or 5-HT7 in L2 based on the results of RT-qPCR, our data and those of others [58] suggest that 5-HT2B may be the only serotonin receptor abundantly expressed in L2 cells.

We did not observe evidence of any serotonin receptor expression in L1 neurons using the serotonin receptor MiMIC-T2A-GAL4 lines to drive MCFO. In agreement with this observation, RT-qPCR from isolated L1 cells showed virtually no receptor expression, apart from one sample weakly enriched for 5-HT1B (Fig 4E and Table 1). In sum, MCFO sparse labeling in combination with RT-qPCR and RNA-Seq showed that T1 neurons express 5-HT1A and 5-HT1B, and L2 neurons express 5-HT2B, whereas L1 neurons do not express any serotonin receptor subtypes that are detectable using these methods (Fig 4).

Our data complement a recent computational genomics study that reported a high probability of expression for 5-HT2B in L2, 5-HT1A and 5-HT1B in T1, and a low likelihood of any serotonin receptor expression in L1 neurons [58]. This study did not report a high probability of either 5-HT2A or 5-HT7 expression in L2 neurons, perhaps consistent with our observation that 5-HT7 and 5-HT2A may be present either at low levels or within a subset of cells.

Fig 4. L2 neurons express 5-HT2B and T1 neurons express both 5-HT1A and 5-HT1B serotonin receptors. (**A**) RT-qPCR performed on cDNA from isolated T1 neurons expressing GFP showed enrichment for serotonin receptors 5-HT1A and 5-HT1B relative to other GFP-negative cells from the optic lobe. (**B**) T1 RNA-Seq transcript abundance (color low to high, blue to yellow) Transcripts Per Kilobase Million (TPMs) revealed enriched 5-HT1A and 5-HT1B compared to other serotonin receptors. (**C**) FACS isolates from L2 cells showed enrichment of 5-HT2B and 5-HT7 in RT-qPCR. (**D**) L2 RNA-Seq showed higher 5-HT2B TPMs in two of three samples. (**E**) L1 RT-qPCR enrichment was not detectable for any serotonin receptors. RT-qPCR error bars represent mean±SEM. N=3-6 biological replicates pooled from 18-40 brains per replicate.

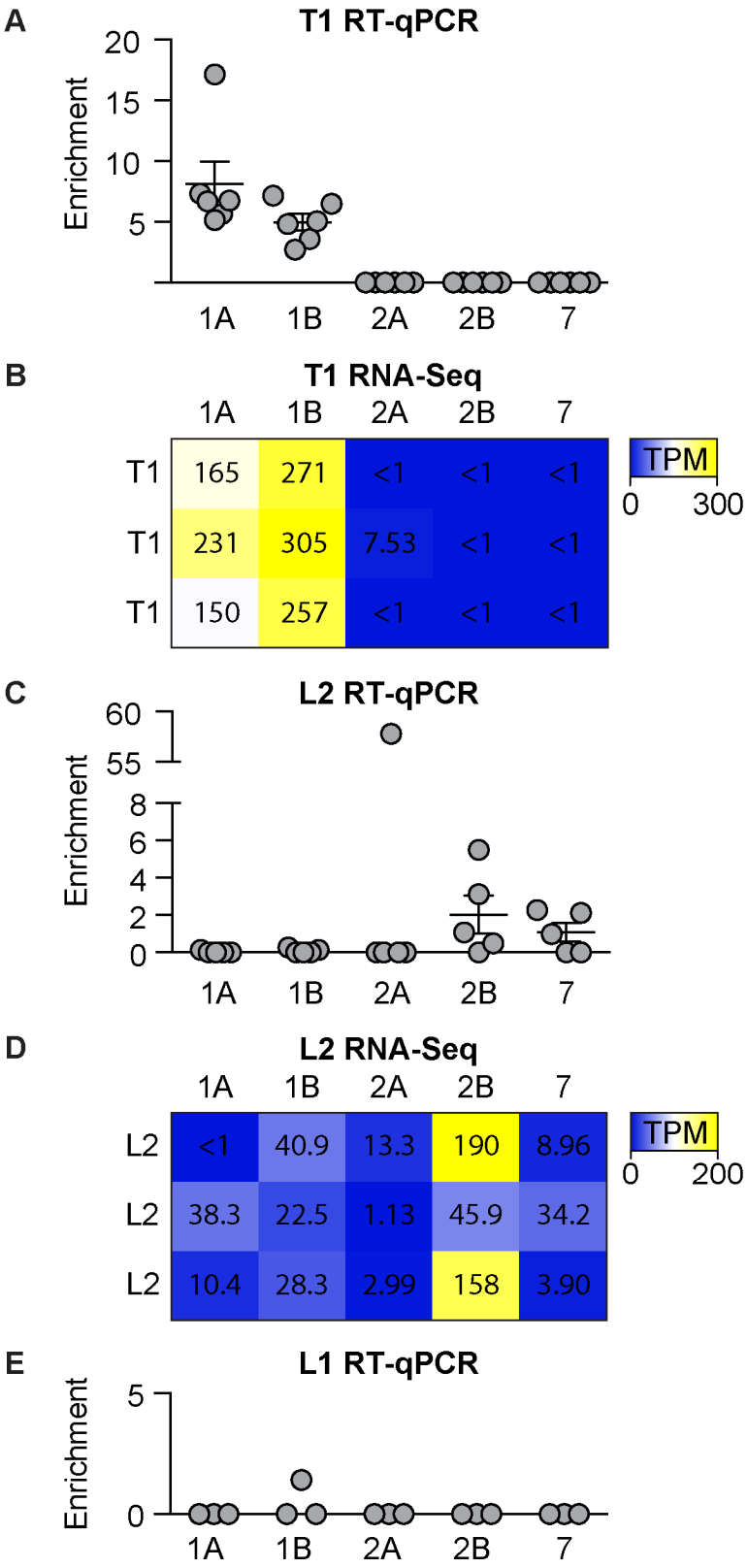
A
T1 RT-qPCR
Enrichment
20
15
10
5
1A
1B
2A
2B
7
B
T1 RNA-Seq
1A
1B
2A
2B
7
T1
165
271
<1
<1
<1
T1
231
305
7.53
<1
<1
T1
150
257
<1
<1
<1
TPM
0
300
C
L2 RT-qPCR
Enrichment
60
55
8
6
4
2
0
1A
1B
2A
2B
7
D
L2 RNA-Seq
1A
1B
2A
2B
7
L2
<1
40.9
13.3
190
8.96
L2
38.3
22.5
1.13
45.9
34.2
L2
10.4
28.3
2.99
158
3.90
TPM
0
200
E
L1 RT-qPCR
Enrichment
5
0
1A
1B
2A
2B
7

5-HT2B and 5-HT1A receptors localize to M2

Both T1 and L2 neurons have dense projections in the lamina neuropil and arborize in layer 2 (M2) of the medulla neuropil. Serotonin neurons directly innervate M1 and M2 of the medulla neuropil raising the possibility that serotonergic signaling might occur at this site. If so, we reasoned that the serotonin receptors expressed in L2 and T1 might localize to M1 and/or M2. To test this possibility, we took advantage of a 5-HT1A allele that had been tagged at the C-terminus with GFP [90]. The tag was inserted into the endogenous 5-HT1A gene, such that, similar to MiMIC-T2A-GAL4 lines [79, 80], the receptor::GFP fusion protein product is putatively expressed at the same level and in the same cells as the endogenous protein [90]. In 5-HT1A::GFP flies, we observed enrichment of the tagged protein in layer M2 of the medulla relative to other subcellular sites (Fig 5A-A"). This signal could be derived from 5-HT1A::GFP in T1 cells or other columnar neurons expressing 5-HT1A. We also observed anti-serotonin immunoreactivity that co-labeled with 5-HT1A::GFP in the medulla (Fig 5B, arrows), suggesting that 5-HT1A acts as both an autoreceptor in serotonergic projection neurons innervating the medulla and as a hetereoreceptor in columnar neurons that project into in the medulla.

Since we were unable to obtain an endogenously tagged allele of 5-HT2B, we relied on expression of a UAS-5-HT2B::GFP transgene [91] under the control of L2 split-GAL4 to investigate its subcellular localization (Fig 5C). 5-HT2B::GFP was enriched in terminals within M2 of the medulla as compared to the lamina neuropil (Fig 5C-C"), and showed additional punctate labeling in L2 cell bodies (Fig 5C', arrowhead). As a control, we expressed UAS-mCD8::GFP using the same L2 split-GAL4 driver. In contrast to 5-HT2B::GFP, labeling with 5-HT2B mCD8::GFP was most prominent in the cell body and proximal processes with progressively weaker labeling through the lamina and medulla neuropil and no enrichment in layer M2 (Fig 5D"). These data suggest that both 5-HT2B and 5-HT1A preferentially localize to the arborizations of L2 and T1 in the medulla rather than the lamina neuropil. Serotonergic

boutons also localize near these arborizations in M1/M2 but are not found in the lamina neuropil near the arborizations of either neuron (see Fig 1G). Although serotonergic boutons are also found in the lamina cortex near the somata of L2 and T1 neurons, we are not aware of any evidence in support of direct signaling to neuronal somata in *Drosophila*. We therefore conclude that serotonergic signaling to L2 and T1 via 5-HT2B and 5-HT1A most likely occurs in the medulla. However, since other receptors are expressed in both cell types, we cannot rule out the possibility that serotonergic signaling also occurs at other locations, and perhaps via neurohumoral mechanisms rather than release from proximal serotonergic boutons.

Fig 5. Serotonin receptors 5-HT1A and 5-HT2B are enriched in layer M2 of the medulla. (**A-A”**) 5-HT1A::GFP localized to layer M2 of the medulla, adjacent to some of the boutons in the medulla neuropil immunogenic for serotonin. Neuropil (anti-N-Cadherin, blue) and serotonin (magenta) labeling provide anatomical context for the lamina (la) and medulla (me). The region specified by the dotted lines in (**A’**) is enlarged in (**A”**). (**B-B”**) In some cases, serotonin immunoreactive boutons appear to be co-labeled rather than adjacent to 5-HT1A::GFP (arrow) possibly representing projections from serotonergic neurons in the central brain. (**C-C”**) Subcellular localization of 5-HT2B was visualized by expressing the fusion construct UAS-5-HT2B::sfGFP in L2 neurons specified by L2-split-Gal4. L2>5-HT2B::sfGFP labeling is stronger in the L2 terminals in medulla layer 2 (M2) compared to L2 projections in the lamina (la). Punctate GFP signal is observed in the L2 cell bodies (arrowhead). The region specified by the dotted lines in (**C’**) is enlarged in (**C”**). (**D-D”**) For comparison, membrane-directed UAS-mCD8::GFP was expressed in L2 neurons. L2>mCD8::GFP signal is similar in the medulla and lamina compartments. Strong GFP signal was observed in the cell bodies (arrowhead). The area within the dotted lines in (**D’**) is enlarged in (**D”**). Scale bars are 20 μm in **A-A’**, **B-B”**, **C-C’** and **D-D’**. Scale bars are 10 μm in **A”** and 8 μm in both **C”** and **D”**. Biological replicates are N=6 for 5-HT1A::GFP (**A-B**), N=15 for L2>5-HT2B::GFP (**C-C”**), and N=10 for L2>mCD8::GFP (**D-D”**).

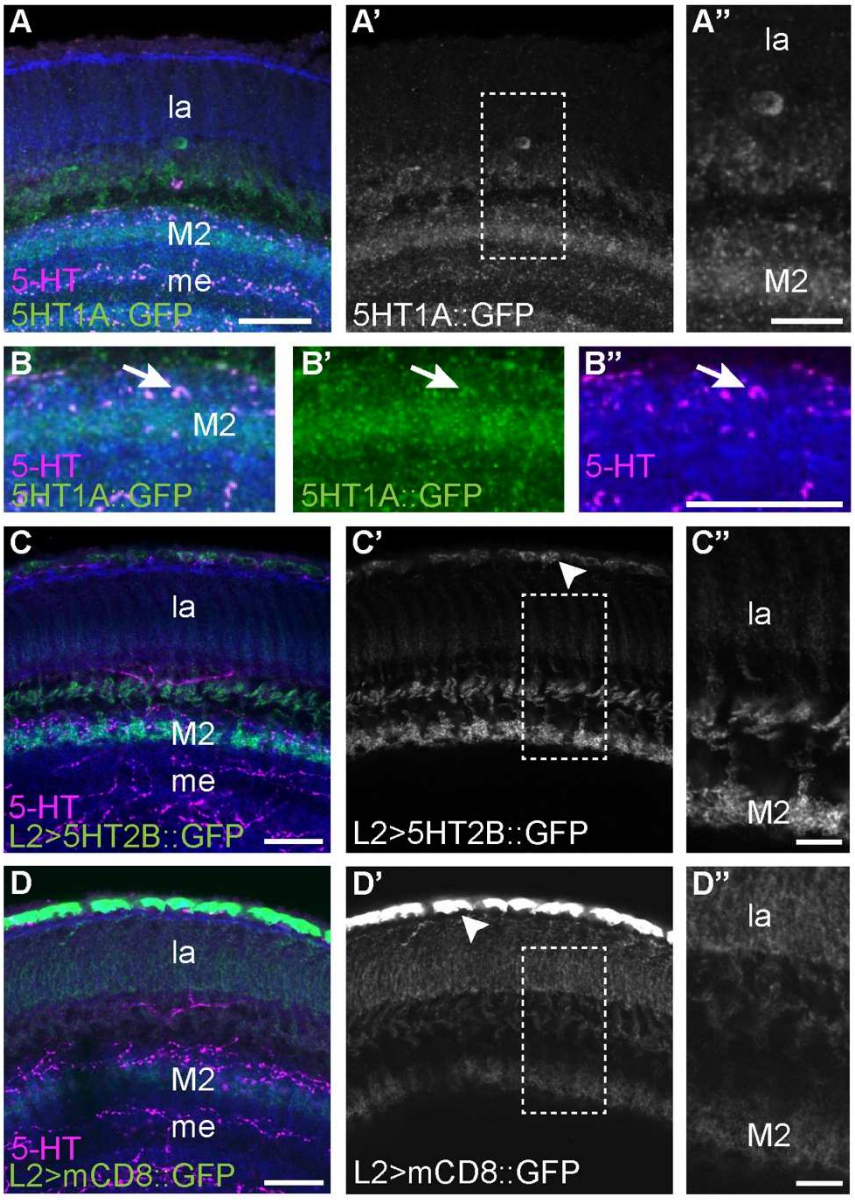
A
la
M2
me
5-HT
5HT1A::GFP
A'
5HT1A::GFP
A''
la
M2
B
M2
5-HT
5HT1A::GFP
B'
5HT1A::GFP
B''
5-HT
C
la
M2
me
5-HT
L2>5HT2B::GFP
C'
L2>5HT2B::GFP
C''
la
M2
D
la
M2
me
5-HT
L2>mCD8::GFP
D'
L2>mCD8::GFP
D''
la
M2

Serotonin increases calcium levels in L2 and L1 neurons

The data presented here and by others [58, 87] strongly suggest that L2 and other cells in the visual system express serotonin receptors but do not address their function. To address the potential effects of serotonin on L2 neurons, we bath applied serotonin to the optic lobe and used live imaging to monitor cellular activity. The data for receptor expression in L2 was strongest for 5-HT2B receptors, which couple with $G_{q/11}$ to increase intracellular calcium *in vitro* [78, 92]. We therefore used the genetically encoded calcium indicator GCaMP6f [93] to follow changes in L2 activity that might be induced by serotonin. We again employed the L2 split-GAL4 driver used for transcriptional analysis (Fig 4) to specifically express GCaMP6f in L2 neurons (Fig 6A). Since we observed enrichment of 5-HT2B::sfGFP in L2 terminals in M2, we focused our recordings of calcium signaling on these sites. For each experiment, we first recorded a baseline while perfusing the tissue with saline; the perfusion solution was then switched to either saline containing 100 μM serotonin or saline alone. We included tetrodotoxin (TTX) in the perfusion solution to reduce inputs to L2 neurons and also to reduce muscle activity driven by action potentials in motor neurons in the head. TTX has been used by others to study the effects of serotonin in *Drosophila,* and represents a standard method to reduce cell-non autonomous neuronal inputs [94-96].

We consistently observed a large increase in GCaMP6f fluorescence in L2 terminals following serotonin application (Fig 6B). This increase continued throughout the time course of recording, peaking at 1.73 $\Delta F/F \pm 0.77$ SEM (compared to saline control -0.03 $\Delta F/F \pm 0.05$ SEM at the same timepoint; $p=0.0095$ by two-tailed Wilcoxon rank sum test). Thus, serotonin leads to an accumulation of cytosolic calcium in L2 cells, consistent with the predicted outcome of activating $G_{q/11}$ coupled 5-HT2B receptors [78, 92]. However, since local neurons in the optic lobe use graded electrical signaling, rather than action potentials, and may be insensitive to

TTX, we did not block all synaptic inputs to L2 neurons in these experiments, and we cannot rule out cell non-autonomous effects of serotonin on L2 neurons.

Fig 6. Bath application of serotonin leads to increased calcium in L2 and L1 neurons, but not T1 neurons. (**A-C**) GCaMP6f was paired with L2, L1 and T1 split-GAL4 drivers to monitor responses to 100 μM serotonin (colored traces) or saline controls (gray traces). (**A**) The experimental setup is shown in the top panel, along with a sample image of L2 terminals (bottom panel) as imaged in the medulla (gray). For bath application experiments (**B, C, E, F**), the perfusion change occurs approximately 105 s into the trace as shown. In L2 terminals (**B**), serotonin application led to a significant increase in GCaMP6f signal indicating increased calcium levels as compared to saline controls (p=00095). L1 terminals (**C**) showed a similar increase in calcium following a switch to serotonin (p=0.02). (**D**) RT-qPCR from cell isolates revealed enrichment of the gap junction protein ShakB in L2 and L1, but not T1 neurons. (**E**) T1 cells expressing GCaMP6f showed no significant change in calcium following serotonin application (p>0.05). (**F**) T1 cells expressing the voltage sensor ArcLight similarly displayed no significant change following serotonin application (p>0.05). (**G**) RNA-Seq of L2 neurons showed high transcript abundance for SHakB (innexin 8, Inx8) compared to the innexin other gap junction channels. For (**B**, **C**, **E**, **F**) N=4-8 individual flies; the dark trace is an average of all traces and the shaded region is 1 SD; saline vs. serotonin comparisons are two-tailed Wilcoxon rank sum tests. For (**D** and **G**), N=3 individual isolates for each cell type. Bars in (**D**) represent the mean±SEM.

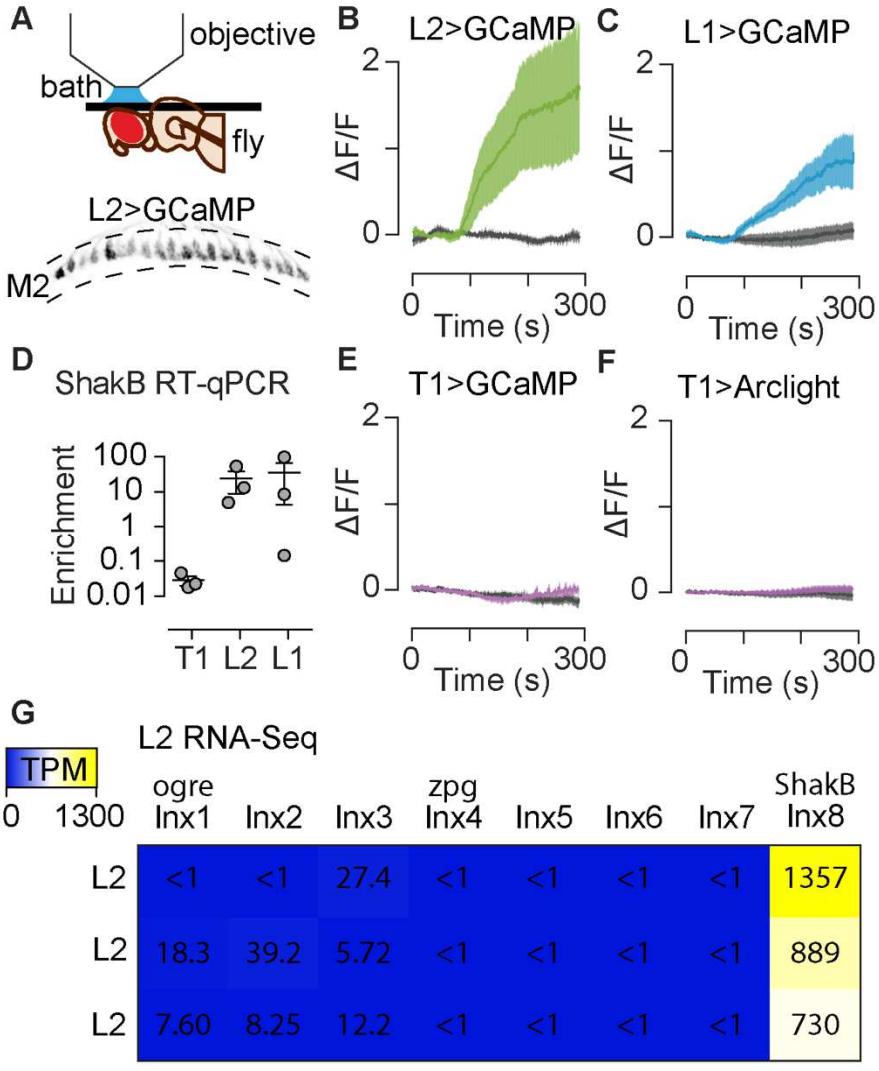

Since we did not detect serotonin receptors in L1 neurons, we did not expect serotonin to measurably change intracellular calcium levels in these cells. However, with GCaMP6f expressed in L1 cells using a cell-specific driver, we regularly observed a robust increase in baseline fluorescence following serotonin exposure (Fig 6C). Although the increase in GCaMP6f signal did not reach the same response amplitude as observed in L2 neurons, the time course was similar: the signal persisted throughout the recording and peaked at 0.98 $\Delta F/F \pm 0.34$ SEM (compared to saline control at 0.07 $\Delta F/F \pm 0.09$ SEM; $p=0.02$ by two-tailed Wilcoxon rank sum test). A direct action of serotonin on L1 is unlikely since we did not detect endogenous serotonin receptors (see Fig 4). The possibility of action potential driven inputs is also low since TTX was included in the perfusion solution. Other possible mechanisms include graded inputs from neurons unaffected by TTX or coupling between L1 and L2 [82]. In support of previous data showing electrical coupling between L1 and L2, we find that transcripts for the gap junction protein Shaking-B (ShakB or Inx8) are enriched in L1 and L2 neurons, but not T1 neurons, using RT-qPCR (Fig 6D) and RNA-Seq (Fig 6G).

We next examined whether serotonin could affect the activity of T1 cells. Both 5-HT1A and 5-HT1B receptors, expressed in T1 neurons, are expected to couple with G_i proteins and negatively regulate adenylyl cyclase [76, 92]. Due to the generally inhibitory function of these receptors, we hypothesized that serotonin would dampen activity in T1 neurons, possibly manifested as a decrease in cytosolic calcium or membrane potential [97]. Using the T1 split-GAL4 driver [54] to express either GCaMP6f or the voltage sensor Arclight [98], we did not observe a significant change in fluorescence during perfusion with serotonin (Fig 6E, 6F; $p>0.1$). Thus, further experiments will be needed to determine the effects of serotonin on T1 neurons. These negative data are nonetheless important for the current study, since the absence of a GCaMP6f response in T1 neurons indicates that the response observed in L1 and L2 is not an artifact or a generalized phenomenon common to all cells in the lamina.

Discussion

Serotonergic modulation occurs by activation of multiple receptors and associated second messenger cascades [7, 9]. Understanding how serotonergic signaling tunes circuit activity requires functional experiments to determine the effects on specific cells in addition to mapping the cellular and subcellular cites of individual receptors. Previous studies have mapped the expression pattern of multiple receptor subtypes to specific cells within the visual system [58, 87]. To develop the fly visual system as a new molecular-genetic model to study serotonergic neuromodulation we have confirmed the expression of the five *Drosophila* serotonin receptors in a subset of experimentally tractable cells in the lamina and used live imaging to determine their potential function. To our knowledge, these represent the first functional data for serotonergic neuromodulation of the *Drosophila* visual system with the exception of a single report in 1995 [62]. We also present the first data on the subcellular localization of serotonin receptors in the visual system. In addition, our data mapping the cellular expression pattern of the receptors are complementary to two previous transcriptomic analyses [58, 87] since we have used a different experimental approach.

We focused primarily on the lamina to identify a subset of cells that might express serotonin receptors. Our goal was to identify cells that could be used for functional studies and the function of several lamina neurons have been previously characterized [53-56]. In addition, the lamina contains a relatively small number of neurons, allowing identification based on morphology alone [51]. MiMIC-T2A-GAL4 drivers [79] are useful for replicating the endogenous expression patterns and provided a convenient method to screen for cells that express each receptor (Fig 1-3). To validate receptor expression before performing functional studies we used a combination of MiMIC-based reporter lines, RNA-Seq and RT-qPCR. All of these techniques indicated that 5-HT2B is expressed in L2 lamina monopolar neurons, which are involved in motion [82, 99] and contrast vision [56]. The idea that L2 cells express 5-HT2B is further

supported by data from a previous report that mapped neurotransmitter receptor transcripts to cells throughout the visual system [58]. Although our RT-qPCR findings support the possibility that L2 neurons might also express 5-HT7, neither we nor others detect an enrichment of 5-HT7 using RNA-Seq [58].

We observed consistent expression of 5-HT1A and 5-HT1B in T1 neurons, whose function remains poorly understood [54]. We did not detect expression of any serotonin receptors in the L1 subclass of lamina monopolar neurons, which acts in parallel to L2 for visual processing. Our data on T1 and L1 are consistent with recent transcriptional studies of these and other cells in the visual system [58, 87]. Konstantinides et al. used FACS-SMART-Seq (GSE103772) and found 5-HT1A and 5-HT1B in T1 cells, 5-HT7 in Mi1 cells, and 5-HT1A in C2 cells. Davis et al. used TAPIN-seq [58] and also reported 5-HT2B in L2 cells, 5-HT1A in C2 cells, and 5-HT7 in L5 cells, consistent with the sparse labeling experiments shown here in Fig 2. In Fig 7 we directly compare serotonin receptor expression reported for each cell type in the current study, Davis et al. [58], and Konstantinides et al. [87].

Differences in the methods used to isolate target cell populations, extract RNA, and create DNA libraries can impact sequencing results. For example, Davis et al. used TAPIN-seq to purify nuclei, subjecting tissue homogenates to two rounds of immunoprecipitation to isolate tagged nuclei before preparing RNA, a process which may lead to non-specific binding. Conversely, our use of FACS can lead to contamination by other cell types due to incomplete dissociation of GFP-tagged cells or due to non-specific labeling by the driver lines. Additionally, differences in cDNA library construction, including different approaches for poly-A mRNA enrichment, can significantly affect the results obtained in different studies. In contrast to Davis et al. we did not detect expression of serotonin receptors in photoreceptor cells or in lamina monopolar neuron L3 using MiMIC-T2A-GAL4>UAS-MCFO. These inconsistencies could be due to biological variability in levels of gene expression or infidelity in the MiMIC-based

approach, which may not perfectly reflect endogenous expression due to disruption of the genetic locus. Further studies may reconcile these differences; meanwhile we suggest that using multiple, overlapping methods may be important to fully evaluate complex patterns of gene expression.

Fig 7. Data sets reporting evidence of serotonin receptor expression in optic lobe neurons. The current study includes MiMIC-T2A-GAL4>MCFO for identification based on morphology (green), and FACS-SMART-seq of cells specified by L2-split-GAL4 or T1-lexA (blue). Davis et al. 2020 employed TAPIN-Seq and reported probability of expressions (GSE116969, Table 7B) for each cell type. Serotonin receptor expression with a p>0.75 are visualized (purple). Konstantinides et al. 2018 used FACS-SMART-Seq for T1, Mi1, C2 and C3 (GSE103772). Serotonin receptors with counts greater than 1,000 in at least two replicates are represented (orange).

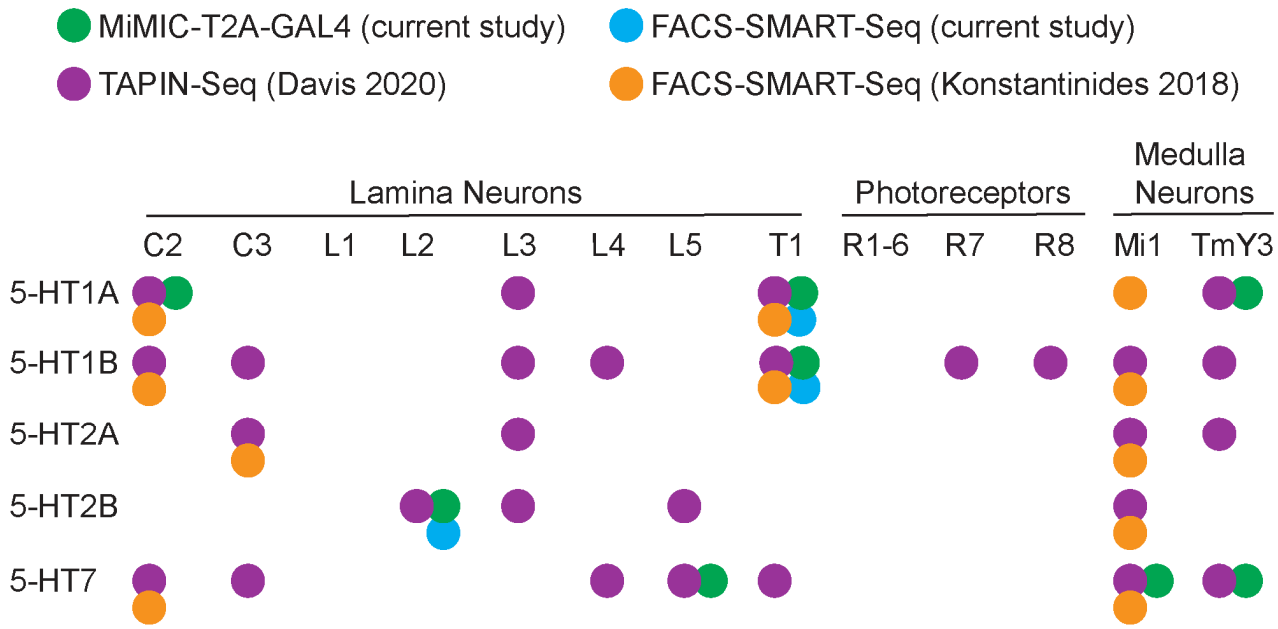

We also reported serotonin receptor expression in lamina glia (Fig 3) [100, 101]. The presence of serotonin receptors in glia immediately adjacent to the basement membrane of the retina raises the possibility that they could regulate photoreceptors cells and perhaps contribute to the indirect regulation of photoreceptor activity [62]. An earlier study also described serotonergic modulation of potassium channels in photoreceptors [62]. However, since the ex vivo preparations used for these experiments may have included other cells or cell fragments it is difficult to determine whether serotonin was acting on receptors expressed in the photoreceptors themselves versus inputs from other cells that regulate photoreceptor activity [20, 62, 102].

Serotonin signaling occurs via G-protein coupled receptors, which can induce immediate or long-term changes in cell physiology. We examined acute responses to serotonin receptor activation by bath applying serotonin onto optic lobe tissue. Consistent with the predicted coupling of 5-HT2B to G_q, we found that L2 neurons respond with a robust increase in calcium measured by GCaMP6f fluorescence (Fig 6B). The simplest explanation for these effects is that 5-HT2B regulates L2 in a cell autonomous manner. However, it remains possible that 5-HT2B expressed in other cells could contribute to the effects we observe. Specific knockdown of 5-HT2B in L2 neurons will be required to address this important issue, but available 5-HT2B RNAi lines have been ineffective in our hands, and additional genetic tools will be needed. We also do not know how either 5-HT2A or 5-HT7 might contribute to the regulation of L2 (Fig 4C). These limitations aside, our data indicate that 5-HT2B plays a role in regulating one of the cells required for most visual processing in the fly and open new avenues of investigation to understand the underlying cellular mechanisms of serotonergic signaling and their effects on circuit output.

In L1 neurons, which do not express serotonin receptors, we unexpectedly observed a large calcium response to serotonin similar to that of L2 neurons (Fig 6C). These data suggest

that L1 cells are indirectly regulated by input from other cells, but further studies will be needed to determine the underlying mechanism. The most likely explanation would be indirect activation of L1 neurons by input from cells that express serotonin receptors either in the optic lobes or perhaps the central brain. For instance, it is possible that the gap junctions that couple L1 and L2 neurons could play a role in the indirect serotonergic regulation of L1 [82]. Alternatively, inputs from neighboring columnar neurons or from wide field neurons that innervate multiple layers of the medulla may play a role. We note that GABAergic C2 neurons [103] express 5-HT1A (Fig 2) and are known to synapse onto L1 in M1 [16]. Likewise, L5 neurons express the 5-HT7 receptor (Fig 2) and reciprocally synapse with L1 neurons in M1 and M5 [16]. Since we used TTX to block sodium channel-based action potentials, inputs to L1 responsible for indirect serotonergic responses are more likely to be based on graded potentials, which have been well documented in the insect brain including photoreceptor cells and other optic lobe neurons [104-106]. Regardless of the underlying mechanism, our data underscore the potential importance of an indirect pathway for serotonergic neuromodulation in this circuit.

In T1 neurons, we were unable to detect any acute changes in baseline calcium or voltage in response to serotonin application (Fig 6E-F) and other probes (e.g., for cAMP) may be necessary to detect the acute response of T1 to serotonin. However, it is also possible that activation of 5-HT1 receptors does not induce any acute physiological response, and that more chronic indices will necessary to detect the potential effects of serotonin on T1 neurons.

Our neuroanatomical data suggest that serotonergic modulation of L2 (and perhaps T1) cells by 5-HT2B and (perhaps 5-HT1A) occurs in layers M1 and M2 of the medulla. Photoreceptors R1-6 synapse onto the dendrites of monopolar cells in the lamina neuropil while the nerve terminals of photoreceptors R7 and R8 and the lamina monopolar neurons synapse onto downstream cells in the medulla neuropil. Multiple neuroanatomical experiments, including data presented here, show that serotonergic boutons are distributed within several layers of the

medulla neuropil including M1, M2, M4 and the inner medulla [45, 47, 84, 85]. By contrast, they are absent from the lamina neuropil. Our observation that molecularly tagged versions of 5-HT2B in L2 neurons and 5-HT1A in T1 neurons are enriched in the medulla neuropil, underscores the likelihood that the medulla rather than the lamina is the most relevant site for serotonergic regulation of these cells. The lamina cortex, which contains the somata of L2 and other monopolar cells is also innervated by serotonergic processes, offering another potential pathway by which serotonin could regulate L2 neurons. However, to our knowledge there is no data in flies in support of the aminergic innervation of cells bodies rather than the neuropil. It is conceivable, however, that serotonin release in the lamina cortex could somehow indirectly regulate L2, perhaps via glia in the lamina cortex that appear to express serotonin receptors (see Fig 3).

We found that both L1 and L2 neurons respond to serotonin with an increase in intracellular serotonin. This suggests that serotonin could modulate visual integration of ON/OFF computations. Additionally, these data suggest a molecular-mechanism for previous observations made in larger insects including serotonin-induced changes field recordings in blowfly representing the output of lamina neurons [70]. Further examination of the serotonin system in the *Drosophila* optic lobe in combination with visual stimulation can be used to test additional hypotheses related to insect vision.

Changes in calcium levels at the nerve terminal suggests that serotonin might regulate inputs to L2 nerve terminals, or perhaps regulate neurotransmitter release, with increased calcium levels possibly driving an increase in neurotransmitter release onto postsynaptic neurons. Dissecting these potential mechanisms will require analysis of neurons downstream of L2, but these too, may undergo direct or indirect serotonergic regulation independent of the effects of serotonin on L2 neurons [17, 107, 108]. Studies in mammals have already begun to dissect the contributions of serotonergic tuning in multiple cells within individual circuits

including the visual system [32, 109-112]. The way in which this information is integrated remains poorly understood. The interactions between receptors expressed on L2 and other neurons in the fly visual system provide a new framework to dissect the mechanism by which multiplexed serotonergic inputs combine to regulate circuit function.

Conclusion

The diversity of serotonin receptors has made it challenging to understand the network level mechanisms by which the modulator serotonin exerts its influence. In this study we identified several cells in the *Drosophila* optic lobe that express specific serotonin receptor subtypes. We also demonstrate that subsets of neurons involved in the initial steps of visual processing are regulated by serotonin through both cell autonomous and non-autonomous mechanisms. In L2 neurons, serotonin signaling via 5-HT2B can regulate baseline calcium changes. We have established a new platform to study the cellular mechanisms by which serotonin and other modulators regulate sensory circuits.

Methods

Fly Husbandry and Genetic Lines

Flies were maintained on a standard cornmeal and molasses-based agar media with a 12:12 hour light/dark cycle at room temperature (22-25°C). All fly strains used in this study are listed in Table 3. Serotonin receptor MiMIC-T2A-GAL4 lines described in [79] were a gift from Herman Dierick (Baylor College of Medicine), and include 5-HT1A-T2A-GAL4^{MI01468}, 5-HT1A-T2A-GAL4^{MI01140}, 5-HT1A-T2A-GAL4^{MI04464}, 5-HT1B-T2A-GAL4^{MI05213}, 5-HT2A-T2A-GAL4 ^{MI0459}, 5-HT2A-GAL4^{MI03299}, 5-HT2B-T2A-GAL4^{MI06500}, 5-HT2B-T2A-GAL4^{MI5208}, 5-HT2B-GAL4^{MI7403}, and 5-HT7-GAL4 ^{MI00215}. L1 and T1 split-GAL4 lines [54], as well as unpublished LexA lines for L1 and T1, were provided by Aljoscha Nern (HHMI/Janelia Research Campus). L. Zipursky

generously provided L2-split-GAL4 and L2-LexA (RRID:BDSC_52510). Yi Rao (Peking University) generously shared 5-HT2B-KO-GAL4 SII (5-HT2B mutant) [91], 5-HT1A::sfGFP [90], and UAS-5-HT2B::sfGFP [91].

Reporter lines include: UAS-mCD8::GFP (RRID:BDSC_5137), UAS-MCFO-1 (RRID:BDSC_64085), UAS-GCaMP6f (RRID:BDSC_42747), UAS-ArcLight (RRID:BDSC_51056), UAS-DenMark, UAS-Syt.eGFP (RRID:BDSC_33064 and RRID:BDSC_33065), and LexAop-mCD8::GFP (RRID:BDSC_32229).

Immunohistochemistry and Imaging

Flies were dissected 5-10 days after eclosion, and equal numbers of males and females were used for all experiments unless otherwise noted. Brains were dissected in ice-cold PBS (Alfa Aesar, Cat#J62036, Tewksbury, MA), then fixed in 4% paraformaldehyde (FisherScientific, Cat#50-980-493, Waltham, MA) in PBS with 0.3% Triton X-100 (Millipore Sigma, Cat#X100, Burlington, MA) (PBST) for one hour at room temperature. After fixation, brains were washed three times with PBST for 10 minutes, then blocked for 30 minutes in PBST containing 0.5% normal goat serum (NGS) (Cayman Chemical, Cat#10006577, Ann Arbor, MA) PBST. Antibodies were diluted in 0.5% NGS/PBST. Primary antibodies were incubated with the tissue overnight at 4°C. The next day, the brains were washed three times with PBST for 10 minutes, then incubated with secondary antibodies for 2 hours in the dark at room temperature. Brains were washed three times with PBST for 10 minutes before mounting.

For frontal mounting, brains were washed with 60% and 80% glycerol (Millipore Sigma, Cat#G5516) and mounted in Fluoromount-G (SouthernBiotech, Cat#0100-01, Birmingham, AL). For dorsal-ventral mounting, brains were fixed in 2% PFA/PBST overnight. The next day, brains were washed three times with PBST. Brains were dehydrated with a series of 10 min ethanol baths of increasing concentrations (30%, 50%, 75%, 95%, 100%, 100%, and 100%). Brains

were then transferred to 100% xylene before mounting in DPX (FisherScientific, Cat#50-980-370).

Serotonin immunolabeling was performed with 1:25 rat anti-serotonin (Millipore Sigma, Cat#MAB352, RRID:AB_11213564), 1:1000 rabbit anti-serotonin (ImmunoStar, Cat#20080, Hudson, WI ,RRID:AB_572263) or 1:1000 goat anti-serotonin (ImmunoStar, Cat#20079, RRID:AB_572262). Where noted, GFP was labeled with 1:250 mouse anti-GFP (Sigma-Aldrich, Cat#G6539, RRID:AB_259941; or, ThermoFisher, Waltham, MA, Cat#A-11120, RRID:AB_221568). Secondary antibodies were used at 1:400 and include: Donkey anti-mouse Alexa Fluor 488, Donkey anti-Rabbit Alexa Fluor 594 or Alexa Fluor Donkey anti-rat 647 (Jackson ImmunoResearch Laboratories, Westgrove, PA, Cat#715-545-151, # 711-585-152, # 712-605-153) or Alexa Fluor 555 (Life Technologies, ThermoFisher, Cat#A-21428).

MultiColor FlpOut (MCFO-1) sparse labeling was induced by heat activation at 37°C for 10-15 minutes at least 2 days prior to dissection as described [86]. Primary antibodies included 1:300 rabbit anti-HA (Cell Signaling Technology, Cat#3724, Danvers, MA, RRID:AB_1549585), 1:150 rat anti-FLAG (Novus, Littleton, CA, Cat#NBP1-06712, RRID:AB_1625982), and 1:400 mouse anti-V5::Dylight-550 (Bio-Rad, Hercules, CA, Cat#MCA1360D550GA, RRID:AB_2687576). Secondary antibodies used for MCFO are listed above.

Imaging was performed with a Zeiss LSM 880 Confocal with Airyscan (Zeiss, Oberkochen, Germany) using a 40x water or 63x oil immersion objective. Post-hoc processing of images was done with Fiji [113] or Adobe Photoshop (Adobe, San Jose, CA) .

FACs and RNA Extraction

L2 and L1 neurons were labeled using split-GAL4 drivers combined with UAS-mCD8::GFP (RRID:BDSC_5137). For RNA-Seq in Fig 4, N=3 T1-LexA samples were tested. For RT-qPCR in Fig 4, we included N=3 T1-split-GLA4 samples and N=3 T1-LexA samples.

Brains were dissected on the day of eclosion and optic lobes were dissociated according to previously published methods [114]. The dissociated optic lobe cells were separated by fluorescence-activated cell sorting (FACS) into GFP-positive and GFP-negative isolates using a BD FACS Aria II high-speed cell sorter in collaboration with the UCLA Jonsson Comprehensive Cancer Center (JCCC) and Center for AIDS Research Flow Cytometry Core Facility (http://cyto.mednet.ucla.edu/home.html). For FACS, each experiment was performed with 18-40 brains, and yielded between 1,700-7,800 GFP^+ cells. RNA was extracted from isolated cells with ARCTURUS® PicoPure® RNA Isolation Kit (ThermoFisher, KIT0204) or RNeasy Plus Micro Kit (QIAGEN, 74034).

RT-qPCR

RNA extracted from FACS isolates was reverse transcribed using SuperScript III (Invitrogen, ThermoFisher, Cat#18080093). RT-qPCR was performed for receptor cDNA using validated primers (Table 4) and SYBR Green Power PCR Mix (Applied Biosystems, ThermoFisher) on an iQ5 real-time qPCR detection system (Bio-Rad). Primers were designed using Primer-Blast (https://www.ncbi.nlm.nih.gov/tools/primer-blast/) or were from the DGRC FlyPrimerBank [115]; oligonucleotides were obtained from Integrated DNA Technologies (Coralville, Iowa). Primer pairs were validated to amplify a single product, verified by a single melting temperature and single band on an electrophoresis gel. The efficiency for each primer pair was between 85-115%. Comparisons between GFP^+ and GFP^- samples were calculated as enrichment (i.e., fold change) using the comparative CT method [116]. A zero value was imputed for samples with no amplification (i.e., no CT value). Raw CT values are shown in Table 1.

RNA-Seq

RNA-Seq was performed using a SMART-Seq protocol adapted from [114, 117, 118]. Libraries were constructed using the SMART-seq v4 Ultra Low-input RNA sequencing kit with Nextera XT (Takara Bio). Paired-end sequencing was conducted by the UCLA genomic core facility (https://www.semel.ucla.edu/ungc/services). After demultiplexing, we obtained between 39-270 (average 105) million reads per sample. Quality control was performed on base qualities and nucleotide composition of sequences. Alignment to the *Drosophila melanogaster* genome (BDGP6) was performed using the STAR spliced read aligner [119] with default parameters. Additional QC was performed after the alignment to examine the following: level of mismatch rate, mapping rate to the whole genome, repeats, chromosomes, and key transcriptomic regions (exons, introns, UTRs, genes). Between 75-85% of the reads mapped uniquely to the fly genome. Total counts of read fragments aligned to candidate gene regions within the reference gene annotation were derived using HTSeq program and used as a basis for the quantification of gene expression. Only uniquely mapped reads were used for subsequent analyses. Following alignment and read quantification, we performed quality control using a variety of indices, including consistency of replicates and average gene coverage. For Fig 4 and Fig 6G, L2 samples were run in two separate sequencing runs and we did not perform corrections for any potential batch effects. Data is shown as Transcripts Per Million (TPMs).

Live Cell Imaging

Calcium imaging was performed as previously described [120]. Briefly, flies were anesthetized at 4°C and placed into a chemically etched metal shim within a larger custom-built fly holder. The fly holder was based on a previously described design (Weir and Dickinson, 2015). The head capsule and the thorax were glued to the metal shim using UV-curable glue (www.esslinger.com). The legs, proboscis and antennae were immobilized using beeswax

applied with a heated metal probe (Waxelectric-1, Renfert). The head capsule was immersed in insect saline (103 mM NaCl, 3 mM KCl, 1.5mM CaCl2, 4 mM MgCl2, 26 mM NaHCO3, 1 mM NaH2PO4, 10 mM trehalose, 10 mM glucose, 5 mM TES, 2 mM sucrose) [121]. A small window on the right rear head capsule was opened using sharp forceps (Dumont, #5SF). Muscles and fat covering the optic lobe were cleared before placing the fly under the 2-photon microscope (VIVO, 3i: Intelligent Imaging Innovations, Denver, CO). Neurons expressing GCaMP6f were imaged at 920-nm using a Ti:Sapphire Laser (Chameleon Vision, Coherent). Images were acquired at 10-20 frames/s for Fig 6 live imaging. Only female flies were used for live imaging experiments.

A custom-built gravity perfusion system was used for bath application of either serotonin or saline control to the fly's exposed optic lobe for Fig 6. For Fig 6, the tissue was first perfused with insect saline containing 1μm tetrodotoxin citrate (TTX) (Alomone Labs, Jerusalem, Israel, Cat#T-550) for at least 5 minutes at 2 mL/min, prior to each recording. TTX remained present throughout the experiment. To examine the effects of serotonin on calcium levels, baseline GCaMP6f fluorescence was recorded for one minute before switching to the second input containing either 100 μM serotonin hydrochloride (Sigma Aldrich, Cat# H9523) or saline alone for an additional five minutes of recording. Due to perfusion tubing length and dead volume, the perfusion switch took approximately 1 min 45 s to reach the tissue. Fig 6 does not show the first minute of the recording, so the solution switch will occur around 45 s on the x axis.

Analysis

Calcium imaging data were analyzed with Matlab R2017a (Mathworks, Natick, MA). Post hoc, recordings were corrected for movement of the brain within the imaging plane using a custom algorithm [122]. Regions of interest (ROIs) were found semi-automatically: first, the median intensity of all pixels across all image frames was found; this value was used as a

threshold and all pixels with mean intensity below the threshold, typically within the image background, were discarded. The 1-D time series of intensity for each remaining pixel was then extracted. K-means clustering was used to identify pixels with similar activity over the course of the experiment: three clusters were identified and the cluster with the highest number of pixels was retained. This reliably identified the pixels within active neurons in the imaging data and aided in identifying preparations with out-of-plane movement, which were discarded. We plotted $\Delta F/F$, defined as $(F_t-F_0)/F_0$, where F_t is the mean fluorescence across all individual terminal ROIs at the indicated time and F_0 is the mean of 30 seconds baseline recording. Approximately half of the bath application recordings showed oscillations in activity due to slow, periodic movement of the brain at around 0.04 Hz; we applied a second-order notch filter at this frequency with a bandwidth of 0.005 Hz to remove these oscillations.

Replicates

Each biological replicate (N) represents one fly, except for RT-qPCR and RNA-Seq (Fig 4) where each biological replicate was pooled from 18+ flies. RT-qPCR experiments include 3 technical replicates, which are averaged to represent a single biological replicate. Animals from at least 3 crosses were used for each experiment. Data for each experiment was collected over 2-6 months in at least 3 experiments. No outliers were removed from any data set. Live imaging recordings with too much movement were excluded and not analyzed.

Data Availability

The RNA-Seq data (raw and processed files) are available on the Gene Expression Omnibus (GSE154085).

Tables

Table 1. RT-qPCR Threshold Cycle (CT) measurements and calculated enrichment for FACS-isolated T1, L2, and L1 samples as shown in Fig 4. Enrichment (i.e., fold change) was calculated for cDNA from GFP-labeled cell isolates relative to pooled, unlabeled optic lobe cell isolates using the comparative CT method.

Target	T1 - Sample 1 (T1-split-GAL4)			T1 - Sample 2 (T1-split-GAL4)			T1 - Sample 3 (T1-split-GAL4)		
	GFP+ Ave CT	GFP- Ave CT	Enrichment	GFP+ Ave CT	GFP- Ave CT	Enrichment	GFP+ Ave CT	GFP- Ave CT	Enrichment
RP49	39.7	32.6		43.2	37.5		38.1	32.4	
5HT1A	40.3	36.1	7.29	43.3	41.7	17.1	39.4	36.1	5.64
5HT1B	41.4	36.1	3.65	44.9	41.9	6.48	41.2	36.9	2.73
5HT2A	ND	46.9		ND	ND		ND	47.0	
5HT2B	ND	38.2		ND	44.1		ND	39.5	
5HT7	ND	37.1		QC Failure			ND	37.5	
Target	T1 - Sample 4 (T1-LexA)			T1 - Sample 5 (T1-LexA)			T1 - Sample 6 (T1-LexA)		
	GFP+ Ave CT	GFP- Ave CT	Enrichment	GFP+ Ave CT	GFP- Ave CT	Enrichment	GFP+ Ave CT	GFP- Ave CT	Enrichment
RP49	37.0	32.5		37.9	31.9		38.6	33.6	
5HT1A	39.4	37.3	5.16	39.9	36.7	6.70	39.9	37.7	6.74
5HT1B	38.7	36.6	5.04	39.7	36.0	4.80	39.5	37.3	7.14
5HT2A		46.9			46.8			47.4	
5HT2B		39.0			38.3			39.7	
5HT7		37.3			36.2			37.9	
Target	L2 - Sample 1			L2 - Sample 2			L2 - Sample 3		
	GFP+ Ave CT	GFP- Ave CT	Enrichment	GFP+ Ave CT	GFP- Ave CT	Enrichment	GFP+ Ave CT	GFP- Ave CT	Enrichment
RP49	43.7	37.2		40.9	35.1		40.0	32.8	
5HT1A	ND	42.7		ND	38.2		45.9	36.0	0.152
5HT1B	ND	41.0		ND	37.7		45.7	36.6	0.262
5HT2A	49.8	49.1	57.8	ND	ND		ND	46.9	
5HT2B	48.7	43.8	3.12	45.8	42.4	5.49	45.8	38.7	1.07
5HT7	ND	42.9		44.8	40.0	2.13	ND	37.7	
Target	L2 - Sample 4			L2 - Sample 5					
	GFP+ Ave CT	GFP- Ave CT	Enrichment	GFP+ Ave CT	GFP- Ave CT	Enrichment			
RP492	40.1	34.1		38.4	34.3				
5HT1A	ND	35.9		ND	40.2				
5HT1B	45.2	36.4	0.151	ND	40.1				
5HT2A	ND	ND		ND	ND				
5HT2B	44.8	37.7	0.495	ND	43.3				
5HT7	41.6	36.7	2.266	45.0	40.8	0.99			
Target	L1 - Sample 1			L1 - Sample 2			L1 - Sample 3		
	GFP+ Ave CT	GFP- Ave CT	Enrichment	GFP+ Ave CT	GFP- Ave CT	Enrichment	GFP+ Ave CT	GFP- Ave CT	Enrichment
RP49	45.3	36.7		42.4	38.0		41.9	32.8	
5HT1A	ND	36.4		ND	41.5		ND	37.5	
5HT1B	ND	36.8		ND	41.9		45.7	37.1	1.416
5HT2A	ND	41.2		ND	ND		ND	ND	
5HT2B	ND	40.4		ND	43.6		ND	40.6	
5HT7	ND	37.5		ND	45.1		ND	39.1	
Target	L1 - Sample 1			L1 - Sample 2			L1 - Sample 3		
	GFP+ Ave CT	GFP- Ave CT	Enrichment	GFP+ Ave CT	GFP- Ave CT	Enrichment	GFP+ Ave CT	GFP- Ave CT	Enrichment
RP49	45.7	40.2		43.8	33.3		42.1	40.2	
ShakB	42.1	39.7	8.44	38.2	34.3	95.7	45.2	40.6	0.147
Target	L2 - Sample 1			L2 - Sample 2			L2 - Sample 3		
	GFP+ Ave CT	GFP- Ave CT	Enrichment	GFP+ Ave CT	GFP- Ave CT	Enrichment	GFP+ Ave CT	GFP- Ave CT	Enrichment
RP49	40.9	38.2		40.9	32.4		40.3	35.6	
ShakB	36.1	37.1	13.0	36.1	33.3	52.7	39.5	37.2	4.98
Target	T1 - Sample 1			T1 - Sample 2			T1 - Sample 3		
	GFP+ Ave CT	GFP- Ave CT	Enrichment	GFP+ Ave CT	GFP- Ave CT	Enrichment	GFP+ Ave CT	GFP- Ave CT	Enrichment
RP49	38.3	32.3		39.4	31.8		39.4	33.6	
ShakB	43.5	33.1	0.0181	44.8	31.7	0.0226	44.9	33.3	0.0181

Table 2 . RNA-Seq Serotonin Receptor TPMs, averages and standard deviations.

	5-HT1A	**5-HT1B**	**5-HT2A**	**5-HT2B**	**5-HT7**
T1	165	271	0.028	0.024	0.034
T1	231	305	7.53	0.000	0.000
T1	150	257	0.000	0.082	0.000
Average	182	278	2.52	0.035	0.011
STDEV	43.1	24.8	4.34	0.042	0.019
	5-HT1A	5-HT1B	5-HT2A	5-HT2B	5-HT7
L2	0.006	40.9	13.3	190	8.96
L2	38.3	22.5	1.13	45.9	34.2
L2	10.4	28.3	2.99	158	3.90
Average	16.2	30.5	5.80	131	15.7
STDEV	19.8	9.40	6.55	75.6	16.2

Table 3. Fly strains used in this study.

Fly Line	**Source**
5-HT1A-T2A-GAL4 MI01468	H. Dierick (Baylor)
5-HT1A-T2A-GAL4 MI01140	H. Dierick (Baylor)
5-HT1A-T2A-GAL4 MI04464	H. Dierick (Baylor)
5-HT1B-T2A-GAL4 MI05213	H. Dierick (Baylor)
5-HT2A-T2A-GAL4 MI0459	H. Dierick (Baylor)
5-HT2A-GAL4 MI03299	H. Dierick (Baylor)
5-HT2B-T2A-GAL4 MI5208	H. Dierick (Baylor)
5-HT7-GAL4 MI00215	H. Dierick (Baylor)
T1-spGAL4	A. Nern (Janelia)
L2-spGAL4	L. Zipursky (UCLA)
L1-spGAL4	A. Nern (Janelia)
T1-LexA	A. Nern (Janelia)
UAS-mCD8::GFP	RRID:BDSC_5137
UAS-MCFO-1	RRID:BDSC_64085
UAS-GCaMP6f	RRID:BDSC_42747
UAS-ArcLight	RRID:BDSC_51056
5-HT1A::GFP	Y. Rao (Peking U.)
UAS-5-HT2B::GFP	Y. Rao (Peking U.)

Table 4. RT-qPCR primer sequences and mRNA (cDNA) target information.

Fly Line	Source
5-HT1A-T2A-GAL4 MI01468	H. Dierick (Baylor)
5-HT1A-T2A-GAL4 MI01140	H. Dierick (Baylor)
5-HT1A-T2A-GAL4 MI04464	H. Dierick (Baylor)
5-HT1B-T2A-GAL4 MI05213	H. Dierick (Baylor)
5-HT2A-T2A-GAL4 MI0459	H. Dierick (Baylor)
5-HT2A-GAL4 MI03299	H. Dierick (Baylor)
5-HT2B-T2A-GAL4 MI5208	H. Dierick (Baylor)
5-HT7-GAL4 MI00215	H. Dierick (Baylor)
T1-spGAL4	A. Nern (Janelia)
L2-spGAL4	L. Zipursky (UCLA)
L1-spGAL4	A. Nern (Janelia)
T1-LexA	A. Nern (Janelia)
UAS-mCD8::GFP	RRID:BDSC_5137
UAS-MCFO-1	RRID:BDSC_64085
UAS-GCaMP6f	RRID:BDSC_42747
UAS-ArcLight	RRID:BDSC_51056
5-HT1A::GFP	Y. Rao (Peking U.)

Chapter 2: The Role of 5-HT2B in *Drosophila* Visual Processing in the Lamina

Introduction

Sensory systems rely on neuromodulators, such as serotonin, to add flexibility and dynamic range to information processing circuits. In the mammalian visual cortex, serotonin regulates the balance of excitation and inhibition [32], cellular plasticity [109, 123-125], and response gain [34, 126]. In some cases, the contribution of individual receptor subtypes is known; for example, in the mammalian retina, serotonin signaling reduces GABAergic amacrine cell input to retinal ganglion cells (RGCs) via 5-HT1A [112] and can modulate the response of RGCs to visual stimuli [127]. However, for most sensory circuits, the manner in which serotonin receptor activation is integrated to regulate information processing remains poorly understood.

The *Drosophila melanogaster* visual system is a tractable genetic model to study visual neuron activity and the regulation of visual circuits [49, 50]. In *Drosophila* light-sensitive photoreceptors signal to intrinsic monopolar neurons in the lamina neuropil [20]. Lamina monopolar cells L1 and L2 are first-order interneurons that feed into pathways discriminating light “ON” (i.e., increase in luminance) and light “OFF” (i.e., decrease in luminance) stimuli respectively [53, 82]. L1 and L2 neurons respond to changes in luminance in a physiologically identical manner [128-130], while downstream neurons in the medulla transform this information to discriminate ON versus OFF stimuli [53]. Further processing occurs in the lobula and lobula plate to mediate higher-order computations for both motion and contrast detection [53, 56, 131].

Serotonergic neurons innervate the optic ganglia [45, 65-69] and we (Chapter 1) and others [58, 87] have shown that serotonin receptors are expressed in many cells throughout the visual system. Previous studies indicate that serotonin has an impact on both cellular activity and visual behavior in insects [62, 63, 70, 71]. In the blowfly, serotonin altered electrophysiological field recordings representing the combined output of lamina neurons [70]. In the honeybee, single cell recordings in motion-sensitive lobula neurons showed that serotonin

signaling reduces background activity, directional selectivity, and the amplitude of field potentials evoked by moving stripes [63]. In the house fly, serotonin and other neurotransmitters regulate rhythmic size changes in L1 and L2 terminals in the medulla [132] and in *Drosophila*, serotonin was shown to modulate the voltage dependence of potassium channels in photoreceptors [62]. Despite extensive evidence that serotonin modulates the insect visual system, the molecular mechanisms responsible for these effects and the potential contributions of specific subtypes of serotonin receptors remain unclear.

The cellular effects of serotonin signaling are highly complex and the precise effects of serotonin receptor activation in specific cells are difficult if not impossible to predict and necessitate the use of functional assays to complement expression studies. Although previous studies suggest that serotonin affects visual processing, and two recent studies have reported serotonin receptor expression in visual neurons [58, 87], to our knowledge there is no information on the functional effect(s) of any serotonin receptor in any cell within the insect visual system. In this work, we show how a specific serotonin receptor, 5-HT2B, regulates visual responses in L2 lamina monopolar cells, which are critical for the initiation of visual information processing. Expansion of the approach demonstrated here to other receptors and cells may be used to generate a comprehensive picture of serotonergic neuromodulation within a well-defined sensory circuit.

Results

To explore the possibility that serotonergic neuromodulation plays a role in visual processing, we tested whether exogenous serotonin alters visually induced calcium transients in L2 neurons. We used GCaMP6f to record and compare calcium transients in flies receiving saline or serotonin perfusion. Previous studies using voltage indicators found that L2 neurons depolarize in response to dark flashes and hyperpolarize in response to light flashes [129].

Similarly, calcium-indicator recordings showed that intracellular calcium increased in the dark and decreased in the light in [128]. Brief light or dark flashes induce bi-phasic calcium transients [129] that enable analysis of calcium kinetics. For this reason, we used brief dark or light flashes to test whether serotonin might alter the magnitude or kinetics of visually induced calcium transients in L2 terminals. Flies were suspended over an LED arena (see Ch 1 Fig 6A) and either a light or dark flash of the entire LED screen (100 ms) was presented at 5 s intervals. Between each flash, the screen showed an intermediate brightness level, indicated as grey in Fig 1A. One-minute "epochs" consisting of 12 flashes of randomly shuffled polarity were presented six times for each trial (Fig 1A). The first 60 s epoch was recorded in saline alone, followed by a switch to either saline with 100 μM serotonin or saline alone during epoch 2 (Fig 1A). Unlike the experiments shown in Ch 1 Fig 6, we did not include TTX in the perfusion solutions because we did not want to affect neuronal communication in any way that might interfere with the response to visual stimuli. Performing additional further experiments in the absence of TTX was also important to rule out the possibility TTX was responsible for the effects seen in Ch 1 Fig 6.

Dark flashes induced a large increase in calcium that returned to baseline within ~1 second as previously described [129] (Fig 1B). The amplitude of the dark flash induced calcium transients increased over the time course of the experiment for animals receiving either serotonin or saline (Fig 1B). To compare differences between the serotonin and saline control groups and the potential effects of serotonin over the time course of the experiment, we quantified three calcium transient variables: amplitude (1C), the time required for decay from the peak to a subsequent minimum (1C'), and the slope of the decay (1C''). To facilitate the direct comparison of results obtained during perfusion with saline alone versus saline followed by serotonin, we first calculated the average for each variable prior to serotonin exposure

measured during epoch-1. We then subtracted the epoch 1 baseline from each epoch, effectively setting the initial value of each plot to 0 for epoch 1 in Fig 1C-C".

Fig 1C shows the change in calcium transient amplitude, calculated as the difference between the pre-stimulus ΔF/F and the peak ΔF/F, relative to epoch 1. We did not detect a difference between the serotonin and saline groups. Fig 1C' quantifies the decay time from peak amplitude, calculated as the time (s) between the peak ΔF/F and the subsequent minimum ΔF/F, relative to epoch 1. We detected a modest but statistically significant ($p=0.0036$ by Repeated Measures ANOVA) increase in the decay time of the dark flash response in animals perfused with serotonin versus saline alone. In Fig 1C" we quantify the change in the slope of the decay relative to epoch 1; we did not detect a difference in slope between flies treated with serotonin versus saline (Fig 1C").

Light flashes induced a transient decrease in GCaMP6f fluorescence, followed by a secondary sustained rebound (Fig 1D) as previously reported [129]. To analyze calcium transients induced by light flashes, we quantified three variables: the magnitude of the initial calcium decrease relative to the pre-stimulus baseline (Fig 1E), the time from minimal to maximal ΔF/F (Fig 1E'), and the slope of this rebound (Fig 1E''). Baseline values obtained for the response to light flashes in epoch 1 were subtracted from each epoch to set the initial value of each variable to 0 for epoch 1 in the plots in Fig 1E-E". We did not observe any significant differences between saline and serotonin groups when calculating the magnitude of the initial downward deflection (Fig 1E), the time from minimal to maximal ΔF/F (Fig 1E') or the slope of the rebound (Fig 1E"). In sum, serotonin drove a robust increase in intracellular calcium levels of L2 neurons in wildtype flies, regardless of the presence (Ch 1 Fig 6) or absence (Fig 1) of TTX. We also detected a modest, but statistically significant effect of serotonin on the kinetics, but not the amplitude, of the GCaMP6f response of L2 to a dark flash (Fig 1C'). We did not detect any effect of serotonin on the response of L2 to a light flash in 5-HT2B +/+ flies.

Fig 1. Serotonin mediates L2 neuron visually induced calcium transient kinetics. L2-split-GAL4 was crossed to UAS-GCaMP6f to monitor calcium transients following 100-ms light or dark flashes. The optic lobe was initially perfused with saline alone during a 60 s baseline recording designated as “epoch 1”. The solution was then switched to either saline with serotonin or saline control after 105 s, with the switch occurring during epoch 2. (**A**) A sample recording with serotonin perfusion following the initial baseline is shown in the upper panel. Light or dark stimuli (A, middle panel) were flashed at random every 5 s for 6 min. To visualize changes in the response to light and dark flashes in L2, data from each 60 s epoch was binned (see epochs 1-6 in A, lower panel). (**B**) Response to dark flashes. Color coded traces representing each 60 s epoch are shown for flies receiving saline (left panel, cyan to blue) or serotonin perfusion (right panel, yellow to red). In both groups, L2 terminals responded to a dark flash with a strong increase in GCaMP6f fluorescence before returning to baseline. (**C-C”**) Analysis of dark flash response from panel B. For plotting each variable shown in C, the average value for the epoch 1 baseline was subtracted; epoch 1 is therefore always set to 0 in panel C-C”. (**C**) The change in the amplitude of the calcium transient (the difference between pre-stimulus ΔF/F and maximum ΔF/F) relative to epoch 1 is shown in (C) and did not differ between flies exposed to saline versus serotonin. (**C’**) The change in the time (s) to reach a minimum ΔF/F following the maximum ΔF/F relative to epoch 1 is shown in (C’) and was significantly longer ($p \leq 0.01$**) in serotonin-perfused flies compared to saline controls. (**C”**) The change in the slope of the decay from maximum ΔF/F to minimum ΔF/F relative to epoch 1 was not different between the saline and serotonin groups. (**D**) Response to light flashes. When a light flash was presented in control experiments, L2 cells responded with a decrease in GCaMP signal followed by a large sustained rebound. Color coded traces representing each 60 s epoch for saline (left panel, cyan to blue) and serotonin (right panel, yellow to red) are shown. (**E-E”**) Analysis of light flash response from panel D. For plotting each variable shown in E, the average value for the epoch 1 baseline was subtracted; epoch 1 is therefore always set to 0 in panel E-E” as in panel C-C”. (**E**) The change in the amplitude of the initial decrease in calcium (the difference between pre-stimulus ΔF/F and the subsequent minimum ΔF/F) relative to epoch 1 is shown in (E) and was not different between the saline and serotonin groups. (**E’**) The change in the time to reach a maximum ΔF/F (time, s) relative to epoch 1 and (**E”**) the change in the slope of the rebound relative to epoch 1 was not significantly differ between serotonin versus saline controls. Recordings in B-E represent, N=14 and N=20 individual flies perfused with serotonin or saline respectively. Shaded areas show mean +/- SEM. Comparisons are two-way repeated measures ANOVA (brackets show interactions between time and genotype) and Sidak’s multiple comparisons tests, $p \leq 0.05$ *, $p \leq 0.01$**, $p \leq 0.001$***, $p \leq 0.0001$****.

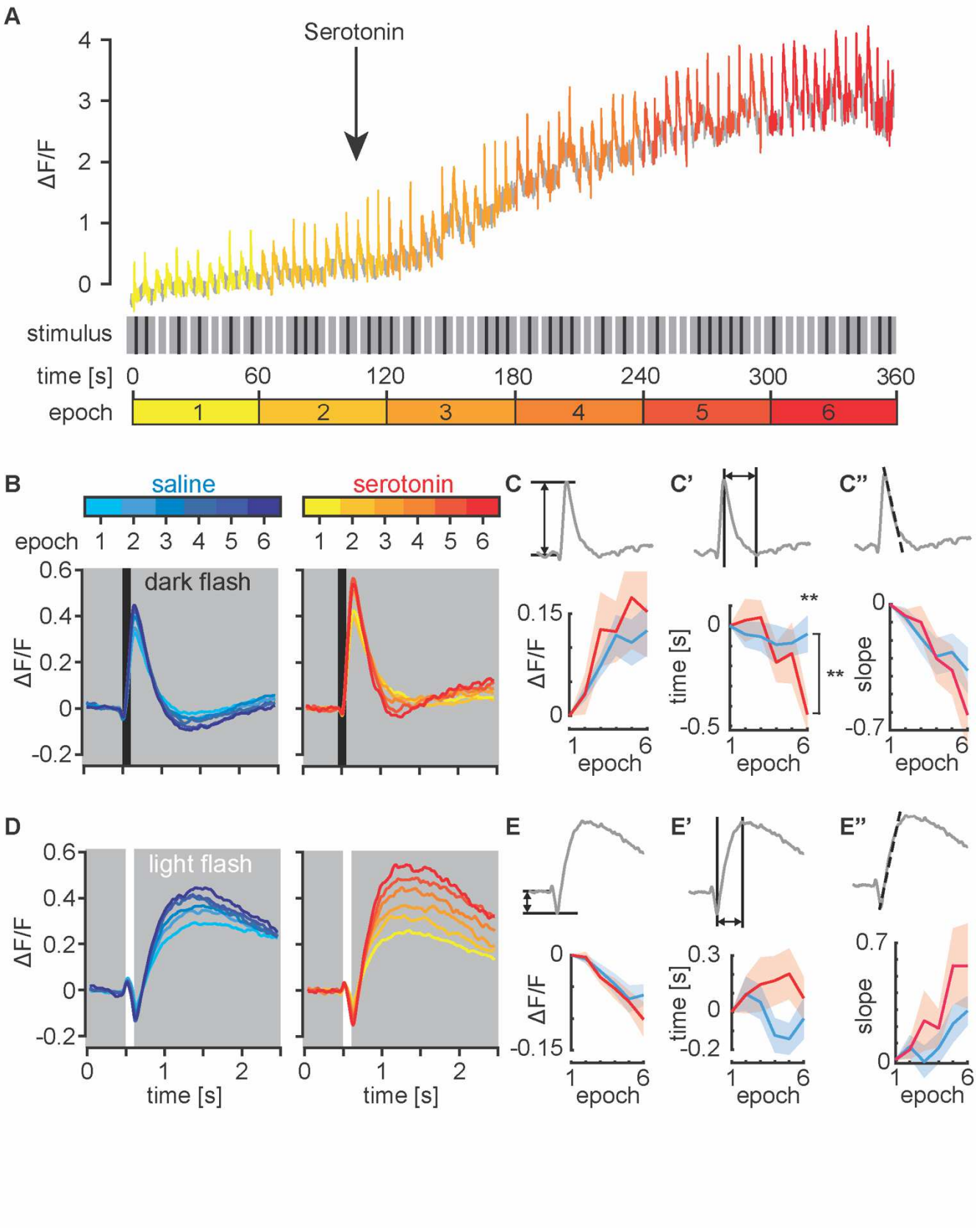
A
Serotonin
ΔF/F
4
3
2
1
0
stimulus
time [s]
0
60
120
180
240
300
360
epoch
1
2
3
4
5
6
B
saline
serotonin
epoch 1 2 3 4 5 6
1 2 3 4 5 6
dark flash
ΔF/F
0.6
0.4
0.2
0
-0.2
C
C'
C"
0.15
0
ΔF/F
time [s]
0
-0.5
slope
-0.7
**
**
1
6
epoch
D
light flash
ΔF/F
0.6
0.4
0.2
0
-0.2
0
1
2
time [s]
E
E'
E"
0
-0.15
ΔF/F
0.3
0
-0.2
time [s]
0.7
0
slope
1
6
epoch

Effects of a 5-HT2B receptor mutant

Since 5-HT2B is expressed in L2 neurons and is predicted to use calcium as a second messenger we hypothesized that it would mediate the response of L2 neurons to serotonin. In flies expressing wild type 5-HT2B we observed a robust serotonin-mediated increase in basal intracellular calcium (Ch 1 Fig 6, with TTX in the perfusion solution and Fig 1, without TTX in the perfusion solution). We next examined whether loss of 5-HT2B would blunt the gradual increase in basal calcium we observed in flies exposed to serotonin (Fig 2B). As a negative control for experiments using the 5-HT2B homozygous mutants (-/-) we used heterozygous siblings (+/-) in which one wild type allele of 5-HT2B was present (Fig 2B). Similar to 5-HT2B +/+ flies (Fig 2A), 5-HT2B heterozygous controls perfused with serotonin showed a gradual increase in basal calcium levels over the six-minute time course of the experiment (Fig 2B). In contrast, in the 5-HT2B -/- mutant, the basal calcium signal was nearly flat over the time course of the experiment ($p=0.0024$ by two-tailed Wilcoxon rank sum test). To more specifically reduce the expression of 5-HT2B in L2, we also tested available RNAi transgenes directed against 5-HT2B but did not detect a significant effect (data not shown). We therefore cannot rule out indirect cell non-autonomous effects from 5-HT2B expression in other cell types. However, the simplest explanation for the observed results is that activation of 5-HT2B in L2 neurons generates a gradual increase in cytosolic calcium.

We next examined whether loss of 5-HT2B would alter the calcium transients in L2 neuron terminals following light or dark flashes. We hypothesized that loss of 5-HT2B would block any changes in the kinetics of the calcium response seen with serotonin perfusion (see Fig 1C'). We also reasoned that a mutation in the serotonergic signaling pathway might provide a "sensitized genetic background" to enhance the detection of serotonin's functional effects. As a negative control, we used heterozygous siblings (5-HT2B +/-). We again graphed averages for each epoch after subtraction of the average for epoch-1. For dark flashes, we plotted the

change in amplitude of the increase from pre-stimulus ΔF/F to the maximum ΔF/F relative to epoch 1 (Fig 2D), the change in the time between the peak ΔF/F and the subsequent minimum ΔF/F relative to epoch 1 (Fig 2D'), and the change in slope of the decay relative to epoch 1 (Fig 2D"). As we observed in 5-HT2B +/+ flies (see Fig 1C'), perfusion of 5-HT2B +/- heterozygous controls with serotonin led to a gradual reduction in the time required for L2 terminals to reach a minimum after responding to a dark flash (Fig 2D'). In striking contrast, in 5-HT2B -/- homozygous loss of function flies, the time between the peak and the subsequent minimum (Fig 2D'), and the slope of the decay (Fig 2D") remained unchanged over the course of the experiment and continuous perfusion with serotonin. In sum, the 5-HT2B mutation ablated the serotonin-dependent change in the kinetics of the L2 response to dark flashes. The effects on amplitude (Fig 2D) were not statistically significant between the 5-HT2B -/- mutant and heterozygous controls.

To compare how 5-HT2B +/- and 5-HT2B -/- flies responded to light flashes, we calculated the change in the amplitude of the initial downward deflection from the pre-stimulus baseline relative to epoch 1 (Fig 2F), the change in the time from minimal to maximal ΔF/F relative to epoch 1 (Fig 2F') and the change in the slope of the rebound relative to epoch 1 (Fig 2F"). The 5-HT2B +/- heterozygotes preparations showed a progressive increase in the magnitude of the initial downward deflection (Fig 2F); strikingly, this progression was absent in 5-HT2B -/- mutants and the difference between the time course of the heterozygotes and homozygotes was highly significant ($p \leq 0.0001$) (Fig 2F). Similarly, the change in both the time required for ΔF/F to progress from a post-stimulus minimum to secondary maximum (Fig 2F') and the slope of the rebound relative to epoch 1 were significantly different (Fig 2F"). Together, the differences between 5HT2B +/- and 5-HT2B -/- in the response to a dark flash (Fig 2D-D") and these data strongly suggest that 5-HT2B mediates the effects of serotonin on the response

of L2 neurons to at least one type of visual stimulus, although we cannot yet conclude whether this occurred in a cell-autonomous manner.

Fig 2. 5-HT2B mediates L2 neuron response serotonin. (**A**) L2-split-GAL4>GCaMP6f was used to monitor intracellular calcium in L2 terminals. The optic lobe was initially perfused with saline alone and was then switched to either saline with serotonin or saline control after 105 s. Serotonin perfusion (in the absence of TTX) induced an increase in baseline calcium in 5-HT2B +/+ lines receiving serotonin compared to saline controls. (**B**) Mutant 5-HT2B-"KO"-GAL4 flies (5-HT2B -/-) were combined with UAS-GCaMP6f to monitor calcium changes in L2 terminals. Homozygous (5-HT2B -/-) and heterozygous (5-HT2B +/-) flies both received serotonin perfusion. The serotonin-mediated baseline increase was seen in 5-HT2B +/- flies, as in wild type flies, but was not observed in 5-HT2B -/- flies. (**C-F**) Homozygous (5-HT2B -/-) and heterozygous (5-HT2B +/-) 5-HT2B- "KO" -GAL4 flies expressing UAS-GCaMP6f were used to record calcium transients following brief light or dark flashes. The preparation was initially perfused with saline alone during a 60 s baseline recording designated as epoch 1 and the solution was then switched to saline with serotonin after 105 s, with the switch occurring in epoch 2. (**C**) Response to dark flashes. Traces representing each 60 s epoch (yellow to red) are shown for 5-HT2B +/- (left) and 5-HT2B -/- (right). All preparations received serotonin perfusion. In both groups, dark flashes induced a strong, transient increase in GCaMP6f fluorescence that returned to baseline. Dark-flash calcium transient amplitude increased over the course of the experiment for 5-HT2B +/- flies, but this was not seen in 5-HT2B -/- flies. (**D-D"**) Analysis of dark-flash data from panel C. For plotting each variable shown in D-D", the average value for epoch 1 was subtracted; epoch 1 is therefore always set to 0. (**D**) The change in the amplitude of the maximum calcium transient (the difference between pre-stimulus ΔF/F and maximum ΔF/F) relative to epoch 1 is shown. (**D'**) The change in the time to reach a minimum ΔF/F following the maximum ΔF/F of the calcium transient relative to epoch 1 was significantly decreased in 5-HT2B +/- flies compared to 5-HT2B -/- flies in which this period was essentially unchanged over the time course of the experiment. (**D"**) The change in the slope of the decay relative to epoch 1 was significantly decreased in 5-HT2B +/- flies compared to 5-HT2B -/- flies; it appeared essentially unchanged for 5-HT2B -/- flies over the course of the experiment. (**E**) Response to light flashes. When a light flash was presented, L2 cells responded with a decrease in the GCaMP6f signal followed by a large sustained rebound. Responses for 5-HT2B +/- (left) and 5-HT2B -/- (right) flies are shown. (**F-F"**) Analysis of light flash data from panel E. For plotting each variable shown in F-F", the average value for the epoch 1 baseline was subtracted; epoch 1 is therefore always set to 0 as in panels D-D". (**F**) The change in the amplitude of the light flash induced a calcium decrease (calculated as the difference between the pre-stimulus ΔF/F and minimum ΔF/F) relative to epoch 1 that was significantly enhanced over the course of the experiment in 5-HT2B +/- flies relative to 5-HT2B -/- flies. (**F'**) The change in the time to reach a maximum relative to epoch 1 was significantly decreased in 5-HT2B -/- flies compared to the response of 5-HT2B +/- flies which appeared unchanged. (**F"**) The change in the rebound slope relative to epoch 1 increased significantly in 5-HT2B +/- flies relative to 5-HT2B -/- flies. For (A), N=14 serotonin and N=20 saline exposed flies were tested. For (B-F), N=13 5-HT2B +/- and N=15 5-HT2B -/- flies, all receiving serotonin, were tested. Shaded areas show mean +/- SEM. Comparisons in (D, F) are two-way repeated measures ANOVA (brackets show interactions between time and genotype) and Sidak's multiple comparisons tests, $p \leq 0.05$ *, $p \leq 0.01$**, $p \leq 0.001$***, $p \leq 0.0001$****.

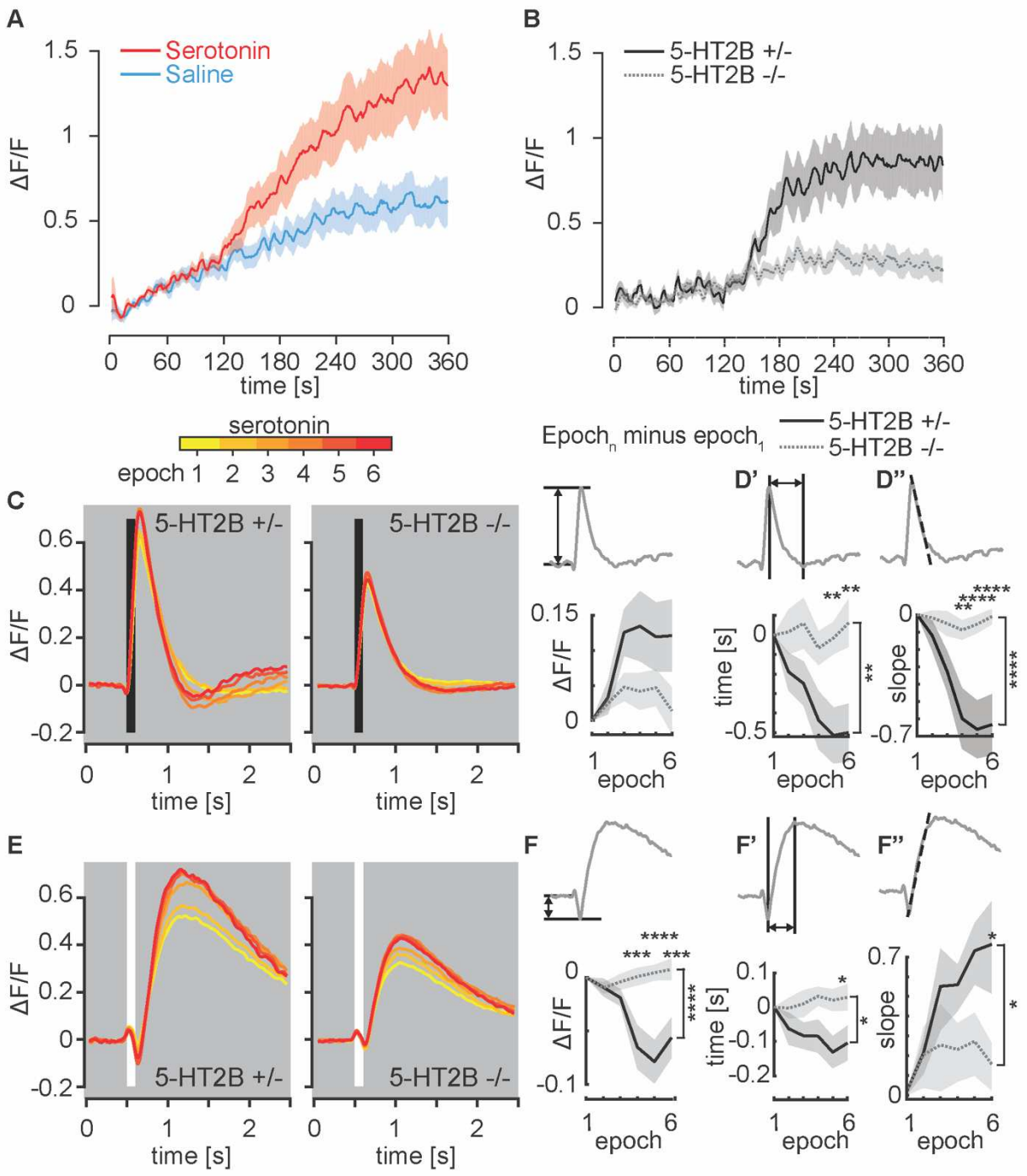
A
Serotonin
Saline
ΔF/F
time [s]
B
5-HT2B +/-
5-HT2B -/-
serotonin
epoch 1 2 3 4 5 6
Epoch$_n$ minus epoch$_1$
C
5-HT2B +/-
5-HT2B -/-
D'
D''
E
F
F'
F''
slope
epoch

Discussion

Serotonin modulation occurs by activation of multiple receptors and associated second messenger cascades [7, 9]. Understanding how serotonergic signaling tunes circuit activity requires functional experiments to determine the effects on specific cells as well as mapping the cellular and subcellular cites of individual receptors. To develop the fly visual system as a new molecular genetic model to study serotonergic neuromodulation we have mapped the expression of the five *Drosophila* serotonin receptors in a subset of experimentally tractable cells in the lamina (Ch 1) and used live imaging to determine their potential function (Fig 1-2). To our knowledge, these represent the first functional data for serotonergic neuromodulation of the *Drosophila* visual system with the exception of a single report in 1995 [62].

We demonstrated that L2 lamina monopolar cells express 5-HT2B using a combination of MiMIC-based reporter lines, RT-PCR and RNA-Seq in Chapter 1. All of these techniques indicated that 5-HT2B is expressed in L2 neurons, which are involved in motion [82, 99] and contrast vision [56]. Our data are consistent with a recent transcriptional study of optic lobe neurons, which also reported high probability of 5-HT2B in L2 cells [58].

In Chapter 1, we found that L2 neurons respond with a robust increase in calcium measured by GCaMP6f fluorescence (Ch 1 Fig 6) in the presence of TTX. In this work, we performed a similar experiment in the absence of TTX and also observed an increase in basal intracellular calcium (Fig 1A). We also found that the serotonin-induced increase in basal calcium was dramatically reduced in 5-HT2B -/- flies (Fig 2B). The simplest explanation for these effects is that 5-HT2B regulates L2 in a cell autonomous manner. However, it remains possible that 5-HT2B expressed in other cells could contribute to the effects we observe. Specific knockdown of 5-HT2B in L2 neurons will be required to address this important issue, but available 5-HT2B RNAi lines have been ineffective in our hands, and additional genetic tools will be needed. We also do not know how either 5-HT2A or 5-HT7 might contribute to the

regulation of L2 (Ch 1 Fig 4). These limitations aside, our data indicate that 5-HT2B plays a role in regulating one of the cells required for most visual processing in the fly and open new avenues of investigation to understand the underlying cellular mechanisms of serotonergic signaling and their effects on circuit output.

In *Drosophila*, L1 and L2 neurons detect changes in luminance and together are necessary for the full complement of motion vision. Both neurons receive synaptic input from photoreceptors, and respond to luminance changes with graded potentials, depolarizing in dark conditions and hyperpolarizing in light [128-130]. These two neurons feed forward into parallel pathways to enable further visual processing such as motion and contrast detection [53, 55, 56]. The modulation of visually induced calcium transients in L2 following serotonin application (Fig 1-2) suggests a role for serotonin in potentiating the response of L2-dependent visual processing pathways [129]. Our data also suggest a molecular-mechanism for previous observations made in larger insects including serotonin-induced changes field recordings in blowfly representing the output of L1 and L2 [70] and honeybee motion detection in the lobula [63]. Further examination of the serotonin system in the *Drosophila* optic lobe using the same approaches we employed here can be used to test additional hypotheses related to insect vision.

We detected serotonin-mediated differences in the kinetics of L2 neurons' response to visual stimuli in wild type flies, but also measured differences in amplitude when comparing 5-HT2B mutants to heterozygous controls. Without inducible knock-down/out experiments, it is not possible to rule out developmental effects of the 5-HT2B mutant on the L2 neurons. The effects of serotonin on calcium signaling in L2 cells were more apparent in the 5-HT2B mutant than wild type flies (Fig 1-2). In particular, we were able to detect serotonin-mediated differences in the kinetics of L2 neurons' response to visual stimuli in wild type flies, but also detected differences in amplitude when comparing 5-HT2B mutants to heterozygous controls.

Without inducible knock-down/out experiments, it is not yet possible to rule out developmental effects of the 5-HT2B mutant on the activity of L2 neurons. Regardless, we suggest that mutation of 5-HT2B generated a useful sensitized genetic background to uncover effects of serotonin that were not detectable in wild type flies.

We speculate that endogenous serotonergic release and activation of 5-HT2B blunted the effects of bath-applied serotonin, making it difficult to detect changes in amplitude due to saturation. A saturation point for neuromodulatory input is critical for circuit stability as has been described previously [2, 133, 134]. In the absence of 5-HT2B, neither endogenous nor exogenous serotonin would have an effect, thus increasing our ability to detect the full spectrum of serotonin's actions. Similarly, the effects of serotonin on pathways mediated by other receptors in the visual system may only become detectable using additional receptor mutants. More generally we suggest that our data underscore the power of a genetically sensitized background to fully understand the mechanisms underlying the aminergic regulation of circuit function. This approach is well developed in the fly compared to mammalian systems and we suggest that it can significantly enhance future analyses of serotonergic neuromodulation.

While the precise function of serotonin signaling in L2 neurons or elsewhere in the fly visual system remains unknown, it may allow neurons to adapt to changes in visual stimuli. We observed stimulus repetition adaptation [102] in flies with endogenous serotonin signaling, but this was completely absent in 5-HT2B mutants even with serotonin perfusion. Likewise, we are struck by the similarities between the changes we observe during perfusion with serotonin and the graded responses of lamina neurons to stimuli of increasing contrast [129].

Conclusion

The diversity of serotonin receptors has made it challenging to understand the network level mechanisms by which this modulator exerts its influence. In L2 neurons, serotonin

signaling via 5-HT2B can regulate baseline calcium changes as well as the amplitude and kinetics of visually induced calcium transients. We have established a new platform to study the cellular mechanisms by which serotonin and other modulators regulate sensory circuits.

Methods

Fly Husbandry and Genetic Lines

Flies were maintained on a standard cornmeal and molasses-based agar media with a 12:12 hour light/dark cycle at room temperature (22-25°C). All fly strains used in this study are listed in Table 1. L. Zipursky generously provided L2-split-GAL4. Yi Rao (Peking University) generously shared 5-HT2B-KO-GAL4 SII (5-HT2B mutant) [91]. UAS-GCaMP6f (RRID:BDSC_42747) was obtained from Bloomington *Drosophila* Stock Center at Indiana University (Bloomington, IN, USA).

Live Cell Imaging

Calcium imaging was performed as previously described [120]. Briefly, flies were anesthetized at 4°C and placed into a chemically etched metal shim within a larger custom-built fly holder. The fly holder was based on a previously described design (Weir and Dickinson, 2015). The head capsule and the thorax were glued to the metal shim using UV-curable glue (www.esslinger.com). The legs, proboscis and antennae were immobilized using beeswax applied with a heated metal probe (Waxelectric-1, Renfert). The head capsule was immersed in insect saline (103 mM NaCl, 3 mM KCl, 1.5mM CaCl2, 4 mM MgCl2, 26 mM NaHCO3, 1 mM NaH2PO4, 10 mM trehalose, 10 mM glucose, 5 mM TES, 2 mM sucrose) [121]. A small window on the right rear head capsule was opened using sharp forceps (Dumont, #5SF). Muscles and fat covering the optic lobe were cleared before placing the fly under the 2-photon microscope (VIVO, 3i: Intelligent Imaging Innovations, Denver, CO). Neurons expressing GCaMP6f were

imaged at 920-nm using a Ti:Sapphire Laser (Chameleon Vision, Coherent). Images were acquired at 25-30 frames/s for Fig 1-2 live imaging. Only female flies were used for live imaging experiments.

For precise control of perfusion solutions, we used a programmable valve controller (VC-6, Warner Instruments, Hamden, CT). During the first minute, and prior to imaging, the tissue was perfused with saline for a baseline recording. At the end of the first minute, a valve controller (VC-6, Warner Instruments, Hamden, CT) activated by a TTL signal switched the perfusion to either saline with 100 μM serotonin or saline alone; imaging then continued for an additional five minutes, for a total of one baseline set and five post-switch sets of visual stimuli. The perfusion switch took approximately 45 s to reach the tissue using the programmable valve system.

Visual Stimulus

Visual stimuli were shown using an arena composed of 48 eight by eight-pixel LED panels, at 470 nm (Adafruit, NY, NY). The panels were assembled into a curved display that extends 216° along the azimuth and ±35° in elevation. Each pixel subtended an angle of 2.2° on the retina at the equatorial axis. To prevent spurious excitation of the imaging photomultiplier tubes, three layers of blue filter (Rosco no. 59 Indigo) were placed over the LED display.

Each stimulus consisted of a brief increment (light flash) or decrement (dark flash) of the entire display for 100 ms, before returning to a mid-intensity brightness for 4.9 s. Images were acquired at 25-30 frames/s for Fig 1-2 visual stimulation experiments. Stimuli were presented in sets of six bright and six dark flashes randomly shuffled for each minute of the experiment. Responses were then pooled for each minute.

Analysis

Calcium imaging data were analyzed with Matlab R2017a (Mathworks, Natick, MA). Post hoc, recordings were corrected for movement of the brain within the imaging plane using a custom algorithm [122]. Regions of interest (ROIs) were found semi-automatically: first, the median intensity of all pixels across all image frames was found; this value was used as a threshold and all pixels with mean intensity below the threshold, typically within the image background, were discarded. The 1-D time series of intensity for each remaining pixel was then extracted. K-means clustering was used to identify pixels with similar activity over the course of the experiment: three clusters were identified and the cluster with the highest number of pixels was retained. This reliably identified the pixels within active neurons in the imaging data and aided in identifying preparations with out-of-plane movement, which were discarded.

For visual response experiments (Figs 1-2), pixels within the remaining cluster were automatically divided into groups corresponding to individual L2 terminals using a watershed transform. The mean intensity within each ROI was found for each image frame to produce a single time-series for the entire experiment, and the time-series for all terminal ROIs within an individual animal were then averaged. For Fig 2, ROIs of L2 terminals were first identified automatically, as above, then manually selected individually according to layer position because the 5-HT2B GAL4 SII mutant line labeled other cells in addition to L2 neurons.

Approximately half of the bath application recordings showed oscillations in activity due to slow, periodic movement of the brain at around 0.04 Hz; we applied a second-order notch filter at this frequency with a bandwidth of 0.005 Hz to remove these oscillations. For the visual stimulus experiments (Fig 1-2), we plotted $\Delta F/F$, defined as $(F_t-F_0)/F_0$, where F_t is the mean fluorescence across all individual terminal ROIs at the indicated time and F_0 is the mean of 30 seconds of non-consecutive baseline activity between stimulus presentations during epoch 1 at the beginning of the experiment and prior to the change in perfusion (Fig 1A). For the stimulus

response plots (Fig 1B, 1D, 2C, 2E), we found the average ΔF/F time-series within each epoch for each fly after subtracting the average pre-stimulus baseline activity level (0.5 s preceding each flash stimulus) from each time-series, so that all responses started aligned at 0 ΔF/F. For further analysis (Fig 1C, 1E, 2D, 2F, left), we found the changes in response amplitude across epochs, defined for the dark stimulus presentation (top) as the difference between the pre-stimulus baseline and the maximum ΔF/F value that occurred up to 1.75 s after cessation of the 0.1 s flash, and for the light stimulus (bottom) as the minimum ΔF/F value that occurred in the same period of time. For each epoch, we subtracted the value of the responses during epoch 1 at the beginning of the experiment and prior to the change in perfusion, in order to find the change in amplitude relative to epoch 1. We followed a similar procedure for the analysis of peak-peak time (Fig 1C, 1E, 2D, 2F, middle), defined as the length of time between the minimum and maximum □F/F values that occurred within 1.75 s after cessation of the 0.1 s flash. The slope of the transient decay was also calculated (Fig 1C, 1E, 2D, 2F, right).

For the visual experiments we examined the baseline changes in fluorescence (Fig 2A-B) after removing responses to the visual stimuli using a series of second-order notch filters at 0.19-0.21 Hz and 0.38-0.42 Hz.

Statistical Tests

For Fig 1 (C, E) and Fig 2 (D, E) comparisons are two-way repeated measure ANOVA (brackets show interactions between time and genotype) and Sidak's multiple comparisons tests, p≤0.05 *, p≤0.01**, p≤0.001***, p≤0.0001****. These tests were performed using Graphpad Prism Software (San Diego, CA). Differences in baseline calcium shown in Fig 2A-B were calculated by two-tailed Wilcoxon rank sum tests in Matlab R2017a.

Replicates

Each biological replicate (N) represents one fly. Animals from at least 3 crosses were used for each experiment. Data for each experiment was collected over 2-6 months in at least 3 experiments. No outliers were removed from any data set. Live imaging recordings with too much movement were excluded and not analyzed.

Tables

Table 1. Animal strains used in this study.

Fly Line	**Source**
L2-sp-GAL4	L. Zipursky (UCLA)
5-HT2B-GKO-GAL4	Y. Rao (Peking U.)
UAS-GCaMP6f	RRID:BDSC_42747

Chapter 3: The Serotonin System in *Drosophila* Optic Lobe

Introduction

Serotonergic neurons broadly innervate the optic ganglia of *Drosophila* and other insects, including the majors neuropils: lamina, medulla, lobula, and lobula plate [45, 65-69]. In Chapter 1, we found that L2 neurons express 5-HT2B and T1 neurons express both 5-HT1A and 5-HT1B (Ch 1 Fig 4). Subcellular mapping with 5-HT2B::GFP and 5-HT1A::GFP showed enrichment in layer M2 of the medulla (Ch 1, Fig 5). Serotonin neurons also project to M2, which may serve as a hub for serotonergic modulation in the visual system.

Ultrastructural studies in the fly visual system have established a connectome for many neurons in the lamina and medulla including L1, L2 and T1 neurons [15-20, 57]. However, the ultrastructure of serotonergic processes in the optic lobe of *Drosophila* is not known. In both mammals and insects, serotonin can be released extrasynaptically through volume transmission [135, 136] or through synaptic sites [21-23, 66, 137]. Synapses compartmentalize rapid cell-to-cell exchange of chemical messengers between neurons. The synaptic cleft confined space enables rapid changes in neurotransmitter concentrations, controlled by neurotransmitter release, reuptake and metabolism. The synapse also physically limits the communication to specific pre- and post-synaptic partners.

Neurotransmission outside of a synaptic cleft, referred to as volume transmission, allows for neurotransmitter diffusion away from the release site, enabling activation of receptors on many distant neurons. In both synaptic and volume transmission, concentration gradients play a large role in determining the intensity of the signal received by post-synaptic neurons. Serotonin neurons receive input from other cells to influence serotonin release and concentration gradients, but they also rely on their own activity to regulate extracellular levels of serotonin.

Serotonergic neurons modulate extracellular serotonin in part by serotonin re-uptake via the serotonin transporter (SERT), which controls the intensity and duration of the serotonin

signal. Concentration gradients are also mediated by serotonin release, which is partially regulated by feedback from receptors. Autoreceptors detect extracellular neurotransmitter concentrations and provide negative feedback to regulate release. In mammals, serotonergic neurons express 5-HT1A and 5-HT1B as pre-synaptic autoreceptors. Previous work has shown that mammalian 5-HT1A is localized to somatodendritic compartment, while 5-HT1B localized in pre-terminal axons [138, 139].

In *Drosophila*, a previous study sequenced serotonergic neurons and found elevated 5-HT1A, 5-HT1B and 5-HT7 transcripts [140] and another study reported co-labeling between 5-HT1B-GAL4 and serotonin-immunoreactive cell bodies in the subesophageal ganglion [141]. Consistent with these findings, we report additional evidence that 5-HT1A, 5-HT1B and 5-HT7 are expressed by serotonergic neurons and we speculate that these receptors function as autoreceptors. *Drosophila* provide a tractable model for molecular and genetic studies. This model system, combined with the tools developed in Chapter 4, will be useful to examine the role of autoreceptors in serotonin system function in health, disease, and therapeutic response.

Results

Serotonergic neurons likely signal through volume transmission in the optic lobe

Our previous findings suggested that M2 may be a hub for serotonergic modulation of L2 and T1 neurons, which both express serotonin receptors and arborize in M2.To further explore the nature of these neurons in the medulla, we co-expressed the dendritic marker DenMark [142] and the synaptic marker synaptotagmin:eGFP (syt.eGFP) in these cells. In both T1 and L2, we detected strong labeling with both syt.eGFP and DenMark in M2, underscoring the ability of the projections of L2 and T1 to both transmit and receive chemical signals here (Fig 1). For serotonergic neurons, we observed Denmark labeling in all regions where anti-serotonin immunoreactive boutons were present, including M2 in the medulla (Fig 1).

Fig 1. Pre- and post-synaptic labeling with DenMark and syt.eGFP. L2, T1 and SerT-GAL4 lines were crossed with UAS-DenMark, UAS-syt.eGFP to label dendrites and presynaptic boutons, respectively. (**A-A”’**) L2-split-GAL4 and (**B-B”’**) T1-split-GAL4 specified neurons show overlapping syt.eGFP (green) and DenMark (magenta) labeled compartments in the medulla. (**C-C”’**) SerT-GAL4 (BSC 38764) was used to express DenMark (magenta). Serotonin immunoreactivity is shown in green. N=3-4 brains per condition. Scale bars are 25 μm (A-C) and 10 μm for all other panels.

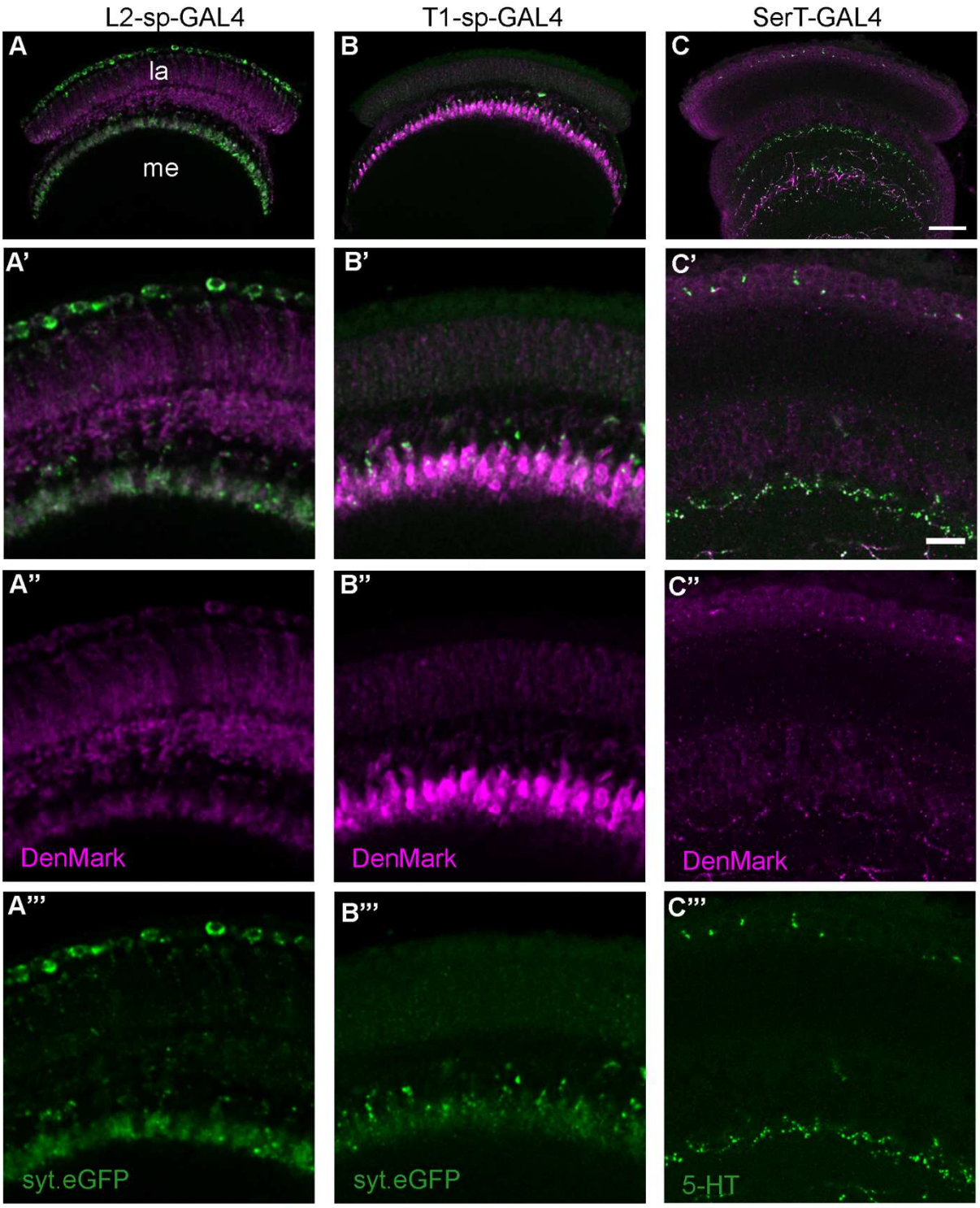
L2-sp-GAL4
T1-sp-GAL4
SerT-GAL4
A
la
me
B
C
A'
B'
C'
A''
B''
C''
DenMark
DenMark
DenMark
A'''
B'''
C'''
syt.eGFP
syt.eGFP
5-HT

When we bath applied serotonin onto the optic lobe we observed increased intracellular calcium in L2 arborizations in M2 (Ch 1 Fig 4). For this reason, we thought it was possible that serotonergic neurons might have direct synaptic contact with L2 in this region. We used sybGRASP to identify potential synaptic connections between serotonergic projections and the arborizations of L2 and T1 in M2 [143]. As a positive control to validate the use of sybGRASP in detecting interactions within M2, we examined previously established ultrastructural connectivity of L2 onto T1 neurons in the medulla [17, 18] and obtained a robust signal (Fig 2). With *SERT*-specified neurons presynaptic to L2, T1 or L1 neurons we did not detect any reconstituted GFP in the medulla (Fig 2) and only occasional GFP puncta in the lamina cortex (3 out of 7 brains, see Fig 2).

Although it remains possible that serotonergic synapses onto L1, L2 or T1 neurons were present but undetectable, this seems unlikely since we observed a robust signal in parallel experiments in which the post-synaptic component of GFP was expressed in serotonergic cells (see Fig 2). Together, these data suggest that most signaling from serotonergic neurons onto L2 and T1 neurons is likely to occur through a non-synaptic mechanism, similar to the extensive use of volume transmission in the mammalian brain [144, 145] as reported for most other aminergic synapses in mammalian systems [136, 144-146].

Fig 2. **Serotonergic neurons do not show sybGRASP signal with postsynaptic T1, L2 or L1 neurons in the medulla.** SybGRASP was used to probe whether serotonergic neurons make synaptic contacts onto L2, T1 or L1 neurons. (**A-A'**) SybGRASP was observed with L2 split-GAL4 presynaptic to T1-LexA in M2. The dashed inset in (**A**) is shown in (**A'**). (**B-E**) A *SERT*-GAL4 driver was used to express the pre-synaptic portion of GFP in serotonergic neurons and LexA drivers were used to express the postsynaptic portion of GFP in L2 (**B-C**) L1 (**D**) or T1 (**E**) as indicated. No sybGRASP signal was detected in the medulla when serotonin neurons were presynaptic to L2 (**B**) however, occasional sparse GFP puncta (arrowhead) were visible in the lamina (**C**). When *SERT*-GAL4 neurons were presynaptic to L1 (**D**) or T1 (**E**) neurons, we did not detect a sybGRASP signal in either the lamina or medulla. All tissue was labeled with primary antibodies to both 5-HT (magenta) and GFP (green). N=7-10 brains. Scale bars are 15 μm (**A**, **B**, **D-E**); 5 μm (**A"** and **C-C"**).

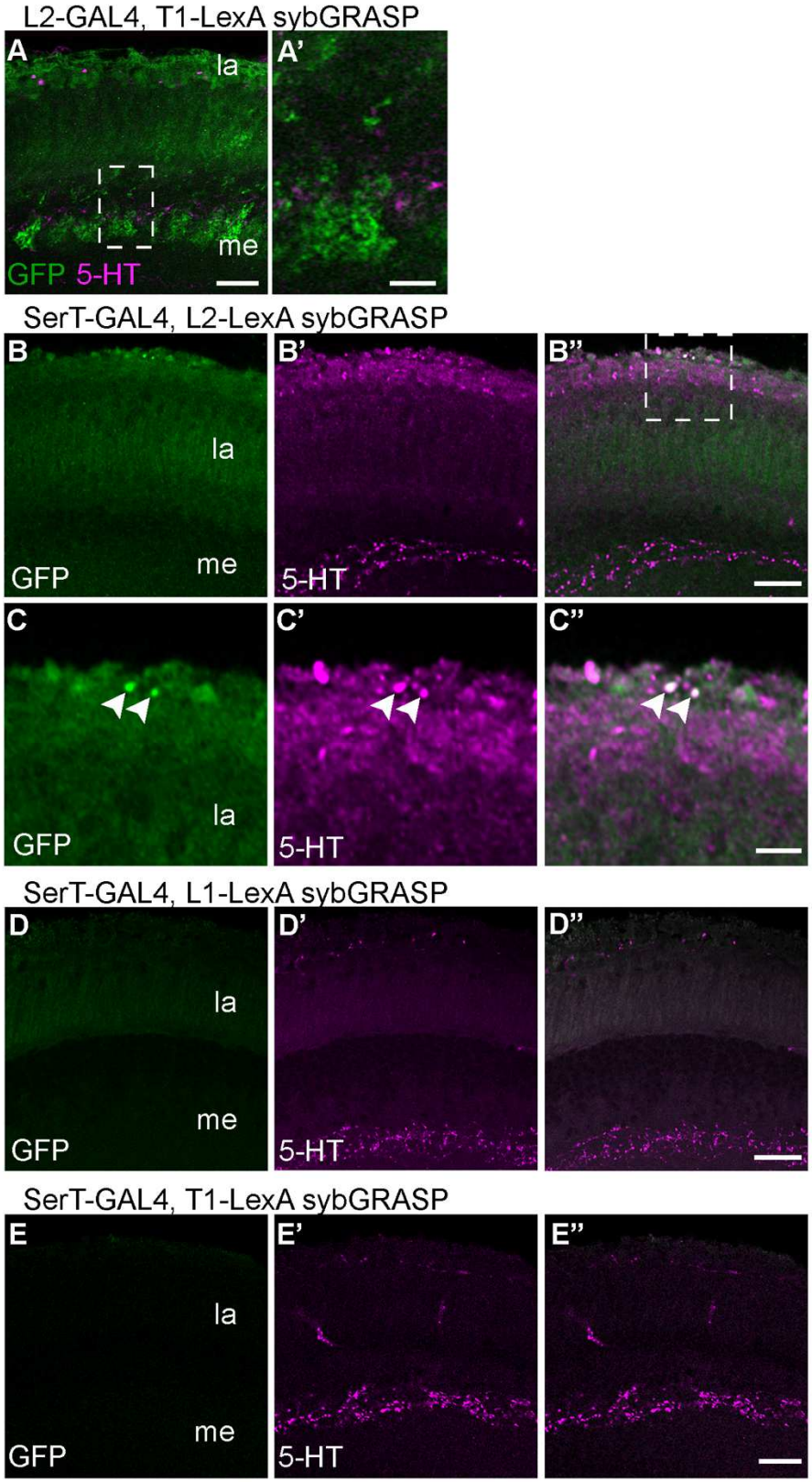
L2-GAL4, T1-LexA sybGRASP
A
la
me
GFP 5-HT
A'
SerT-GAL4, L2-LexA sybGRASP
B
la
GFP
me
B'
5-HT
B''
C
la
GFP
C'
5-HT
C''
SerT-GAL4, L1-LexA sybGRASP
D
la
me
GFP
D'
5-HT
D''
SerT-GAL4, T1-LexA sybGRASP
E
la
me
GFP
E'
5-HT
E''

5-HT1A, 5-HT1B and 5-HT7 are expressed in *Drosophila* serotonergic neurons

The visual system does not contain any serotonergic cell bodies, rather projections from neurons with cell bodies in the accessory medulla and central brain innervate the optic lobes. Immunolabeling for serotonergic boutons can be observed within all optic ganglia neuropil as well as the lamina cortex (Ch 1 Fig 1) [44-48]. Sparse labeling with 5-HT1B-T2A-GAL4 >MCFO co-labeled with serotonin immunolabeled boutons in the inner medulla (iM), medulla layer 4 (M4), and lobula (lo) (Fig 3). We speculate that these processes are serotonergic and expresses 5-HT1B as an autoreceptor, consistent with the fact that 5-HT1B>GFP co-labeled with serotonin-immunoreactive cells in serotonergic cluster LP2 (arrowhead in Ch 1 Fig 1G). Furthermore, we observed co-localization of 5-HT1B-MiMIC-T2A-GAL4 and 5-HT1A-MiMIC-T2A-GAL4>GFP with several anti-serotonin immunolabeled cell bodies in the central brain as shown in Fig 3 and Fig 4. Although we did not comprehensively map all putative serotonin autoreceptors in the central brain, we used serotonin cell mapping described in [44, 45, 47, 48] to identify 5-HT1B+ cell clusters as LP2 (Cb1), PLP (LP1), and PMP, (Fig 3) and 5-HT1A+ serotonergic clusters as PLP (LP1), SEL, AMP and PMP (Fig 4).

Fig 3. Serotonin receptor 5-HT1B co-labels with serotonin immunoreactive sites in optic lobe and cell bodies in the central brains. Anti-serotonin immunolabeling (magenta) was used to identify serotonergic cells and projections in (A-F). (**A-A”**) Serotonin receptor MiMIC-T2A-GAL4 lines were crossed to UAS-MCFO-1 to label individual cells. Using 5-HT1B-MiMIC-T2A-GAL4>MCFO (green), we observed co-labeling between MCFO-labeled cells and serotonergic boutons (magenta) processes in the inner medulla (iM), medulla layer 4 (M4), and lobula (lo). (**B**) A schematic of the fly brain with dashed lines showing the approximate anatomical locations for (A-A”). (**C-C”**) Anti-serotonin immunolabeling (magenta) co-labeled with 5-HT1B-MiMIC-T2A-GAL4>UAS-mCD8::GFP labeled cell bodies in the central brain. 5-HT1B-labeled kenyon cells (KC) are labeled for anatomical reference in (C”). (**D**) The approximate anatomical location for images in (C-C”) are shown in the boundaries of the dashed line. Serotonin co-labeling was performed in N=6 brains for 5-HT1B>MCFO (A-A”) and N=5 for 5-HT1B>GFP (C-C”). Scale bars are 20 μm.

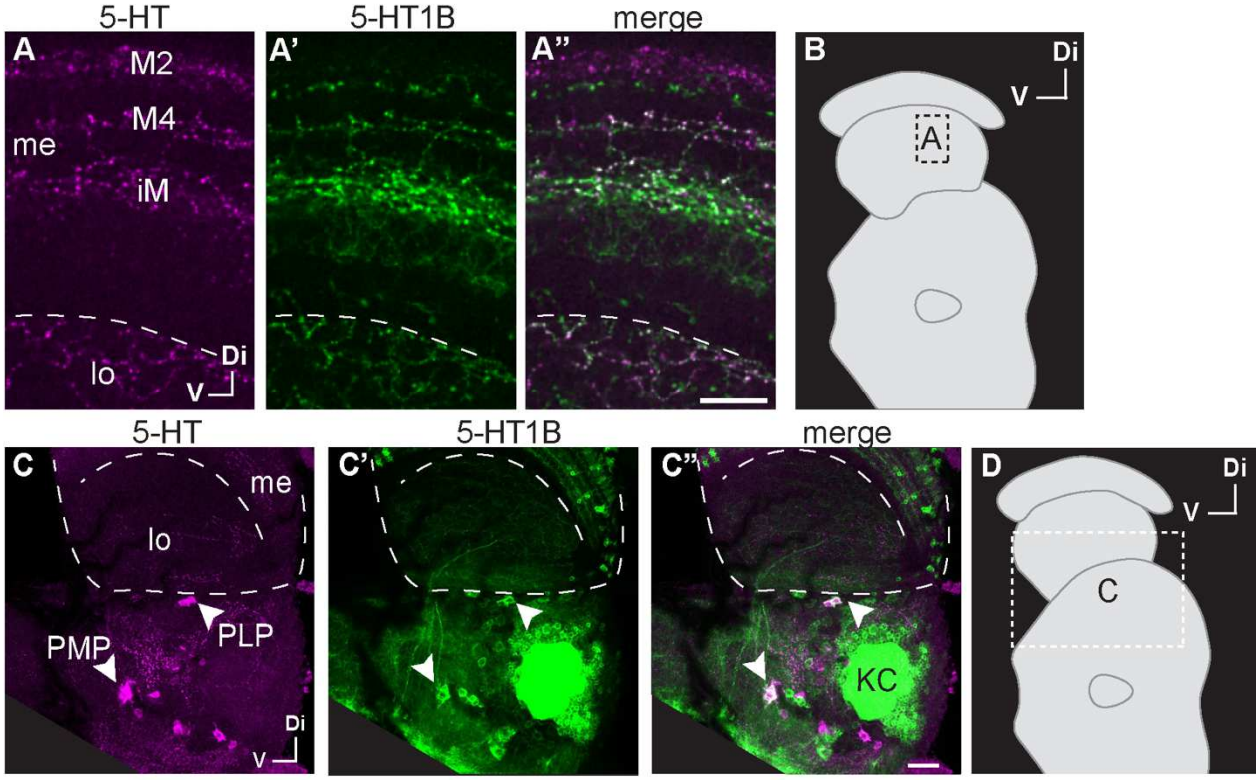

Fig 4. Serotonin receptor 5-HT1A co-labels with serotonin immunoreactive sites in optic lobe and cell bodies in the central brain. (**A**) Schematic of the optic lobe neuropils—lamina (la), medulla (me), lobula (lo) and lobula plate (lp)—and serotonergic PLP cells. (**B-B”**) 5-HT1A-MiMIC-T2A-GAL4 driving UAS-mCD8::GFP (green) was co-stained with anti-serotonin immunolabeling (magenta) to map potential autoreceptors to specific cell clusters in the central brain. PLP neurons co-labeling for 5-HT1A labeling and anti-serotonin immunolabeling are indicated by the arrowhead. (**C-E**) Anterior to posterior images taken in the same brain show several serotonergic cell clusters expressing 5-HT1A (labeled at arrowheads). 5-HT1A-labeled mushroom body (MB) and kenyon cells (KC) are labeled for anatomical reference in (**C** and **E**). (**F**) A cartoon of the fly brain with dashed lines to indicate the approximate anatomical location for (C-E). Scale bars are 20 μm and N=6.

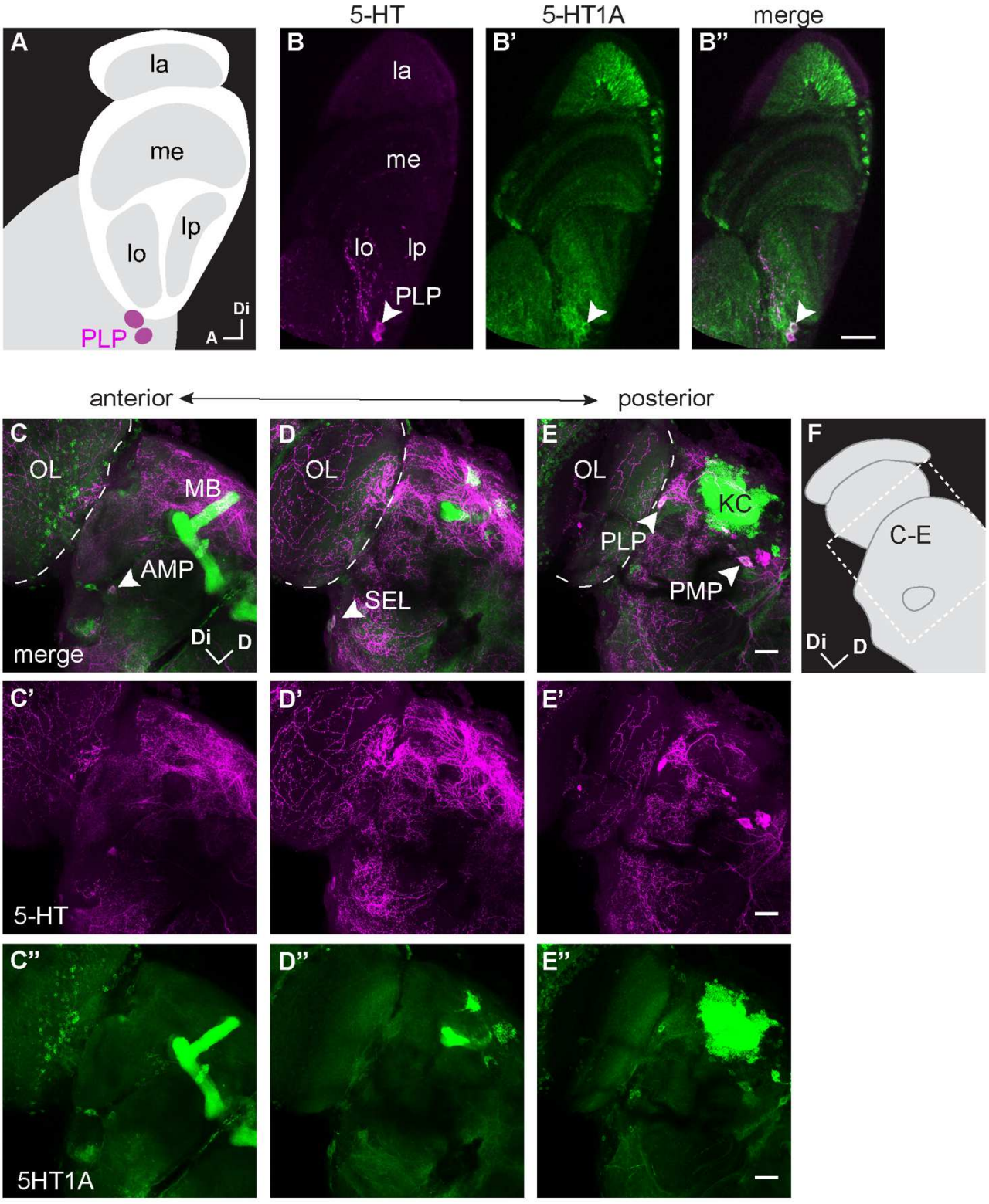
5-HT
5-HT1A
merge
A
la
me
lo
lp
PLP
Di
A
B
B'
B''
anterior
posterior
C
OL
MB
AMP
merge
Di
D
D
SEL
E
KC
PLP
PMP
F
C-E
C'
5-HT
C''
5HT1A
D'
D''
E'
E''

In MCFO experiments, we observed 5-HT1A and 5-HT7 labeled projections into the lamina cortex (Fig 5A-B) and in some cases these co-labeled with anti-serotonin (Fig 5C-D). We also observed co-labeling between 5-HT7-labeled projections and anti-serotonin in the medulla, lobula, and lobula plate neuropils (Fig 5E-E"). We have not yet identified that serotonergic cell body that expressed 5-HT7. In Ch 1 Fig 5 we observed co-labeling between 5-HT1A::GFP constructs and anti-serotonin signal in the medulla, suggesting that 5-HT1A traffics to serotonin release sites. While we have not pursued functional studies of presynaptic serotonergic neurons in this report, the integration of imaging studies in both serotonergic neurons and post-synaptic neurons represents a future goal to assess the interplay between auto- and post-synaptic receptors in visual circuits.

Fig 5. Serotonin Autoreceptors are expressed throughout the Optic Lobe. (**A-D**) Serotonin receptor MiMIC-GAL4 lines were crossed to UAS-MCFO-1 to label individual cells. Anti-serotonin labeling (magenta) was used to identify serotonergic cells. (**A**) A 5-HT1A>MCFO labeled central brain neuron innervates the lamina cortex and the most distal area of the laminar neuropil (**B**) Similarly, 5-HT7>MCFO labeled projections could be seen in the lamina. (**C**) The 5-HT1A>MCFO projection (green) into the lamina co-stains with anti-serotonin (magenta). (**D-E**) 5-HT7>MCFO processes (green) co-labeled with anti-serotonin (magenta) in the lamina (la) and iM, M4, lo (lobula), and lobula plate (lp). Scale bars are 20 μm. N=13 5-HT7>MCFO and N=31 5-HT1A>MCFO brains were imaged per receptor subtype. Projections into the lamina from the central brain were observed N=6 for 5-HT1A>MCFO (A) and N=3 for 5-HT7>MCFO (B). Co-localization with anti-serotonin was observed in N=3 (C), N=3 (D-E).

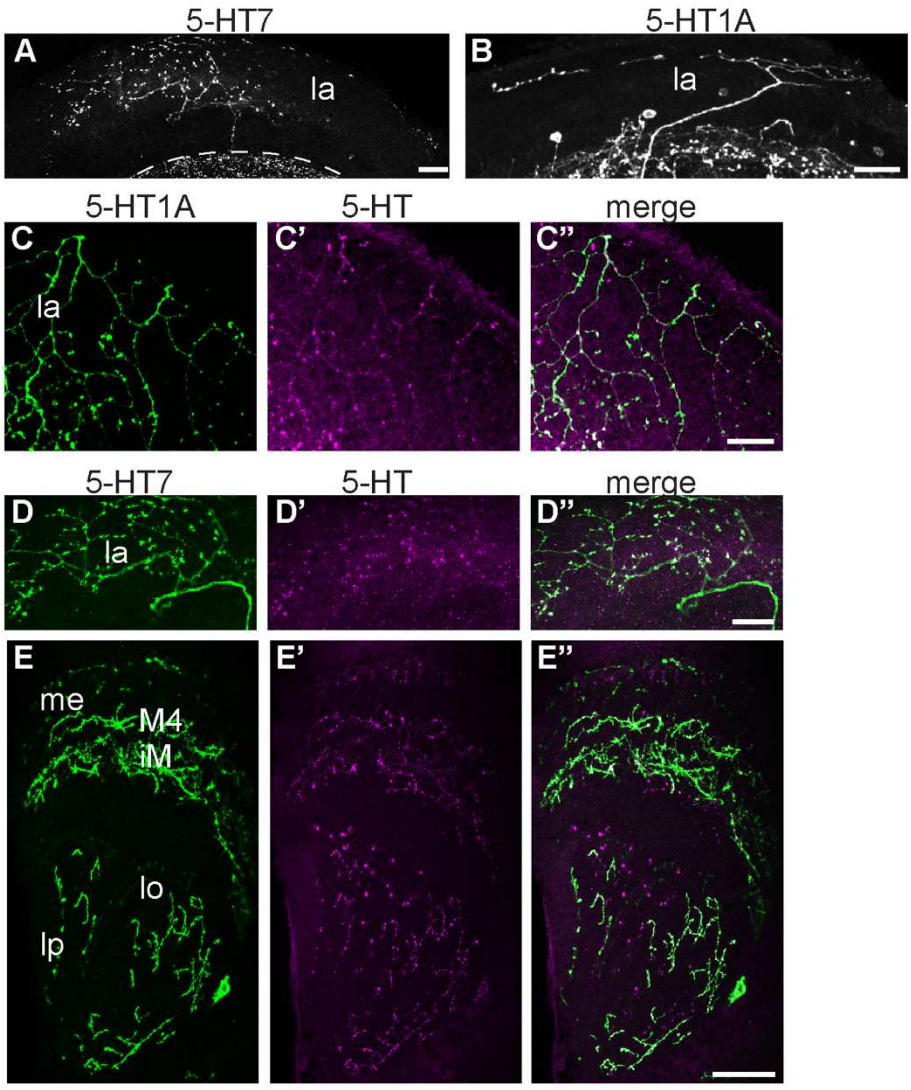

Discussion

Serotonin neurons innervate layer M2 of the medulla, where they converge with arborizations of L2 and T1 neurons. L2 and T1 neurons are both pre- and post-synaptic in M2 suggesting that both receive and transmit information here (Fig 1). L2 and T1 form reciprocal synapses in M2 [17] (Fig 2) and also express serotonin receptors. Previous studies have established a connectome for many neurons in the fly visual system including L1, L2 and T1 neurons [15-20, 57]. By contrast the ultrastructure of serotonergic processes in the optic lobe are not known, but EM studies in other insects have revealed sites likely to represent both synaptic and non-synaptic release [66, 147]. Using GRASP, we found that serotonergic signaling to L2 and T1 in the medulla is likely to occur extrasynaptically (Fig 2). In both mammals and insects, serotonin can be released extrasynaptically through volume transmission [135, 136] or through synaptic sites [21-23, 66, 137]. The majority of mammalian aminergic release sites lack an identifiable synaptic partner, and even synaptic release can lead to spillover and extrasynaptic release.

Serotonergic release sites appear to lack synaptic partners in the lamina of the blowfly *Calliphora* [147] and our data using sybGRASP to test whether serotonergic neurons synapse on L2, T1, and L1 was negative (Fig 2). It is possible that ultrastructural studies will prove more fruitful, but in the absence of true synaptic connections we anticipate that new methods may be needed to unambiguously determine the relationship of aminergic boutons to potential targets in the visual system and other sites in the fly CNS.

In this work we found additional evidence that 5-HT1A, 5-HT1B and 5-HT7 may be expressed by serotonergic neurons that innervate the optic lobes (Fig 3-5). Previous work by the Seghal lab showed co-labeling between 5-HT1B-GAL4 and serotonin-immunoreactive cell bodies in the subesophageal ganglion [141], which is consistent with our findings. Another study by the Kravitz lab sequenced serotonin neurons specified by TRH-GAL4 and found elevated 5-

HT1A, 5-HT1B and 5-HT7 transcripts [140]. Subcellular mapping with 5-HT1A::GFP showed co-localization with serotonin-immunoreactive sites and suggests that 5-HT1A is localized to the serotonin release sites in the medulla, providing further evidence that 5-HT1A might function as an autoreceptor (Ch 1 Fig 5). Serotonin autoreceptors are a critical regulators of the serotonin system and it is increasingly evident that 5-HT1A may play a role in psychological illness and treatment.

Conclusions

Together, these experiments suggest that M2 is a potential hub for serotonin volume transmission targeting L2 and T1 arborizations. It is possible that serotonin also modulates cross talk between these neurons, which form reciprocal synapses in M2. Lastly, we found autoreceptors in serotonergic processes innervating the optic lobe and observed that 5-HT1A::GFP traffics to the outer medulla, including M2. This suggests that negative feedback through 5-HT1A and other serotonin receptors may also occur at this neuromodulatory "hub" in the medulla.

Methods

Fly Husbandry and Genetic Lines

Flies were maintained on a standard cornmeal and molasses-based agar media with a 12:12 hour light/dark cycle at room temperature (22-25°C). All fly strains used in this study are listed in Table 1. Serotonin receptor MiMIC-T2A-GAL4 lines described in [79] were a gift from Herman Dierick (Baylor College of Medicine), and include 5-HT1A-T2A-GAL4^{MI01468}, 5-HT1A-T2A-GAL4^{MI01140}, 5-HT1A-T2A-GAL4^{MI04464}, 5-HT1B-T2A-GAL4^{MI05213}, and 5-HT7-GAL4 ^{MI00215}. L1 and T1 split-GAL4 lines [54], as well as unpublished LexA lines for L1 and T1, were provided

by Aljoscha Nern (HHMI/Janelia Research Campus). L. Zipursky generously provided L2-split-GAL4 and L2-LexA (RRID:BDSC_52510).

SERT-GAL4 (RRID:BDSC_38764) was obtained from Bloomington *Drosophila* Stock Center at Indiana University (Bloomington, IN, USA). Reporter lines include: UAS-MCFO-1 (RRID:BDSC_64085), UAS-DenMark, UAS-Syt.eGFP (RRID:BDSC_33064 and RRID:BDSC_33065) and UAS-nSyb::GFP1-10, LexAop-CD4:GFP11 (RRID:BDSC_64314; provided by Larry Zipursky (UCLA)).

Immunohistochemistry and Imaging

Flies were dissected 5-10 days after eclosion, and equal numbers of males and females were used for all experiments unless otherwise noted. Brains were dissected in ice-cold PBS (Alfa Aesar, Cat#J62036, Tewksbury, MA), then fixed in 4% paraformaldehyde (FisherScientific, Cat#50-980-493, Waltham, MA) in PBS with 0.3% Triton X-100 (Millipore Sigma, Cat#X100, Burlington, MA) (PBST) for one hour at room temperature. After fixation, brains were washed three times with PBST for 10 minutes, then blocked for 30 minutes in PBST containing 0.5% normal goat serum (NGS) (Cayman Chemical, Cat#10006577, Ann Arbor, MA) PBST. Antibodies were diluted in 0.5% NGS/PBST. Primary antibodies were incubated with the tissue overnight at 4°C. The next day, the brains were washed three times with PBST for 10 minutes, then incubated with secondary antibodies for 2 hours in the dark at room temperature. Brains were washed three times with PBST for 10 minutes before mounting in Fluoromount-G (SouthernBiotech, Cat#0100-01, Birmingham, AL).

Serotonin immunolabeling was performed with 1:25 rat anti-serotonin (Millipore Sigma, Cat#MAB352, RRID:AB_11213564), 1:1000 rabbit anti-serotonin (ImmunoStar, Cat#20080, Hudson, WI ,RRID:AB_572263) or 1:1000 goat anti-serotonin (ImmunoStar, Cat#20079, RRID:AB_572262). GFP was labeled with 1:250 mouse anti-GFP (Sigma-Aldrich, Cat#G6539,

RRID:AB_259941; or, ThermoFisher, Waltham, MA, Cat#A-11120, RRID:AB_221568). Secondary antibodies were used at 1:400 and include: Donkey anti-mouse Alexa Fluor 488, Donkey anti-Rabbit Alexa Fluor 594 or Alexa Fluor Donkey anti-rat 647 (Jackson ImmunoResearch Laboratories, Westgrove, PA, Cat#715-545-151, # 711-585-152, # 712-605-153) or Alexa Fluor 555 (Life Technologies, ThermoFisher, Cat#A-21428).

N-Synaptobrevin GFP Reconstitution Across Synaptic Partners (sybGRASP) flies [143] were dissected, fixed and immunolabeled as described above, without KCl induction. The tissue was labeled with mouse antiserum specific to reconstituted GFP (1:250; Sigma-Aldrich, Cat#G6539, RRID:AB_259941) [148] and anti-serotonin (antibodies listed above).

Imaging was performed with a Zeiss LSM 880 Confocal with Airyscan (Zeiss, Oberkochen, Germany) using a 40x water or 63x oil immersion objective. Post-hoc processing of images was done with Fiji [113] or Adobe Photoshop (Adobe, San Jose, CA).

Tables

Table 1. Animal strains used in this study.

Fly Line	**Source**
L2-sp-GAL4	L. Zipursky (UCLA)
L2-LexA	RRID:BDSC_52510
L1-sp-GAL4	A. Nern (Janelia)
L1-LexA	A. Nern (Janelia)
T1-sp-GAL4	A. Nern (Janelia)
T1-LexA	A. Nern (Janelia)
5-HT1B-T2A-GAL4 MI05213	H. Dierick (Baylor)
5-HT1A-T2A-GAL4 MI01468	H. Dierick (Baylor)
5-HT7-GAL4 MI00215	H. Dierick (Baylor)
SERT-Gal4 (P(GMR50H05-GAL4)attP2)	RRID:BDSC_38764
(sybGRASP) UAS-nSyb::GFP1-10, LexAop-CD4:GFP11	RRID:BDSC_64314
UAS-mCD8::GFP	RRID:BDSC_5137
UAS-MCFO-1	RRID:BDSC_64085

Chapter 4: Tools for Studying SERT in *Drosophila*

Introduction

The serotonin transporter (SERT) localizes to the plasma membrane of serotonergic neurons where it transports serotonin from the extracellular space. Serotonin selective reuptake inhibitors (SSRIs) are commonly prescribed antidepressants that inhibit SERT. SERT inhibition decreases serotonin clearance from the extracellular space and subsequently increases serotonergic signaling. Serotonin regulates a wide variety of physiological processes beyond mood and anxiety, and changes in SERT function can have an enormous influence on brain function and behavior. Here we develop tools to study the molecular mechanisms by which SERT activity alters circuits and behaviors that are regulated by serotonin.

Drosophila melanogaster is a genetically tractable model organism that provides a flexible platform for generating transgenes and mutants to study gene function. We leveraged this system to develop new tools to study how SERT activity regulates serotonin biology. We first developed an epitope-tagged *Drosophila* SERT (HA-dSERT) for localization studies because there is not a commercial antibody available for dSERT. We also used several molecular genetic approaches to humanize dSERT. Lastly, we tested how a loss of function mutation of dSERT (*SERT*16) affects sleep behavior in flies. This behavioral paradigm will be used to characterize other transgenic d*SERT* lines we developed in this study.

In mice, several m*SERT* mutants [149-151] have been developed and used to study SERT function [152, 153]. Surprisingly, the only published d*SERT* mutations are a hypomorph that decreases its expression by 46.5% [154] and a dominant-negative insertion [46], both of which reduce but do not eliminate SERT function. *SERT* mutants have been used to model SSRI therapies [149, 152, 153], but have major caveats that limit data interpretation. *SERT* knockout animals do not re-capitulate SSRI treatment because SERT is not completely non-functional during drug treatment. A null *SERT* mutant represents an extreme state that likely does not likely reflect the biology of SSRI treatment. Additionally, there may be developmental or

adaptive effects in constitutive knockouts that are not relevant to SSRI therapeutic state. Lastly, SERT loss of function animals are unable to model drug pharmacokinetics and pharmacodynamics including off-target effects. These limitations are critical for data interpretation; however, gene knockout animals continue to be a gold standard for demonstrating gene and protein function through rescue experiments.

Many studies in *Drosophila* have used SSRIs such as fluoxetine [141, 155-157], but there are important differences in the pharmacodynamics of dSERT and hSERT [158-162]. A humanized version of dSERT with a higher affinity to psychotropic drugs will be important for the modeling human therapies using dSERT. For this reason, we sought to develop a way to conduct drug studies in *Drosophila* and used several strategies to “humanize” dSERT to enable studies using drugs in the *Drosophila* model system. To this end, we induced the point mutation M167I [163] and designed human-*Drosophila* chimeras that replaced large portions of d*SERT* with the homologous h*SERT* sequence

To establish a behavior paradigm to test the newly developed “humanized” *SERT* transgenic lines, we collaborated with Henrike Scholz (University of Cologne, Germany) to obtain two unpublished *SERT* mutants that were generated by p-transposon excision. The imprecise excision mutants are protein nulls according to western blot using a dSERT antibody generated in the Scholz lab [164]. Serotoninergic modulation targets most circuits in the brain, which means that altering the serotonin system will affect many behaviors. We identified sleep behavior as a reproducible behavioral paradigm to asses changes in SERT function.

Results

The Krantz lab previously generated an HA-dSERT construct that transports serotonin in S2 cell culture [165]. In the current work, this construct was used to generate a fly expressing HA-dSERT by inserting the sequence into the MiMIC site [80] by recombinase-mediated

cassette exchange (RMCE). This approach generated a fly that expresses a combination of both endogenous dSERT and HA-dSERT from the endogenous d*SERT* locus. Antibodies targeting HA (green) and serotonin (red) show co-labeling in both cell bodies and projections when the construct was inserted in the forward direction (HA-dSERT-FWD) (Fig 1). In some cases, RMCE of the HA-dSERT insertion occurred in an inverted orientation and these flies are used as a negative control (HA-dSERT-REV) in Fig 1.

Fig 1. Epitope-tagged dSERT expressed in vivo. (**A-D**) Flies expressing MiMIC-HA-dSERT were stained for anti-HA and anti-serotonin (red, 5-HT). (**A**) Co-labeling was observed in optic lobe (OL) and central brain (CB) processes and cell bodies, as shown for serotonergic cluster LP2, when the construct was inserted in the forward (FWD) orientation. (**B**). When the construct was inserted in reverse (REV), very little anti-HA staining was observed and it did not correlate with anti-serotonin labeling. (**C**) For HA-dSERT-FWD, co-labeling was seen throughout the central brain including projections in the ellipsoid body (EB). (**D**) In some regions, such as the mushroom bodies (MB), projections showed anti-HA staining, but not anti-serotonin staining. All scale bars are 20 μm.

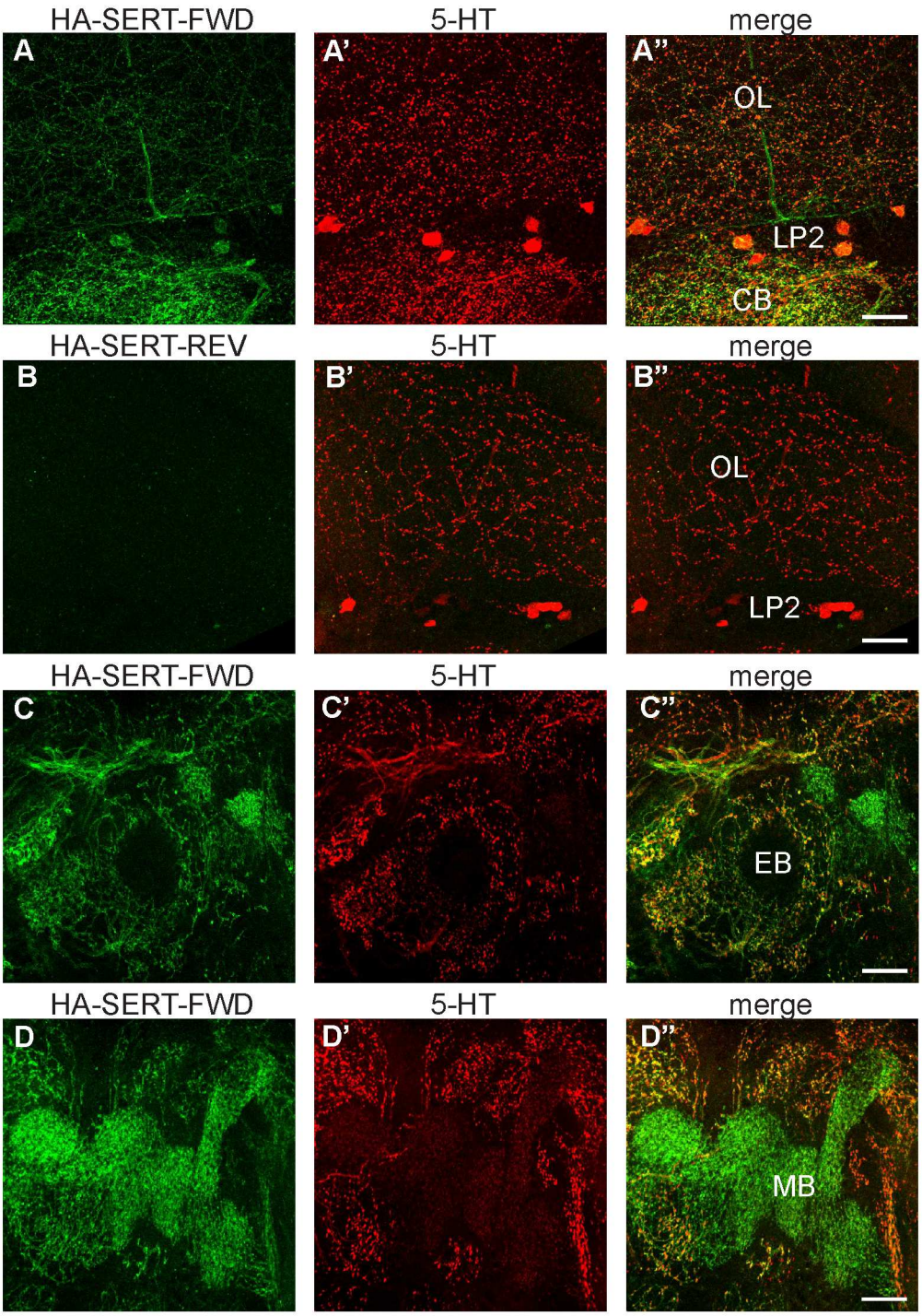
HA-SERT-FWD
5-HT
merge
A
A'
A''
OL
LP2
CB
HA-SERT-REV
5-HT
merge
B
B'
B''
OL
LP2
HA-SERT-FWD
5-HT
merge
C
C'
C''
EB
HA-SERT-FWD
5-HT
merge
D
D'
D''
MB

Human SERT (hSERT) and *Drosophila* SERT (dSERT) are 53% homologous by amino acid sequence [166]. The transport kinetics for serotonin re-uptake are similar for dSERT and hSERT with K_ms of 490 and 463 nM respectively [160]. However, although dSERT is inhibited by SSRIs, it is less sensitive than hSERT, with fluoxetine K_i of 3 nM for hSERT and 73 nM for dSERT expressed in heterologous mammalian cells [160]. To elicit a more robust response to SSRI treatment, we first "humanized" dSERT by insertion of a single point mutation M167I (Fig 2). Amino acid 167 is located in transmembrane domain three in dSERT. The corresponding isoleucine amino acid (Ile-172) is conserved in mammals, whereas insects have a methionine (Met-167). Previously, mammalian Ile-172 was replaced with methionine (hSERT I172M) and was shown to dramatically reduce fluoxetine and citalopram inhibition of serotonin transport in vitro [163].

We generated the M167I point mutant using CRISPR-cas9 homologous repair. Guide RNAs targeted cas9 to cut in the *SERT* locus in an intronic region (Table 1). The donor repair vector consisted homologous R- and L-arm sequences flanking a loxP-DsRed-loxP construct. Dsred was expressed in photoreceptors and enabled visual identification of successful insertions. The M167I mutation was introduced into the R-arm sequence using a mutagenesis primer (Table 1).

In addition to the point mutant, we also generated a chimeric SERT (dSERT-Chi1) that includes cytosolic N- and C-termini of dSERT flanking the twelve hSERT transmembrane domains: $dSERT^{1-73}$-$hSERT^{74-586}$-$dSERT^{587-622}$ (Fig 2). The hSERT domains included in this chimera contain the serotonin and SSRI binding sites. Chimeras containing both dSERT and hSERT for in vitro structure function experiments have been created previously [161, 162], and we added a HA tag to a cytosolic region for easy visualization of this chimeric protein in fly. When the HA-dSERT-Chi1 construct was inserted into the MiMIC site using RMCE, we found that the HA-Chi1-SERT staining was limited to cell bodies, suggested the chimera failed to

traffic (Fig 3). For HA-dSERT-Chi1 we replaced the transmembrane region of the dSERT protein with the hSERT amino acid sequence. As a next step, we collaborated with Thomas Stockner (Med Uni, Vienna) to design 4 additional chimeras using different boundaries for the hSERT replacement (Fig 2).

Fig 2. Serotonin transporter amino acid sequences from *Drosophila* (dSERT, NP_523846.2) and *homo sapiens* (hSERT, NP_001036.1) are aligned with sequences of the constructs designed to "humanize" dSERT. A single point mutation in was made in d*SERT* to generate dSERTM167I (highlighted in red). For dSERT Chimeras 1-5, N-terminal and C-terminal regions are *Drosophila* sequences and potential drug-binding regions in the transmembrane domains were replaced with hSERT sequences. Sequences were aligned using CLUSTAL Omega (1.2.4) multiple sequence alignment. Amino acids highlighted in grey represent dSERT. Alignment data can be accessed here: https://www.ebi.ac.uk/Tools/services/rest/clustalo/result/clustalo-I20200502-174931-0094-36718259-p2m/aln-clustal_num.

```
dSERT           ----------MDRSGSSDFAGAAATTGRSNPAPWSDDKESPNNEDDSNEDDGDHTTP-A        48
hSERT           METTPLNSQKQLSACEDGEDCQENGVLQKVVPTPGDKVESG-------QISNGYSAVPSP        53
dSERTM167I      ----------MDRSGSSDFAGAAATTGRSNPAPWSDDKESPNNEDDSNEDDGDHTTP-A        48
dSERTChi1       ----------MDRSGSSDFAGAAATTGRSNPAPWSDDKESPNNEDDSNEDDGDHTTP-A        48
dSERTChi2       ----------MDRSGSSDFAGAAATTGRSNPAPWSDDKESPNNEDDSNEDDGDHTTP-A        48
dSERTChi3       ----------MDRSGSSDFAGAAATTGRSNPAPWSDDKESPNNEDDSNEDDGDHTTP-A        48
dSERTChi4       ----------MDRSGSSDFAGAAATTGRSNPAPWSDDKESPNNEDDSNEDDGDHTTP-A        48
dSERTChi5       ----------MDRSGSSDFAGAAATTGRSNPAPWSDDKESPNNEDDSNEDDGDHTTP-A        48

dSERT           KVTDPLAPKLANNERILVVSVTERTRETWGQKAEFLLAVIGFAVDLGNVWRFPYICYQNG        108
hSERT           GAGDDTRHSIPATTTTLVAELHQGERETWGKKVDFLLSVIGYAVDLGNVWRFPYICYQNG        113
dSERTM167I      KVTDPLAPKLANNERILVVSVTERTRETWGQKAEFLLAVIGFAVDLGNVWRFPYICYQNG        108
dSERTChi1       KVTDPLAPKLANNERILVVSVTERTRETWGKKVDFLLSVIGYAVDLGNVWRFPYICYQNG        108
dSERTChi2       KVTDPLAPKLANNERILVVSVTERTRETWGKKVDFLLSVIGYAVDLGNVWRFPYICYQNG        108
dSERTChi3       KVTDPLAPKLANNERILVVELHQGERETWGKKVDFLLSVIGYAVDLGNVWRFPYICYQNG        108
dSERTChi4       KVTDPLAPKLANNERILVVELHQGERETWGKKVDFLLSVIGYAVDLGNVWRFPYICYQNG        108
dSERTChi5       KVTDPLAPKLANNERILVVSVTERTRETWGKKVDFLLSVIGYAVDLGNVWRFPYICYQNG        108

dSERT           GGAFLVPYCLFLIFGGLPLFYMELALGQFHRCGCLSIWKRICPALKGVGYAICLIDIYMG        168
hSERT           GGAFLLPYTIMAIFGGIPLFYMELALGQYHRNGCISIWRKICPIFKGIGYAICIIAFYIA        173
dSERTM167I      GGAFLVPYCLFLIFGGLPLFYMELALGQFHRCGCLSIWKRICPALKGVGYAICLIDIYIG        168
dSERTChi1       GGAFLLPYTIMAIFGGIPLFYMELALGQYHRNGCIIWRKICPIFKGIGYAICIIAFYIA         168
dSERTChi2       GGAFLLPYTIMAIFGGIPLFYMELALGQYHRNGCISIWRKICPIFKGIGYAICIIAFYIA        168
dSERTChi3       GGAFLLPYTIMAIFGGIPLFYMELALGQYHRNGCISIWRKICPIFKGIGYAICIIAFYIA        168
dSERTChi4       GGAFLLPYTIMAIFGGIPLFYMELALGQYHRNGCISIWRKICPIFKGIGYAICIIAFYIA        168
dSERTChi5       GGAFLLPYTIMAIFGGIPLFYMELALGQYHRNGCISIWRKICPIFKGIGYAICIIAFYIA        168

dSERT           MYYNTIIGWAVYYLFASFTSKLPWTSCDNPWNTENCMQVTSEN---FTELATSPAKEFFE        225
hSERT           SYYNTIMAWALYYLISSFTDQLPWTSCKNSWNTGNCTNYFSEDNITWTLHSTSPAEEFYT        233
dSERTM167I      MYYNTIIGWAVYYLFASFTSKLPWTSCDNPWNTENCMQVTSEN---FTELATSPAKEFFE        225
dSERTChi1       SYYNTIMAWALYYLISSFTDQLPWTSCKNSWNTGNCTNYFSEDNITWTLHSTSPAEEFYT        228
dSERTChi2       SYYNTIMAWALYYLISSFTDQLPWTSCKNSWNTGNCTNYFSEDNITWTLHSTSPAEEFYT        228
dSERTChi3       SYYNTIMAWALYYLISSFTDQLPWTSCKNSWNTGNCTNYFSEDNITWTLHSTSPAEEFYT        228
dSERTChi4       SYYNTIMAWALYYLISSFTDQLPWTSCKNSWNTGNCTNYFSEDNITWTLHSTSPAEEFYT        228
dSERTChi5       SYYNTIMAWALYYLISSFTDQLPWTSCKNSWNTGNCTNYFSEDNITWTLHSTSPAEEFYT        228

dSERT           RKVLESYKGNGLDFMGPVKPTLALCVFGVFVLVYFSLWKGVRSAGKVVWVTALAPYVVLI        285
hSERT           RHVLQIHRSKGLQDLGGISWQLALCIMLIFTVIYFSIWKGVKTSGKVVWVTATFPYIILS        293
dSERTM167I      RKVLESYKGNGLDFMGPVKPTLALCVFGVFVLVYFSLWKGVRSAGKVVWVTALAPYVVLI        285
dSERTChi1       RHVLQIHRSKGLQDLGGISWQLALCIMLIFTVIYFSIWKGVKTSGKVVWVTATFPYIILS        288
dSERTChi2       RHVLQIHRSKGLQDLGGISWQLALCIMLIFTVIYFSIWKGVKTSGKVVWVTATFPYIILS        288
dSERTChi3       RHVLQIHRSKGLQDLGGISWQLALCIMLIFTVIYFSIWKGVKTSGKVVWVTATFPYIILS        288
dSERTChi4       RHVLQIHRSKGLQDLGGISWQLALCIMLIFTVIYFSIWKGVKTSGKVVWVTATFPYIILS        288
dSERTChi5       RHVLQIHRSKGLQDLGGISWQLALCIMLIFTVIYFSIWKGVKTSGKVVWVTATFPYIILS        288

dSERT           ILLVRGVSLPGADEGIKYYLTPEWHKLKNSKVWIDAASQIFFSLGPGFGTLLALSSYNKF        345
hSERT           VLLVRGATLPGAWRGVLFYLKPNWQKLLETGVWIDAAAQIFFSLGPGFGVLLAFASYNKF        353
dSERTM167I      ILLVRGVSLPGADEGIKYYLTPEWHKLKNSKVWIDAASQIFFSLGPGFGTLLALSSYNKF        345
dSERTChi1       VLLVRGATLPGAWRGVLFYLKPNWQKLLETGVWIDAAAQIFFSLGPGFGVLLAFASYNKF        348
dSERTChi2       VLLVRGATLPGAWRGVLFYLKPNWQKLLETGVWIDAAAQIFFSLGPGFGVLLAFASYNKF        348
dSERTChi3       VLLVRGATLPGAWRGVLFYLKPNWQKLLETGVWIDAAAQIFFSLGPGFGVLLAFASYNKF        348
dSERTChi4       VLLVRGATLPGAWRGVLFYLKPNWQKLLETGVWIDAAAQIFFSLGPGFGVLLAFASYNKF        348
dSERTChi5       VLLVRGATLPGAWRGVLFYLKPNWQKLLETGVWIDAAAQIFFSLGPGFGVLLAFASYNKF        348

dSERT           NNNCYRDALITSSINCLTSFLAGFVIFSVLGYMAYVQKTSIDKVG-LEGPGLVFIVYPEA        404
hSERT           NNNCYQDALVTSVVNCMTSFVSGFVIFTVLGYMAEMRNEDVSEVAKDAGPSLLFITYAEA        413
dSERTM167I      NNNCYRDALITSSINCLTSFLAGFVIFSVLGYMAYVQKTSIDKVG-LEGPGLVFIVYPEA        404
dSERTChi1       NNNCYQDALVTSVVNCMTSFVSGFVIFTVLGYMAEMRNEDVSEVAKDAGPSLLFITYAEA        408
dSERTChi2       NNNCYQDALVTSVVNCMTSFVSGFVIFTVLGYMAEMRNEDVSEVAKDAGPSLLFITYAEA        408
dSERTChi3       NNNCYQDALVTSVVNCMTSFVSGFVIFTVLGYMAEMRNEDVSEVAKDAGPSLLFITYAEA        408
dSERTChi4       NNNCYQDALVTSVVNCMTSFVSGFVIFTVLGYMAEMRNEDVSEVAKDAGPSLLFITYAEA        408
dSERTChi5       NNNCYQDALVTSVVNCMTSFVSGFVIFTVLGYMAEMRNEDVSEVAKDAGPSLLFITYAEA        408

dSERT           IATMSGSVFWSIIFFLMLITLGLDSTFGGLEAMITALCDEYPRVIGRRRELFVLLLLAFI        464
```

```
hSERT           IANMPASTFFAIIFFLMLITLGLDSTFAGLEGVITAVLDEFPHVWAKRRERFVLAVVITC          473
dSERTM167I      IATMSGSVFWSIIFFLMLITLGLDSTFGGLEAMITALCDEYPRVIGRRRELFVLLLLAFI          464
dSERTChi1       IANMPASTFFAIIFFLMLITLGLDSTFAGLEGVITAVLDEFPHVWAKRRERFVLAVVITC          468
dSERTChi2       IANMPASTFFAIIFFLMLITLGLDSTFAGLEGVITAVLDEFPHVWAKRRERFVLAVVITC          468
dSERTChi3       IANMPASTFFAIIFFLMLITLGLDSTFAGLEGVITAVLDEFPHVWAKRRERFVLAVVITC          468
dSERTChi4       IANMPASTFFAIIFFLMLITLGLDSTFAGLEGVITAVLDEFPHVWAKRRERFVLAVVITC          468
dSERTChi5       IANMPASTFFAIIFFLMLITLGLDSTFAGLEGVITAVLDEFPHVWAKRRERFVLAVVITC          468

dSERT           FLCALPTMTYGGVVLVNFLNVYGPGLAILFVVFVEAAGVFWFYGVDRFSSDVEQMLGSKP          524
hSERT           FFGSLVTLTFGGAYVVKLLEEYATGPAVLTVALIEAVAVSWFYGITQFCRDVKEMLGFSP          533
dSERTM167I      FLCALPTMTYGGVVLVNFLNVYGPGLAILFVVFVEAAGVFWFYGVDRFSSDVEQMLGSKP          524
dSERTChi1       FFGSLVTLTFGGAYVVKLLEEYATGPAVLTVALIEAVAVSWFYGITQFCRDVKEMLGFSP          528
dSERTChi2       FFGSLVTLTFGGAYVVKLLEEYATGPAVLTVALIEAVAVSWFYGITQFCRDVKEMLGFSP          528
dSERTChi3       FFGSLVTLTFGGAYVVKLLEEYATGPAVLTVALIEAVAVSWFYGITQFCRDVKEMLGFSP          528
dSERTChi4       FFGSLVTLTFGGAYVVKLLEEYATGPAVLTVALIEAVAVSWFYGITQFCRDVKEMLGFSP          528
dSERTChi5       FFGSLVTLTFGGAYVVKLLEEYATGPAVLTVALIEAVAVSWFYGITQFCRDVKEMLGFSP          528

dSERT           GLFWRICWTYISPVFLLTIFIFSIMGYKEMLGEEYYYPDWSYQVGWAVTCSSVLCIPMYI          584
hSERT           GWFWRICWVAISPLFLLFIICSFLMSPPQLRLFQYNYPYWSIILGYCIGTSSFICIPTYI          593
dSERTM167I      GLFWRICWTYISPVFLLTIFIFSIMGYKEMLGEEYYYPDWSYQVGWAVTCSSVLCIPMYI          584
dSERTChi1       GWFWRICWVAISPLFLLFIICSFLMSPPQLRLFQYNYPYWSIILGYCIGTSSFICIPTYI          588
dSERTChi2       GWFWRICWVAISPLFLLFIICSFLMSPPQLRLFQYNYPYWSIILGYCIGTSSFICIPTYI          588
dSERTChi3       GWFWRICWVAISPLFLLFIICSFLMSPPQLRLFQYNYPYWSIILGYCIGTSSFICIPTYI          588
dSERTChi4       GWFWRICWVAISPLFLLFIICSFLMSPPQLRLFQYNYPYWSIILGYCIGTSSFICIPTYI          588
dSERTChi5       GWFWRICWVAISPLFLLFIICSFLMSPPQLRLFQYNYPYWSIILGYCIGTSSFICIPTYI          588

dSERT           IYKFFFASKGGCRQRLQESFQPED----NCGSVVPGQQGTSV          622
hSERT           AYRLII-TPGTFKERIIKSITPET----PTEIPCGDIRLNAV          630
dSERTM167I      IYKFFFASKGGCRQRLQESFQPED----NCGSVVPGQQGTSV          622
dSERTChi1       AYKFFFASKGGCRQRLQESFQPED----NCGSVVPGQQGTSV          626
dSERTChi2       AYRLII-TPGTFKERIIKSITPET----PTESVVPGQQGTSV          625
dSERTChi3       AYRLII-TPGTFKERIIKSITPET----PTEIPCGGQQGTSV          625
dSERTChi4       AYRLII-TPGTFKERIIKSITPET----PTESVVPGQQGTSV          625
dSERTChi5       AYRLII-TPGTFKERIIKSITPET----PTEIPCGGQQGTSV          625
```

Fig 3. Chimeric dSERT expressed in vivo. (**A-D**) Flies expressing MiMIC-HA-dSERT-Chi1 or MiMIC-HA-dSERT were stained for anti-HA and anti-serotonin (red, 5-HT). (**A**) The chimera showed very little anti-HA labeling in projections, including the fan-shaped body (FB). (**B**) In contrast, MiMIC-HA-dSERT-FWD shows strong anti-HA labeling that co-stains with anti-serotonin. (**C-D**) Both lines show co-labeling in the cell bodies. All scale bars are 20 μm.

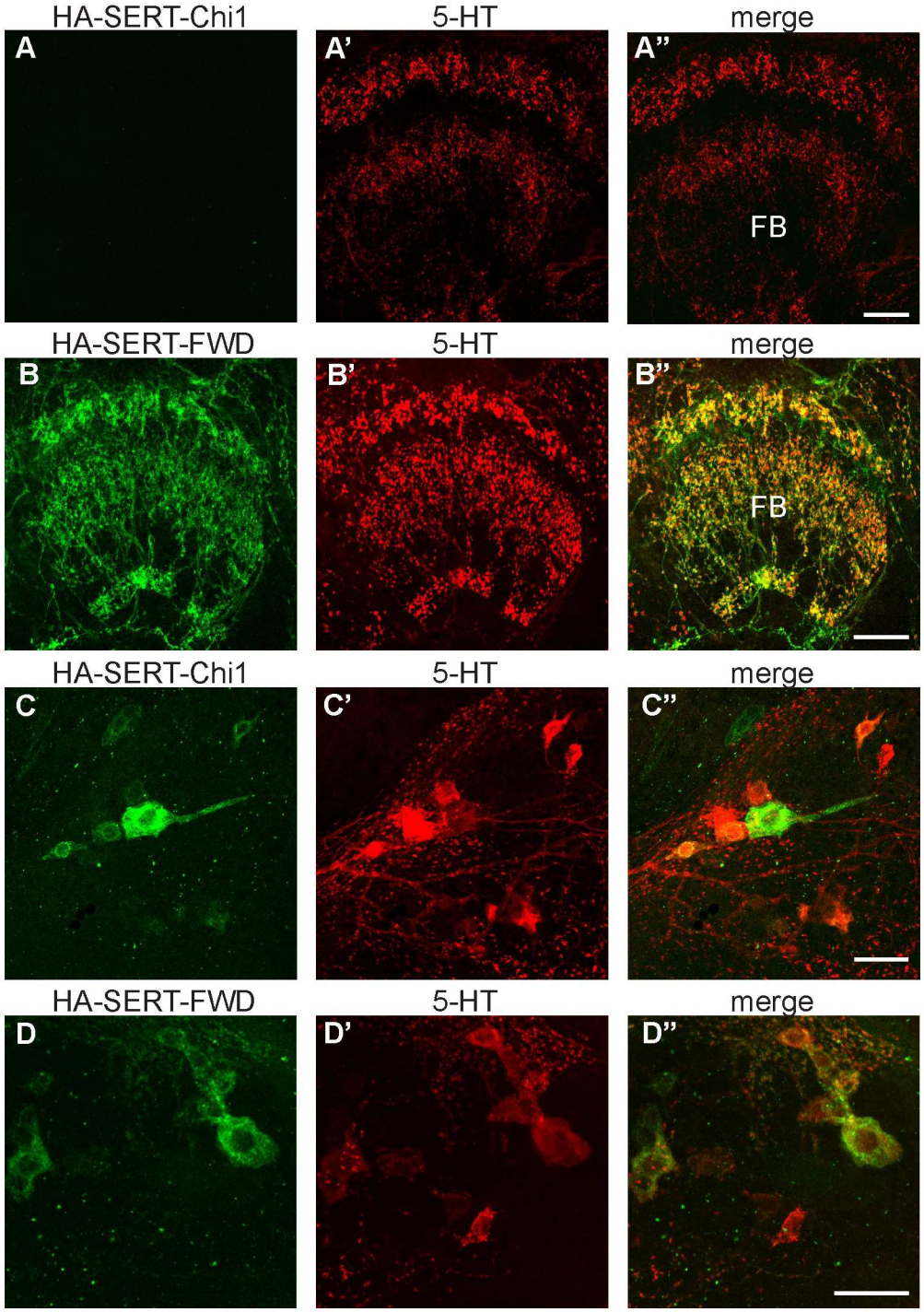

Serotonin regulates many diverse behaviors in flies including courtship and mating [167], sleep and circadian rhythm [141, 168, 169], memory [170], feeding [47, 171], and aggression [172, 173]. For this reason, we expected that constitutive *SERT* mutants would influence many behaviors and we considered many paradigms to test the M167I and chimeric dSERT flies. We found a robust and reproducible behavior phenotype using sleep. The *SERT*16 imprecise excision line was generated from the parent line previously backcrossed to the Scholz lab W1118 line. In these experiments, we compare *SERT*16 (-/-), W1118 (+/+), and a heterozygous cross (+/-) of both lines. Overall, the *SERT*16 flies slept more than control flies in both the day and night (Fig 4). The *SERT*16 flies had an average of 56 min of sleep per hour for ZT 13-24, near the ceiling of possible sleep behavior, compared to 39 min in W1118 flies. The *SERT* +/- flies exhibited sleep behavior that was not significantly different from W1118, suggesting that either partial loss of SERT was not sufficient to drive a change in this behavior or SERT function was not significantly reduced in the heterozygous line.

Fig 4. Flies lacking SERT sleep more than wild-type controls. Flies were tracked with activity monitors and sleep was classified as 5-minute intervals of inactivity. The *SERT*16 mutant (*SERT* -/-) is compared to W1118 controls (*SERT* +/+) and a heterozygous cross (*SERT* +/-). (**A**) The 24-hour activity tracking data was binned into 1-hour intervals and the resulting trace is shown. (**B**) Total sleep (ZT 1-24). (**C**) Total night sleep (ZT 13-24). N=32 flies per genotype, data was collected and averaged over 3 consecutive days. Error is SEM across the daily average. Comparisons in (B-C) are one-way ANOVA tukey's multiple comparisons tests, p-value in (B) is 0.0079 and (C) is 0.0001.

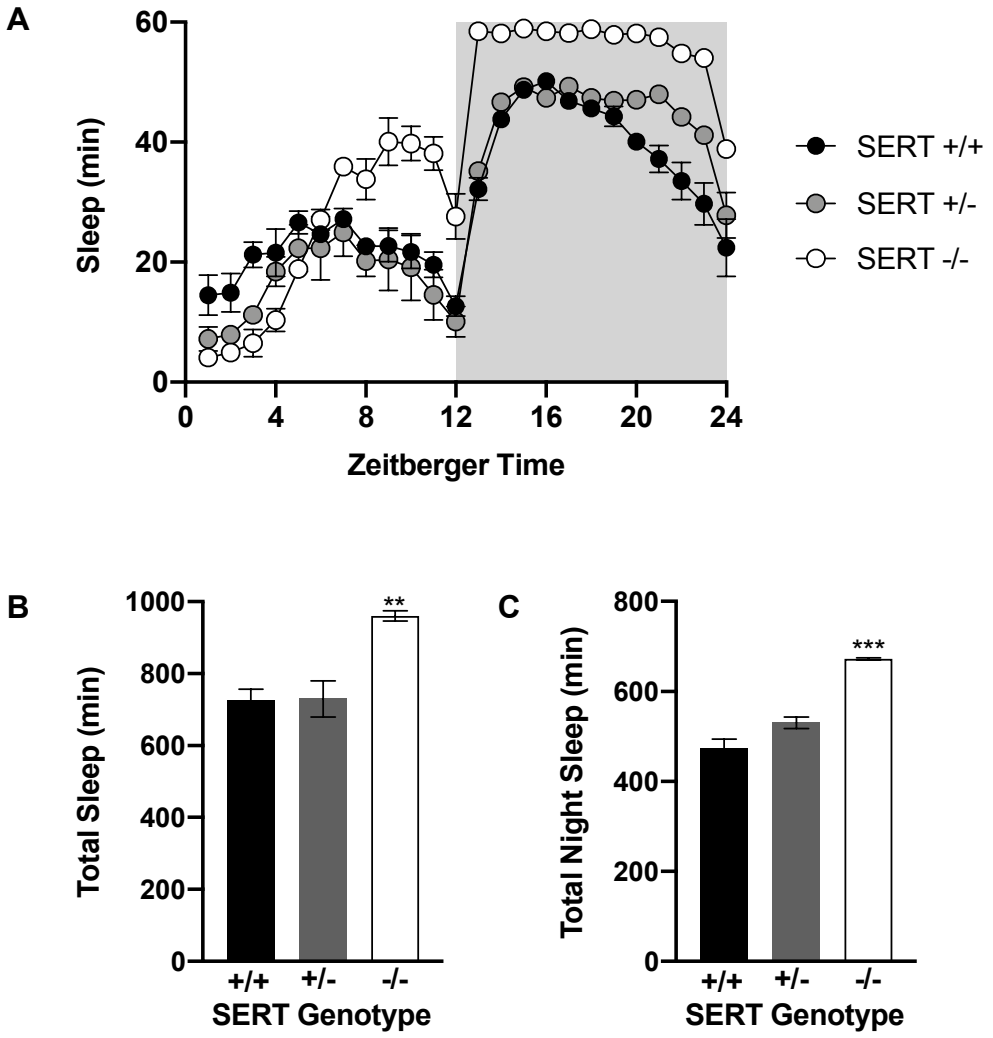

Discussion

The focus of Chapter 4 was to develop new tools for studying SERT function in *Drosophila*. We used two genetic approaches to manipulate the *SERT* locus: RMCE at the *SERT* MiMIC site and CRISPR-cas9 homologous repair. Insertion of constructs, such as HA-dSERT, in the MiMIC site result in expression of both endogenous SERT and HA-dSERT, due to exon skipping of the insertion. It is also possible to insert mutant SERT cDNA in the MiMIC site to create a dominant-negative system, similar to the $SERT^{DN}$ developed by the Scholz lab [46]. We also inserted HA-dSERT-Chi1 into the MiMIC site to evaluate whether chimeric SERT would traffic similarly to HA-dSERT (Fig 1). We found that HA-dSERT-Chi1 did not traffic outside of the cell bodies (Fig 3), possibly due improper folding at the first and last transmembrane domains. For this reason, we designed four additional chimeras with slightly different boundaries in these regions.

In the future work, humanized dSERT constructs (Fig 2) should be expressed in S2 cells for kinetic and pharmacodynamic validation experiments. Specifically, transport assays using tritium-labeled serotonin to measure V_{max} and K_m for serotonin uptake should be performed. It is possible that the HA tag interferes with SERT structure and function, however a previous study has included HA epitopes in their chimeras and reported no interference with serotonin transport [162]. We should also compare pharmacodynamic response to SSRI inhibition by measuring the IC50 of the chimeric dSERTs, dSERT, and hSERT expressed in S2 cells. The SSRIs fluoxetine and sertraline are good candidates for testing. Sertraline is the most potent inhibitor of hSERT and it has become one of the most prescribed SSRIs. Fluoxetine is the most well studied SSRI and remains a first-line treatment for anxiety and depression.

Serotonin has been implicated in sleep behavior in *Drosophila*, which exhibit diurnal sleep patterns. Increasing serotonin by feeding of the serotonin-precursor 5-HTP was associated with increases in total sleep [169]. Activation of specific serotonergic neurons that

innervate the mushroom bodies also result in increased total sleep [174]. Loss of serotonin signaling, such as by genetic knock-out or RNAi knockdown of the synthetic enzyme TRH, led to decreases in total sleep [91, 174]. Our experiments similarly found that constitutive loss of SERT function increased total sleep (Fig 4), which is consistent with observations in SERT knock-out mice [175].

Activation of specific serotonin receptors including 5-HT1A in the mushroom bodies [169] or 5-HT2B in the dorsal fan-shaped body [91] promotes sleep behavior. In contrast, loss of 5-HT7 function by knock-down or pharmacological antagonist leads to more fragmented sleep and may be important for maintaining sleep architecture, rather than total sleep. In the future, we will combine the *SERT*16 mutant with receptor knockouts to determine which receptor is responsible for the sleep defects we observe.

Conclusions

We developed new tools for studying serotonin and SERT biology in *Drosophila*. We generated a fly expressing epitope-tagged SERT for subcellular mapping. To enable studies of serotonergic drugs that target SERT, we humanized d*SERT* by point mutation M167I and various dSERT-hSERT-dSERT chimeras. This work is ongoing and these constructs will need to be evaluated pharmacologically and behaviorally. We identified sleep as a potential behavior to screen the humanized dSERTs described here.

Methods

Generation of MiMIC-HA-dSERT flies

Epitope-tagged SERT cDNA was previously generated and the constructed was cloned out of pMT(HA-dSERT) [165] and into the MiMIC RMCE vector: pBS-KS-attB1-2-PT-SA-SD-1. Bestgene service (Chino Hills, USA) was used to inject the RMCE vector into the SERT MiMIC MI02578 (BSC 36004) fly line. HA-dSERT-FWD images are from lines 2 and 4. HA-dSERT-REV images are line 3.

Generation of dSERT-M167I flies

The M167I point mutant was generated using CRISPR-cas9 homologous repair. Primers for amplifying the homology arms, gRNAs and mutagenesis primers are listed in Table 1. Guide RNAs targeted an intronic region of SERT and were designed using http://cistrome.org/crispr/tool. Homology arms were approximately 1000 bp and were amplified using gDNA isolated from Vas-Cas9-3xP3-GFP (III) flies. The donor vector consisted homologous R- and L-arm sequences flanking a loxP-DsRed-loxP construct, which was previously generated by Piero Sanfilippo in the lab of L. Zipursky. The homology arms, DsRed construct and pHD were assembled using Gibson Assembly NEB HiFi DNA Assembly Cloning Kit (NEB, Cat# E5520S). The Gibson assembled vector was transformed into XL10 Gold Ultracompetent cells (Agilent Technologies, Cat #200315). The M167I mutation was introduced into the R-arm sequence in the assembled donor vector using QuikChange XL Site-Directed Mutagenesis Kit (Agilent Technologies, Cat# 200516). Bestgene initially performed injection of the donor vector and gRNA into vas-Cas9 (III) embryos but this was not successful. The insertion was successful using vas-Cas9 (X) embryos.

Generation of pMT(HA-dSERT-Chi) and HA-SERT-Chi1 flies

The dSERT chimeras were cloned from the HA-dSERT plasmid [165] and hSERT cDNA (https://www.addgene.org/15483/). All final constructs are inserted into pMT/V5-HisA (https://www.addgene.org/browse/sequence_vdb/3645/) for testing in S2 cells. The first chimera, HA-dSERT-Chi1, has been used to generate transgenic fly with the epitope tagged chimeric construct inserted into the MiMIC site using the same approach as for MiMIC-HA-dSERT. Images show HA-dSERT-Chi1 Line 4.

Immunohistochemistry and Imaging

Flies were dissected 5-10 days after eclosion, and equal numbers of males and females were used for all experiments unless otherwise noted. Brains were dissected in ice-cold PBS (Alfa Aesar, Cat#J62036, Tewksbury, MA), then fixed in 4% paraformaldehyde (FisherScientific, Cat#50-980-493, Waltham, MA) in PBS with 0.3% Triton X-100 (Millipore Sigma, Cat#X100, Burlington, MA) (PBST) for one hour at room temperature. After fixation, brains were washed three times with PBST for 10 minutes, then blocked for 30 minutes in PBST containing 0.5% normal goat serum (NGS) (Cayman Chemical, Cat#10006577, Ann Arbor, MA) PBST. Antibodies were diluted in 0.5% NGS/PBST. Primary antibodies were incubated with the tissue overnight at 4°C. Primary antibodies were 1:25 rat anti-serotonin (Millipore Sigma, Cat#MAB352, RRID:AB_11213564) and 1:300 rabbit anti-HA (Cell Signaling Technology, Cat#3724, Danvers, MA, RRID:AB_1549585). The next day, the brains were washed three times with PBST for 10 minutes, then incubated with secondary antibodies for 2 hours in the dark at room temperature. Secondary antibodies were diluted 1:400 and include: Donkey anti-rat 488 (Thermofisher, Cat# A-21209) and Donkey anti-rabbit 594 (Thermofisher, Cat# A-

21207). Brains were washed three times with PBST for 10 minutes before mounting in Fluoromount-G (SouthernBiotech, Cat#0100-01, Birmingham, AL).

Imaging was performed with a Zeiss LSM 880 Confocal with Airyscan (Zeiss, Oberkochen, Germany) using a 63x oil immersion objective. Post-hoc processing of images was done with Fiji [113] or Adobe Photoshop (Adobe, San Jose, CA).

Sleep

Sleep was measured as previously described [176, 177]. On the day of eclosion, flies were transported to the Donlea lab for habituation lasting at least 3 days. Females flies 3-7 day old were loaded into 65 mm-long glass tubes for activity monitoring (Trikinetics Inc; Waltham MA, USA). Flies habituated in the activity monitors overnight before data collection began. Data was collected for 3 consecutive 24-hour periods. Inactive periods of at least 5 minutes were classified as sleep. Trikinetics activity data was analyzed using custom Visual Basic scripts [176] in Microsoft Excel and was graphed using Graphpad Prism Software (San Diego, CA). In the experiment shown, N=32 flies per genotype, data was collected and averaged over 3 consecutive days. Comparisons in (Fig 4 B-C) are one-way ANOVA tukey's multiple comparisons tests.

Tables

Table 1. Primers used in this study.

Primer	Sequence
F_SERT_sg1_chr2_24407700	TTCGAGGACCCTTAAACTTCCTCT
R_SERT_sg1_chr2_24407700	AAACAGAGGAAGTTTAAGGGTCCT
F1_SERT_Larm	tggggtgtcgcccttcgctgaagcaggtgg**cgcagcgtggccctgcgaaaag**
R1_SERT_Larm	cgttagggatgccaactcgtatgttaaatgctcagtaaggacccttaaacttcctctgCg
F1_lox-3xP3DsRed-lox	gagttggcatccctaacgcg
R1_lox-3xP3DsRed-lox	ataacttcgcaagttaacaacaacaattg
F1_SERT_Rarm	cgaagttatcaattgttgttgttaacttg**aatgcgctccaaacttgcaggcgtgggc**
R1_SERT_Rarm	tcgcccttgaactcgattgacggaagagccggtgctgtccagtcccaggg
F_M167I Mutagenesis	TGCCTAATCGACATTTAT**ATT**GGCATGTACTACAACACG
R_M167I Mutagenesis	CGTGTTGTAGTACATGCCAATATAAATGTCGATTAGGCA

Table 2. Animal strains used in this study.

Fly Line	**Source**
MiMIC-HA-dSERT-FWD (Line 2 or 4)	Generated in this study
MiMIC-HA-dSERT-REV (Line 3)	Generated in this study
MiMIC-HA-dSERT-Chi1 (Line 4)	Generated in this study
W1118; SERT16	H. Scholz
W1118; SERT10	H. Scholz
W1118	H. Scholz
SerT MiMIC MI02578	BSC 36004
Vas-Cas9-3xP3-GFP (III)	Supplied by Bestgene
Vas-Cas9-3xP3-GFP (x)	Supplied by Bestgene

Conclusions and Future Directions

This study contributes to our understanding of serotonergic modulation in the *Drosophila* visual system and established a model for future studies of serotonergic signaling. Serotonin is involved in many complex processes that are mediated through concentration gradients controlled by release sites, SERT, and flow of cerebral fluid, as well as many receptors with differential expression, dimerization, and serotonin binding affinities. The remarkable flexibility of the serotonin system is such that there will not be a single common cellular response to serotonin in post-synaptic neurons. We demonstrated that tracing the molecular mechanisms of serotonergic modulation will require a combination of receptor mapping to individual cells and subcellular compartments with complementary functional assays.

Serotonin is implicated in the treatment of mood and anxiety disorders, but these processes are currently challenging to model in the fly. To address this, we developed several approaches to humanize d*SERT*, which will enable improved SSRI studies in flies. Bypassing the pharmacological differences between invertebrates and mammals will enable us to employ the genetic tools available in *Drosophila* to ask questions relevant to the mammalian serotonin system. Specifically, we would like to evaluate the post-synaptic response to SSRI treatment over time to compare immediate vs. long-term transcriptomic changes in single cells types in adult *Drosophila*.

In this work, we focused on mapping serotonin receptor expression. However, it is increasingly recognized that serotonin neurons can release other neuromodulatory compounds, such as peptides. In the next stages of this research, it will be important to examine how other modulatory systems overlay the connectome and serotonin receptor mapping described here. Overall, this work informs our understanding of basic principles of neuromodulation and the integration of neuromodulatory signaling in sensory processing.

Bibliography

1. Kupfermann I. Modulatory actions of neurotransmitters. Annual review of neuroscience. 1979;2:447-65. doi: 10.1146/annurev.ne.02.030179.002311. PubMed PMID: 44174.

2. Marder E. Neuromodulation of neuronal circuits: back to the future. Neuron. 2012;76(1):1-11. doi: 10.1016/j.neuron.2012.09.010. PubMed PMID: 23040802; PubMed Central PMCID: PMC3482119.

3. Marder E, O'Leary T, Shruti S. Neuromodulation of circuits with variable parameters: single neurons and small circuits reveal principles of state-dependent and robust neuromodulation. Annual review of neuroscience. 2014;37:329-46. doi: 10.1146/annurev-neuro-071013-013958. PubMed PMID: 25032499.

4. Nadim F, Bucher D. Neuromodulation of neurons and synapses. Current opinion in neurobiology. 2014;29:48-56. doi: 10.1016/j.conb.2014.05.003. PubMed PMID: 24907657; PubMed Central PMCID: PMC4252488.

5. Katz PS. Beyond Neurotransmission : Neuromodulation and its Importance for Information Processing. Oxford ; New York: Oxford University Press; 1999. xiii, 391 p. p.

6. Millan MJ, Marin P, Bockaert J, Mannoury la Cour C. Signaling at G-protein-coupled serotonin receptors: recent advances and future research directions. Trends Pharmacol Sci. 2008;29(9):454-64. Epub 2008/08/05. doi: 10.1016/j.tips.2008.06.007. PubMed PMID: 18676031.

7. Nichols DE, Nichols CD. Serotonin receptors. Chemical reviews. 2008;108(5):1614-41. doi: 10.1021/cr078224o. PubMed PMID: 18476671.

8. Palacios JM. Serotonin receptors in brain revisited. Brain research. 2016;1645:46-9. Epub 2016/01/08. doi: 10.1016/j.brainres.2015.12.042. PubMed PMID: 26740406.

9. McCorvy JD, Roth BL. Structure and function of serotonin G protein-coupled receptors. Pharmacology & therapeutics. 2015;150:129-42. Epub 2015/01/21. doi: 10.1016/j.pharmthera.2015.01.009. PubMed PMID: 25601315; PubMed Central PMCID: PMCPMC4414735.

10. Giulietti M, Vivenzio V, Piva F, Principato G, Bellantuono C, Nardi B. How much do we know about the coupling of G-proteins to serotonin receptors? Mol Brain. 2014;7:49. Epub 2014/07/12. doi: 10.1186/s13041-014-0049-y. PubMed PMID: 25011628; PubMed Central PMCID: PMCPMC4105882.

11. Hanlon CD, Andrew DJ. Outside-in signaling--a brief review of GPCR signaling with a focus on the Drosophila GPCR family. J Cell Sci. 2015;128(19):3533-42. Epub 2015/09/09. doi: 10.1242/jcs.175158. PubMed PMID: 26345366; PubMed Central PMCID: PMCPMC4610211.

12. Pierce KL, Premont RT, Lefkowitz RJ. Seven-transmembrane receptors. Nat Rev Mol Cell Biol. 2002;3(9):639-50. Epub 2002/09/05. doi: 10.1038/nrm908. PubMed PMID: 12209124.

13. Maroteaux L, Bechade C, Roumier A. Dimers of serotonin receptors: Impact on ligand affinity and signaling. Biochimie. 2019;161:23-33. Epub 2019/01/28. doi: 10.1016/j.biochi.2019.01.009. PubMed PMID: 30685449.

14. Herrick-Davis K. Functional significance of serotonin receptor dimerization. Exp Brain Res. 2013;230(4):375-86. Epub 2013/07/03. doi: 10.1007/s00221-013-3622-1. PubMed PMID: 23811735; PubMed Central PMCID: PMCPMC3788847.

15. Rivera-Alba M, Vitaladevuni SN, Mishchenko Y, Lu Z, Takemura SY, Scheffer L, et al. Wiring economy and volume exclusion determine neuronal placement in the Drosophila brain. Current biology : CB. 2011;21(23):2000-5. doi: 10.1016/j.cub.2011.10.022. PubMed PMID: 22119527; PubMed Central PMCID: PMC3244492.

16. Takemura SY, Lu Z, Meinertzhagen IA. Synaptic circuits of the Drosophila optic lobe: the input terminals to the medulla. The Journal of comparative neurology. 2008;509(5):493-513. doi: 10.1002/cne.21757. PubMed PMID: 18537121; PubMed Central PMCID: PMC2481516.

17. Takemura SY, Bharioke A, Lu Z, Nern A, Vitaladevuni S, Rivlin PK, et al. A visual motion detection circuit suggested by Drosophila connectomics. Nature. 2013;500(7461):175-81. doi: 10.1038/nature12450. PubMed PMID: 23925240; PubMed Central PMCID: PMC3799980.

18. Takemura SY, Xu CS, Lu Z, Rivlin PK, Parag T, Olbris DJ, et al. Synaptic circuits and their variations within different columns in the visual system of Drosophila. Proceedings of the National Academy of Sciences of the United States of America. 2015;112(44):13711-6. doi: 10.1073/pnas.1509820112. PubMed PMID: 26483464; PubMed Central PMCID: PMC4640747.

19. Takemura SY, Nern A, Chklovskii DB, Scheffer LK, Rubin GM, Meinertzhagen IA. The comprehensive connectome of a neural substrate for 'ON' motion detection in. Elife. 2017;6. Epub 2017/04/22. doi: 10.7554/eLife.24394. PubMed PMID: 28432786; PubMed Central PMCID: PMCPMC5435463.

20. Meinertzhagen IA, O'Neil SD. Synaptic organization of columnar elements in the lamina of the wild type in Drosophila melanogaster. The Journal of comparative neurology. 1991;305(2):232-63. doi: 10.1002/cne.903050206. PubMed PMID: 1902848.

21. Moukhles H, Bosler O, Bolam JP, Vallee A, Umbriaco D, Geffard M, et al. Quantitative and morphometric data indicate precise cellular interactions between serotonin terminals and postsynaptic targets in rat substantia nigra. Neuroscience. 1997;76(4):1159-71. PubMed PMID: 9027876.

22. Herve D, Pickel VM, Joh TH, Beaudet A. Serotonin axon terminals in the ventral tegmental area of the rat: fine structure and synaptic input to dopaminergic neurons. Brain research. 1987;435(1-2):71-83. PubMed PMID: 2892580.

23. Gaspar P, Lillesaar C. Probing the diversity of serotonin neurons. Philosophical transactions of the Royal Society of London Series B, Biological sciences. 2012;367(1601):2382-94. doi: 10.1098/rstb.2011.0378. PubMed PMID: 22826339; PubMed Central PMCID: PMC3405676.

24. Mojtabai R, Olfson M. National trends in long-term use of antidepressant medications: results from the U.S. National Health and Nutrition Examination Survey. The Journal of clinical psychiatry. 2014;75(2):169-77. doi: 10.4088/JCP.13m08443. PubMed PMID: 24345349.

25. Taylor MJ, Freemantle N, Geddes JR, Bhagwagar Z. Early onset of selective serotonin reuptake inhibitor antidepressant action: systematic review and meta-analysis. Archives of general psychiatry. 2006;63(11):1217-23. doi: 10.1001/archpsyc.63.11.1217. PubMed PMID: 17088502; PubMed Central PMCID: PMC2211759.

26. Marjoribanks J, Brown J, O'Brien PM, Wyatt K. Selective serotonin reuptake inhibitors for premenstrual syndrome. The Cochrane database of systematic reviews. 2013;(6):CD001396. doi: 10.1002/14651858.CD001396.pub3. PubMed PMID: 23744611.

27. Sepede G, Sarchione F, Matarazzo I, Di Giannantonio M, Salerno RM. Premenstrual Dysphoric Disorder Without Comorbid Psychiatric Conditions: A Systematic Review of Therapeutic Options. Clinical neuropharmacology. 2016;39(5):241-61. doi: 10.1097/WNF.0000000000000173. PubMed PMID: 27454391.

28. Steinberg EM, Cardoso GM, Martinez PE, Rubinow DR, Schmidt PJ. Rapid response to fluoxetine in women with premenstrual dysphoric disorder. Depression and anxiety. 2012;29(6):531-40. doi: 10.1002/da.21959. PubMed PMID: 22565858; PubMed Central PMCID: PMC3442940.

29. Grillon C, Levenson J, Pine DS. A single dose of the selective serotonin reuptake inhibitor citalopram exacerbates anxiety in humans: a fear-potentiated startle study. Neuropsychopharmacology : official publication of the American College of Neuropsychopharmacology. 2007;32(1):225-31. doi: 10.1038/sj.npp.1301204. PubMed PMID: 16971899.

30. Browning M, Reid C, Cowen PJ, Goodwin GM, Harmer CJ. A single dose of citalopram increases fear recognition in healthy subjects. Journal of psychopharmacology. 2007;21(7):684-90. doi: 10.1177/0269881106074062. PubMed PMID: 17259206.

31. Berton O, McClung CA, Dileone RJ, Krishnan V, Renthal W, Russo SJ, et al. Essential role of BDNF in the mesolimbic dopamine pathway in social defeat stress. Science. 2006;311(5762):864-8. doi: 10.1126/science.1120972. PubMed PMID: 16469931.

32. Moreau AW, Amar M, Le Roux N, Morel N, Fossier P. Serotoninergic fine-tuning of the excitation-inhibition balance in rat visual cortical networks. Cereb Cortex. 2010;20(2):456-67. Epub 2009/06/11. doi: 10.1093/cercor/bhp114. PubMed PMID: 19520765.

33. Arechiga H, Banuelos E, Frixione E, Picones A, Rodriguez-Sosa L. Modulation of crayfish retinal sensitivity by 5-hydroxytryptamine. The Journal of experimental biology. 1990;150:123-43. PubMed PMID: 2355208.

34. Seillier L, Lorenz C, Kawaguchi K, Ott T, Nieder A, Pourriahi P, et al. Serotonin Decreases the Gain of Visual Responses in Awake Macaque V1. The Journal of neuroscience : the official journal of the Society for Neuroscience. 2017;37(47):11390-405. doi: 10.1523/JNEUROSCI.1339-17.2017. PubMed PMID: 29042433; PubMed Central PMCID: PMC5700422.

35. Kloppenburg P, Ferns D, Mercer AR. Serotonin enhances central olfactory neuron responses to female sex pheromone in the male sphinx moth manduca sexta. The Journal of neuroscience : the official journal of the Society for Neuroscience. 1999;19(19):8172-81. PubMed PMID: 10493719.

36. Dacks AM, Christensen TA, Hildebrand JG. Modulation of olfactory information processing in the antennal lobe of Manduca sexta by serotonin. Journal of neurophysiology. 2008;99(5):2077-85. doi: 10.1152/jn.01372.2007. PubMed PMID: 18322001.

37. Lottem E, Lorincz ML, Mainen ZF. Optogenetic Activation of Dorsal Raphe Serotonin Neurons Rapidly Inhibits Spontaneous But Not Odor-Evoked Activity in Olfactory Cortex. The Journal of neuroscience : the official journal of the Society for Neuroscience. 2016;36(1):7-18. doi: 10.1523/JNEUROSCI.3008-15.2016. PubMed PMID: 26740645.

38. Brunert D, Tsuno Y, Rothermel M, Shipley MT, Wachowiak M. Cell-Type-Specific Modulation of Sensory Responses in Olfactory Bulb Circuits by Serotonergic Projections from the Raphe Nuclei. The Journal of neuroscience : the official journal of the Society for Neuroscience. 2016;36(25):6820-35. doi: 10.1523/JNEUROSCI.3667-15.2016. PubMed PMID: 27335411; PubMed Central PMCID: PMC4916254.

39. Petzold GC, Hagiwara A, Murthy VN. Serotonergic modulation of odor input to the mammalian olfactory bulb. Nature neuroscience. 2009;12(6):784-91. doi: 10.1038/nn.2335. PubMed PMID: 19430472.

40. Papesh MA, Hurley LM. Modulation of auditory brainstem responses by serotonin and specific serotonin receptors. Hearing research. 2016;332:121-36. doi: 10.1016/j.heares.2015.11.014. PubMed PMID: 26688176.

41. Fotowat H, Harvey-Girard E, Cheer JF, Krahe R, Maler L. Subsecond Sensory Modulation of Serotonin Levels in a Primary Sensory Area and Its Relation to Ongoing Communication Behavior in a Weakly Electric Fish. eNeuro. 2016;3(5). doi: 10.1523/ENEURO.0115-16.2016. PubMed PMID: 27844054; PubMed Central PMCID: PMC5093153.

42. Andres M, Seifert M, Spalthoff C, Warren B, Weiss L, Giraldo D, et al. Auditory Efferent System Modulates Mosquito Hearing. Current biology : CB. 2016;26(15):2028-36. doi: 10.1016/j.cub.2016.05.077. PubMed PMID: 27476597.

43. Watakabe A, Komatsu Y, Sadakane O, Shimegi S, Takahata T, Higo N, et al. Enriched expression of serotonin 1B and 2A receptor genes in macaque visual cortex and their bidirectional modulatory effects on neuronal responses. Cereb Cortex. 2009;19(8):1915-28. doi: 10.1093/cercor/bhn219. PubMed PMID: 19056862; PubMed Central PMCID: PMC2705701.

44. Nassel DR. Serotonin and serotonin-immunoreactive neurons in the nervous system of insects. Progress in neurobiology. 1988;30(1):1-85. PubMed PMID: 3275407.

45. Valles AM, White K. Serotonin-containing neurons in Drosophila melanogaster: development and distribution. The Journal of comparative neurology. 1988;268(3):414-28. doi: 10.1002/cne.902680310. PubMed PMID: 3129459.

46. Xu L, He J, Kaiser A, Graber N, Schlager L, Ritze Y, et al. A Single Pair of Serotonergic Neurons Counteracts Serotonergic Inhibition of Ethanol Attraction in Drosophila. PloS one. 2016;11(12):e0167518. doi: 10.1371/journal.pone.0167518. PubMed PMID: 27936023; PubMed Central PMCID: PMC5147910.

47. Pooryasin A, Fiala A. Identified Serotonin-Releasing Neurons Induce Behavioral Quiescence and Suppress Mating in Drosophila. The Journal of neuroscience : the official journal of the Society for Neuroscience. 2015;35(37):12792-812. doi: 10.1523/JNEUROSCI.1638-15.2015. PubMed PMID: 26377467.

48. Sitaraman D, Zars M, Laferriere H, Chen YC, Sable-Smith A, Kitamoto T, et al. Serotonin is necessary for place memory in Drosophila. Proceedings of the National Academy of Sciences of the United States of America. 2008;105(14):5579-84. doi: 10.1073/pnas.0710168105. PubMed PMID: 18385379; PubMed Central PMCID: PMC2291120.

49. Borst A, Helmstaedter M. Common circuit design in fly and mammalian motion vision. Nature neuroscience. 2015;18(8):1067-76. doi: 10.1038/nn.4050. PubMed PMID: 26120965.

50. Cheng KY, Frye MA. Neuromodulation of insect motion vision. J Comp Physiol A Neuroethol Sens Neural Behav Physiol. 2019. doi: 10.1007/s00359-019-01383-9. PubMed PMID: 31811398.

51. Fischbach KF, Dittrich APM. The optic lobe of Drosophila melanogaster. I. A Golgi analysis of wild type structure. Cell Tissue Res. 1989;258:441-75.

52. Sanes JR, Zipursky SL. Design principles of insect and vertebrate visual systems. Neuron. 2010;66(1):15-36. doi: 10.1016/j.neuron.2010.01.018. PubMed PMID: 20399726; PubMed Central PMCID: PMC2871012.

53. Strother JA, Nern A, Reiser MB. Direct observation of ON and OFF pathways in the Drosophila visual system. Current biology : CB. 2014;24(9):976-83. Epub 2014/04/03. doi: 10.1016/j.cub.2014.03.017. PubMed PMID: 24704075.

54. Tuthill JC, Nern A, Holtz SL, Rubin GM, Reiser MB. Contributions of the 12 neuron classes in the fly lamina to motion vision. Neuron. 2013;79(1):128-40. doi: 10.1016/j.neuron.2013.05.024. PubMed PMID: 23849200; PubMed Central PMCID: PMC3806040.

55. Maisak MS, Haag J, Ammer G, Serbe E, Meier M, Leonhardt A, et al. A directional tuning map of Drosophila elementary motion detectors. Nature. 2013;500(7461):212-6. doi: 10.1038/nature12320. PubMed PMID: 23925246.

56. Bahl A, Serbe E, Meier M, Ammer G, Borst A. Neural Mechanisms for Drosophila Contrast Vision. Neuron. 2015;88(6):1240-52. doi: 10.1016/j.neuron.2015.11.004. PubMed PMID: 26673659.

57. Shinomiya K, Huang G, Lu Z, Parag T, Xu CS, Aniceto R, et al. Comparisons between the ON- and OFF-edge motion pathways in the Drosophila brain. Elife. 2019;8. doi: 10.7554/eLife.40025. PubMed PMID: 30624205; PubMed Central PMCID: PMC6338461.

58. Davis FP, Nern A, Picard S, Reiser MB, Rubin GM, Eddy SR, et al. A genetic, genomic, and computational resource for exploring neural circuit function. eLife. 2020;9. Epub 2020/01/16. doi: 10.7554/eLife.50901. PubMed PMID: 31939737; PubMed Central PMCID: PMCPMC7034979.

59. Wasserman SM, Aptekar JW, Lu P, Nguyen J, Wang AL, Keles MF, et al. Olfactory neuromodulation of motion vision circuitry in Drosophila. Current biology : CB. 2015;25(4):467-72. doi: 10.1016/j.cub.2014.12.012. PubMed PMID: 25619767; PubMed Central PMCID: PMC4331282.

60. Strother JA, Wu ST, Rogers EM, Eliason JLM, Wong AM, Nern A, et al. Behavioral state modulates the ON visual motion pathway of Drosophila. Proceedings of the National Academy of Sciences of the United States of America. 2018;115(1):E102-E11. doi: 10.1073/pnas.1703090115. PubMed PMID: 29255026; PubMed Central PMCID: PMC5776785.

61. Cheng KY, Colbath RA, Frye MA. Olfactory and Neuromodulatory Signals Reverse Visual Object Avoidance to Approach in Drosophila. Current biology : CB. 2019;29(12):2058-65 e2. doi: 10.1016/j.cub.2019.05.010. PubMed PMID: 31155354; PubMed Central PMCID: PMC6615044.

62. Hevers W, Hardie RC. Serotonin modulates the voltage dependence of delayed rectifier and Shaker potassium channels in Drosophila photoreceptors. Neuron. 1995;14:845-56.

63. Kloppenburg P, Erber J. The modulatory effects of serotonin and octopamine in the visual system of the honey bee (Apis mellifera L.) II. Electrophysiological analysis of motion-sensitive neurons in the lobula. J Comp Physiol A Neuroethol Sens Neural Behav Physiol. 1995;176:119-29.

64. Suver MP, Mamiya A, Dickinson MH. Octopamine neurons mediate flight-induced modulation of visual processing in Drosophila. Current biology : CB. 2012;22(24):2294-302. doi: 10.1016/j.cub.2012.10.034. PubMed PMID: 23142045.

65. Leitinger G, Pabst MA, Kral K. Serotonin-immunoreactive neurones in the visual system of the praying mantis: an immunohistochemical, confocal laser scanning and electron microscopic study. Brain research. 1999;823(1-2):11-23. PubMed PMID: 10095007.

66. Nassel DR, Meyer EP, Klemm N. Mapping and ultrastructure of serotonin-immunoreactive neurons in the optic lobes of three insect species. The Journal of comparative neurology. 1985;232(2):190-204. doi: 10.1002/cne.902320205. PubMed PMID: 3973090.

67. Nassel DR, Ohlsson L, Sivasubramanian P. Postembryonic differentiation of serotonin-immunoreactive neurons in fleshfly optic lobes developing in situ or cultured in vivo without eye discs. The Journal of comparative neurology. 1987;255(3):327-40. doi: 10.1002/cne.902550302. PubMed PMID: 3546409.

68. Hamanaka Y, Kinoshita M, Homberg U, Arikawa K. Immunocytochemical localization of amines and GABA in the optic lobe of the butterfly, Papilio xuthus. PloS one. 2012;7(7):e41109. doi: 10.1371/journal.pone.0041109. PubMed PMID: 22844431; PubMed Central PMCID: PMC3402530.

69. Schafer S, Bicker G. Common projection areas of 5-HT- and GABA-like immunoreactive fibers in the visual system of the honeybee. Brain research. 1986;380(2):368-70. PubMed PMID: 3530374.

70. Chen B, Meinertzhagen IA, Shaw SR. Circadian rhythms in light-evoked responses of the fly's compound eye, and the effects of neuromodulators 5-HT and the peptide PDF. J Comp Physiol [A]. 1999;185:393-404.

71. Ichikawa T. Light suppresses the activity of serotonin-immunoreactive neurons in the optic lobe of the swallowtail butterfly. Neurosci Lett. 1994;172(1-2):115-8. PubMed PMID: 8084513.

72. Araneda R, Andrade R. 5-Hydroxytryptamine2 and 5-hydroxytryptamine 1A receptors mediate opposing responses on membrane excitability in rat association cortex. Neuroscience. 1991;40(2):399-412. doi: 10.1016/0306-4522(91)90128-b. PubMed PMID: 1851255.

73. Celada P, Puig MV, Artigas F. Serotonin modulation of cortical neurons and networks. Frontiers in integrative neuroscience. 2013;7:25. doi: 10.3389/fnint.2013.00025. PubMed PMID: 23626526; PubMed Central PMCID: PMC3630391.

74. Colas JF, Launay JM, Kellermann O, Rosay P, Maroteaux L. Drosophila 5-HT2 serotonin receptor: coexpression with fushi-tarazu during segmentation. Proceedings of the National Academy of Sciences of the United States of America. 1995;92(12):5441-5. PubMed PMID: 7777527; PubMed Central PMCID: PMC41710.

75. Gasque G, Conway S, Huang J, Rao Y, Vosshall LB. Small molecule drug screening in Drosophila identifies the 5HT2A receptor as a feeding modulation target. Scientific reports. 2013;3:srep02120. doi: 10.1038/srep02120. PubMed PMID: 23817146; PubMed Central PMCID: PMC3698492.

76. Saudou F, Boschert U, Amlaiky N, Plassat JL, Hen R. A family of Drosophila serotonin receptors with distinct intracellular signalling properties and expression patterns. The EMBO journal. 1992;11(1):7-17. PubMed PMID: 1310937; PubMed Central PMCID: PMC556419.

77. Witz P, Amlaiky N, Plassat JL, Maroteaux L, Borrelli E, Hen R. Cloning and characterization of a Drosophila serotonin receptor that activates adenylate cyclase. Proceedings of the National Academy of Sciences of the United States of America. 1990;87(22):8940-4. PubMed PMID: 2174167; PubMed Central PMCID: PMC55076.

78. Blenau W, Daniel S, Balfanz S, Thamm M, Baumann A. Dm5-HT2B: Pharmacological Characterization of the Fifth Serotonin Receptor Subtype of Drosophila melanogaster. Front Syst Neurosci. 2017;11:28. Epub 2017/05/11. doi: 10.3389/fnsys.2017.00028. PubMed PMID: 28553207; PubMed Central PMCID: PMCPMC5425475.

79. Gnerer JP, Venken KJ, Dierick HA. Gene-specific cell labeling using MiMIC transposons. Nucleic acids research. 2015;43(8):e56. doi: 10.1093/nar/gkv113. PubMed PMID: 25712101; PubMed Central PMCID: PMC4417149.

80. Venken KJ, Schulze KL, Haelterman NA, Pan H, He Y, Evans-Holm M, et al. MiMIC: a highly versatile transposon insertion resource for engineering Drosophila melanogaster genes.

Nature methods. 2011;8(9):737-43. PubMed PMID: 21985007; PubMed Central PMCID: PMC3191940.

81. Diao F, Ironfield H, Luan H, Shropshire WC, Ewer J, Marr E, et al. Plug-and-play genetic access to drosophila cell types using exchangeable exon cassettes. Cell Rep. 2015;10(8):1410-21. Epub 2015/02/26. doi: 10.1016/j.celrep.2015.01.059. PubMed PMID: 25732830; PubMed Central PMCID: PMCPMC4373654.

82. Joesch M, Schnell B, Raghu SV, Reiff DF, Borst A. ON and OFF pathways in Drosophila motion vision. Nature. 2010;468(7321):300-4. doi: 10.1038/nature09545. PubMed PMID: 21068841.

83. Edwards TN, Meinertzhagen IA. The functional organisation of glia in the adult brain of Drosophila and other insects. Progress in neurobiology. 2010;90(4):471-97. doi: 10.1016/j.pneurobio.2010.01.001. PubMed PMID: 20109517; PubMed Central PMCID: PMC2847375.

84. Chang H-Y, Grygoruk A, Brooks ES, Ackerson LC, Maidment NT, Bainton RJ, et al. Over-expression of the Drosophila vesicular monoamine transporter increases motor activity and courtship but decreases the behavioral response to cocaine. Molecular psychiatry. 2006;11:99-113.

85. Monastirioti M. Biogenic amine systems in the fruit fly Drosophila melanogaster. Microscopy research and technique. 1999;45(2):106-21. doi: 10.1002/(SICI)1097-0029(19990415)45:2<106::AID-JEMT5>3.0.CO;2-3. PubMed PMID: 10332728.

86. Nern A, Pfeiffer BD, Rubin GM. Optimized tools for multicolor stochastic labeling reveal diverse stereotyped cell arrangements in the fly visual system. Proceedings of the National Academy of Sciences of the United States of America. 2015;112(22):E2967-76. doi: 10.1073/pnas.1506763112. PubMed PMID: 25964354; PubMed Central PMCID: PMC4460454.

87. Konstantinides N, Kapuralin K, Fadil C, Barboza L, Satija R, Desplan C. Phenotypic Convergence: Distinct Transcription Factors Regulate Common Terminal Features. Cell. 2018;174(3):622-35 e13. Epub 2018/06/19. doi: 10.1016/j.cell.2018.05.021. PubMed PMID: 29909983; PubMed Central PMCID: PMCPMC6082168.

88. Hasegawa E, Kitada Y, Kaido M, Takayama R, Awasaki T, Tabata T, et al. Concentric zones, cell migration and neuronal circuits in the Drosophila visual center. Development. 2011;138(5):983-93. doi: 10.1242/dev.058370. PubMed PMID: 21303851.

89. DeSalvo MK, Hindle SJ, Rusan ZM, Orng S, Eddison M, Halliwill K, et al. The Drosophila surface glia transcriptome: evolutionary conserved blood-brain barrier processes. Front Neurosci. 2014;8:346. Epub 2014/11/27. doi: 10.3389/fnins.2014.00346. PubMed PMID: 25426014; PubMed Central PMCID: PMCPMC4224204.

90. Deng B, Li Q, Liu X, Cao Y, Li B, Qian Y, et al. Chemoconnectomics: Mapping Chemical Transmission in Drosophila. Neuron. 2019;101(5):876-93 e4. doi: 10.1016/j.neuron.2019.01.045. PubMed PMID: 30799021.

91. Qian Y, Cao Y, Deng B, Yang G, Li J, Xu R, et al. Sleep homeostasis regulated by 5HT2b receptor in a small subset of neurons in the dorsal fan-shaped body of drosophila. eLife.

2017;6. Epub 2017/10/07. doi: 10.7554/eLife.26519. PubMed PMID: 28984573; PubMed Central PMCID: PMCPMC5648528.

92. Hoyer D, Hannon JP, Martin GR. Molecular, pharmacological and functional diversity of 5-HT receptors. Pharmacol Biochem Behav. 2002;71(4):533-54. PubMed PMID: 11888546.

93. Chen TW, Wardill TJ, Sun Y, Pulver SR, Renninger SL, Baohan A, et al. Ultrasensitive fluorescent proteins for imaging neuronal activity. Nature. 2013;499(7458):295-300. doi: 10.1038/nature12354. PubMed PMID: 23868258; PubMed Central PMCID: PMC3777791.

94. Liu C, Meng Z, Wiggin TD, Yu J, Reed ML, Guo F, et al. A Serotonin-Modulated Circuit Controls Sleep Architecture to Regulate Cognitive Function Independent of Total Sleep in Drosophila. Current biology : CB. 2019;29(21):3635-46 e5. Epub 2019/11/02. doi: 10.1016/j.cub.2019.08.079. PubMed PMID: 31668619; PubMed Central PMCID: PMCPMC6832866.

95. Narahashi T. Tetrodotoxin: a brief history. Proc Jpn Acad Ser B Phys Biol Sci. 2008;84(5):147-54. Epub 2008/10/23. doi: 10.2183/pjab.84.147. PubMed PMID: 18941294; PubMed Central PMCID: PMCPMC2858367.

96. Narahashi T, Moore JW, Scott WR. Tetrodotoxin Blockage of Sodium Conductance Increase in Lobster Giant Axons. The Journal of general physiology. 1964;47:965-74. Epub 1964/05/01. doi: 10.1085/jgp.47.5.965. PubMed PMID: 14155438; PubMed Central PMCID: PMCPMC2195365.

97. Polter AM, Li X. 5-HT1A receptor-regulated signal transduction pathways in brain. Cell Signal. 2010;22(10):1406-12. Epub 2010/04/02. doi: 10.1016/j.cellsig.2010.03.019. PubMed PMID: 20363322; PubMed Central PMCID: PMCPMC2903656.

98. Cao G, Platisa J, Pieribone VA, Raccuglia D, Kunst M, Nitabach MN. Genetically targeted optical electrophysiology in intact neural circuits. Cell. 2013;154(4):904-13. Epub 2013/08/08. doi: 10.1016/j.cell.2013.07.027. PubMed PMID: 23932121; PubMed Central PMCID: PMCPMC3874294.

99. Takemura SY, Nern A, Chklovskii DB, Scheffer LK, Rubin GM, Meinertzhagen IA. The comprehensive connectome of a neural substrate for 'ON' motion detection in Drosophila. eLife. 2017;6. doi: 10.7554/eLife.24394. PubMed PMID: 28432786; PubMed Central PMCID: PMC5435463.

100. Stuart AE, Borycz J, Meinertzhagen IA. The dynamics of signaling at the histaminergic photoreceptor synapse of arthropods. Progress in neurobiology. 2007;82(4):202-27. doi: 10.1016/j.pneurobio.2007.03.006. PubMed PMID: 17531368.

101. Chaturvedi R, Reddig K, Li HS. Long-distance mechanism of neurotransmitter recycling mediated by glial network facilitates visual function in Drosophila. Proceedings of the National Academy of Sciences of the United States of America. 2014;111(7):2812-7. doi: 10.1073/pnas.1323714111. PubMed PMID: 24550312; PubMed Central PMCID: PMC3932938.

102. Nikolaev A, Zheng L, Wardill TJ, O'Kane CJ, de Polavieja GG, Juusola M. Network adaptation improves temporal representation of naturalistic stimuli in Drosophila eye: II

mechanisms. PloS one. 2009;4(1):e4306. doi: 10.1371/journal.pone.0004306. PubMed PMID: 19180195; PubMed Central PMCID: PMC2628722.

103. Kolodziejczyk A, Sun X, Meinertzhagen IA, Nassel DR. Glutamate, GABA and acetylcholine signaling components in the lamina of the Drosophila visual system. PloS one. 2008;3(5):e2110. doi: 10.1371/journal.pone.0002110. PubMed PMID: 18464935; PubMed Central PMCID: PMC2373871.

104. Mu L, Ito K, Bacon JP, Strausfeld NJ. Optic glomeruli and their inputs in Drosophila share an organizational ground pattern with the antennal lobes. The Journal of neuroscience : the official journal of the Society for Neuroscience. 2012;32(18):6061-71. doi: 10.1523/JNEUROSCI.0221-12.2012. PubMed PMID: 22553013; PubMed Central PMCID: PMC3358351.

105. Juusola M, Uusitalo RO, Weckstrom M. Transfer of graded potentials at the photoreceptor-interneuron synapse. The Journal of general physiology. 1995;105(1):117-48. doi: 10.1085/jgp.105.1.117. PubMed PMID: 7537323; PubMed Central PMCID: PMC2216927.

106. Uusitalo RO, Juusola M, Kouvalainen E, Weckstrom M. Tonic transmitter release in a graded potential synapse. Journal of neurophysiology. 1995;74(1):470-3. doi: 10.1152/jn.1995.74.1.470. PubMed PMID: 7472349.

107. Takemura SY, Karuppudurai T, Ting CY, Lu Z, Lee CH, Meinertzhagen IA. Cholinergic circuits integrate neighboring visual signals in a Drosophila motion detection pathway. Current biology : CB. 2011;21(24):2077-84. Epub 2011/12/01. doi: 10.1016/j.cub.2011.10.053. PubMed PMID: 22137471; PubMed Central PMCID: PMCPMC3265035.

108. Shinomiya K, Karuppudurai T, Lin TY, Lu Z, Lee CH, Meinertzhagen IA. Candidate neural substrates for off-edge motion detection in Drosophila. Current biology : CB. 2014;24(10):1062-70. Epub 2014/04/24. doi: 10.1016/j.cub.2014.03.051. PubMed PMID: 24768048; PubMed Central PMCID: PMCPMC4031294.

109. Gagolewicz PJ, Dringenberg HC. Age-Dependent Switch of the Role of Serotonergic 5-HT1A Receptors in Gating Long-Term Potentiation in Rat Visual Cortex In Vivo. Neural Plast. 2016;2016:6404082. Epub 2016/05/10. doi: 10.1155/2016/6404082. PubMed PMID: 27247804; PubMed Central PMCID: PMCPMC4877497.

110. Halberstadt AL. Recent advances in the neuropsychopharmacology of serotonergic hallucinogens. Behav Brain Res. 2015;277:99-120. Epub 2014/07/15. doi: 10.1016/j.bbr.2014.07.016. PubMed PMID: 25036425; PubMed Central PMCID: PMCPMC4642895.

111. Li YH, Xiang K, Xu X, Zhao X, Li Y, Zheng L, et al. Co-activation of both 5-HT1A and 5-HT7 receptors induced attenuation of glutamatergic synaptic transmission in the rat visual cortex. Neurosci Lett. 2018;686:122-6. Epub 2018/09/08. doi: 10.1016/j.neulet.2018.09.013. PubMed PMID: 30205142.

112. Zhou X, Zhang R, Zhang S, Wu J, Sun X. Activation of 5-HT1A receptors promotes retinal ganglion cell function by inhibiting the cAMP-PKA pathway to modulate presynaptic GABA release in chronic glaucoma. The Journal of neuroscience : the official journal of the

Society for Neuroscience. 2018. Epub 2018/12/12. doi: 10.1523/JNEUROSCI.1685-18.2018. PubMed PMID: 30541912.

113. Schindelin J, Arganda-Carreras I, Frise E, Kaynig V, Longair M, Pietzsch T, et al. Fiji: an open-source platform for biological-image analysis. Nature methods. 2012;9(7):676-82. Epub 2012/06/28. doi: 10.1038/nmeth.2019. PubMed PMID: 22743772; PubMed Central PMCID: PMCPMC3855844.

114. Tan L, Zhang KX, Pecot MY, Nagarkar-Jaiswal S, Lee PT, Takemura SY, et al. Ig Superfamily Ligand and Receptor Pairs Expressed in Synaptic Partners in Drosophila. Cell. 2015;163(7):1756-69. doi: 10.1016/j.cell.2015.11.021. PubMed PMID: 26687360; PubMed Central PMCID: PMC4804707.

115. Hu Y, Sopko R, Foos M, Kelley C, Flockhart I, Ammeux N, et al. FlyPrimerBank: an online database for Drosophila melanogaster gene expression analysis and knockdown evaluation of RNAi reagents. G3 (Bethesda). 2013;3(9):1607-16. Epub 2013/09/04. doi: 10.1534/g3.113.007021. PubMed PMID: 23893746; PubMed Central PMCID: PMCPMC3755921.

116. Schmittgen TD, Livak KJ. Analyzing real-time PCR data by the comparative C(T) method. Nature protocols. 2008;3(6):1101-8. PubMed PMID: 18546601.

117. Picelli S, Bjorklund AK, Faridani OR, Sagasser S, Winberg G, Sandberg R. Smart-seq2 for sensitive full-length transcriptome profiling in single cells. Nature methods. 2013;10(11):1096-8. doi: 10.1038/nmeth.2639. PubMed PMID: 24056875.

118. Picelli S, Faridani OR, Bjorklund AK, Winberg G, Sagasser S, Sandberg R. Full-length RNA-seq from single cells using Smart-seq2. Nature protocols. 2014;9(1):171-81. doi: 10.1038/nprot.2014.006. PubMed PMID: 24385147.

119. Dobin A, Davis CA, Schlesinger F, Drenkow J, Zaleski C, Jha S, et al. STAR: ultrafast universal RNA-seq aligner. Bioinformatics. 2013;29(1):15-21. doi: 10.1093/bioinformatics/bts635. PubMed PMID: 23104886; PubMed Central PMCID: PMC3530905.

120. Keles MF, Frye MA. Object-Detecting Neurons in Drosophila. Current biology : CB. 2017;27(5):680-7. doi: 10.1016/j.cub.2017.01.012. PubMed PMID: 28190726; PubMed Central PMCID: PMCPMC5340600.

121. Wilson RI, Turner GC, Laurent G. Transformation of olfactory representations in the Drosophila antennal lobe. Science. 2004;303(5656):366-70. Epub 2003/12/18. doi: 10.1126/science.1090782. PubMed PMID: 14684826.

122. Akin O, Zipursky SL. Frazzled promotes growth cone attachment at the source of a Netrin gradient in the Drosophila visual system. Elife. 2016;5. doi: 10.7554/eLife.20762. PubMed PMID: 27743477; PubMed Central PMCID: PMC5108592.

123. Lombaert N, Hennes M, Gilissen S, Schevenels G, Aerts L, Vanlaer R, et al. 5-HTR2A and 5-HTR3A but not 5-HTR1A antagonism impairs the cross-modal reactivation of deprived visual cortex in adulthood. Mol Brain. 2018;11(1):65. Epub 2018/11/06. doi: 10.1186/s13041-018-0404-5. PubMed PMID: 30400993; PubMed Central PMCID: PMCPMC6218970.

124. Gu Q, Singer W. Involvement of serotonin in developmental plasticity of kitten visual cortex. Eur J Neurosci. 1995;7(6):1146-53. PubMed PMID: 7582087.

125. Wang Y, Gu Q, Cynader MS. Blockade of serotonin-2C receptors by mesulergine reduces ocular dominance plasticity in kitten visual cortex. Exp Brain Res. 1997;114(2):321-8. PubMed PMID: 9166921.

126. Shimegi S, Kimura A, Sato A, Aoyama C, Mizuyama R, Tsunoda K, et al. Cholinergic and serotonergic modulation of visual information processing in monkey V1. Journal of physiology, Paris. 2016;110(1-2):44-51. doi: 10.1016/j.jphysparis.2016.09.001. PubMed PMID: 27619519.

127. Trakhtenberg EF, Pita-Thomas W, Fernandez SG, Patel KH, Venugopalan P, Shechter JM, et al. Serotonin receptor 2C regulates neurite growth and is necessary for normal retinal processing of visual information. Developmental neurobiology. 2017;77(4):419-37. doi: 10.1002/dneu.22391. PubMed PMID: 26999672.

128. Clark DA, Bursztyn L, Horowitz MA, Schnitzer MJ, Clandinin TR. Defining the computational structure of the motion detector in Drosophila. Neuron. 2011;70(6):1165-77. doi: 10.1016/j.neuron.2011.05.023. PubMed PMID: 21689602; PubMed Central PMCID: PMC3121538.

129. Yang HH, St-Pierre F, Sun X, Ding X, Lin MZ, Clandinin TR. Subcellular Imaging of Voltage and Calcium Signals Reveals Neural Processing In Vivo. Cell. 2016;166(1):245-57. doi: 10.1016/j.cell.2016.05.031. PubMed PMID: 27264607; PubMed Central PMCID: PMC5606228.

130. Zheng L, de Polavieja GG, Wolfram V, Asyali MH, Hardie RC, Juusola M. Feedback network controls photoreceptor output at the layer of first visual synapses in Drosophila. The Journal of general physiology. 2006;127(5):495-510. doi: 10.1085/jgp.200509470. PubMed PMID: 16636201; PubMed Central PMCID: PMC2151524.

131. Behnia R, Desplan C. Visual circuits in flies: beginning to see the whole picture. Curr Opin Neurobiol. 2015;34:125-32. doi: 10.1016/j.conb.2015.03.010. PubMed PMID: 25881091; PubMed Central PMCID: PMCPMC4577302.

132. Pyza E, Meinertzhagen IA. Neurotransmitters regulate rhythmic size changes amongst cells in the fly's optic lobe. Journal of comparative physiology A, Sensory, neural, and behavioral physiology. 1996;178(1):33-45. doi: 10.1007/bf00189588. PubMed PMID: 8568723.

133. Marder E. Variability, compensation, and modulation in neurons and circuits. Proceedings of the National Academy of Sciences of the United States of America. 2011;108 Suppl 3:15542-8. doi: 10.1073/pnas.1010674108. PubMed PMID: 21383190; PubMed Central PMCID: PMC3176600.

134. Prinz AA, Thirumalai V, Marder E. The functional consequences of changes in the strength and duration of synaptic inputs to oscillatory neurons. The Journal of neuroscience : the official journal of the Society for Neuroscience. 2003;23(3):943-54. PubMed PMID: 12574423; PubMed Central PMCID: PMC6741924.

135. Descarries L, Mechawar N. Ultrastructural evidence for diffuse transmission by monoamine and acetylcholine neurons of the central nervous system. Prog Brain Res. 2000;125:27-47. doi: 10.1016/S0079-6123(00)25005-X. PubMed PMID: 11098652.

136. Bunin MA, Wightman RM. Paracrine neurotransmission in the CNS: involvement of 5-HT. Trends Neurosci. 1999;22(9):377-82. PubMed PMID: 10441294.

137. Coates KE, Majot AT, Zhang X, Michael CT, Spitzer SL, Gaudry Q, et al. Identified Serotonergic Modulatory Neurons Have Heterogeneous Synaptic Connectivity within the Olfactory System of Drosophila. The Journal of neuroscience : the official journal of the Society for Neuroscience. 2017;37(31):7318-31. doi: 10.1523/JNEUROSCI.0192-17.2017. PubMed PMID: 28659283; PubMed Central PMCID: PMC5546105.

138. Riad M, Garcia S, Watkins KC, Jodoin N, Doucet E, Langlois X, et al. Somatodendritic localization of 5-HT1A and preterminal axonal localization of 5-HT1B serotonin receptors in adult rat brain. The Journal of comparative neurology. 2000;417(2):181-94. PubMed PMID: 10660896.

139. Azmitia EC, Gannon PJ, Kheck NM, Whitaker-Azmitia PM. Cellular localization of the 5-HT1A receptor in primate brain neurons and glial cells. Neuropsychopharmacology : official publication of the American College of Neuropsychopharmacology. 1996;14(1):35-46. doi: 10.1016/S0893-133X(96)80057-1. PubMed PMID: 8719028.

140. Alekseyenko OV, Chan YB, Okaty BW, Chang Y, Dymecki SM, Kravitz EA. Serotonergic Modulation of Aggression in Drosophila Involves GABAergic and Cholinergic Opposing Pathways. Current biology : CB. 2019;29(13):2145-56 e5. Epub 2019/06/25. doi: 10.1016/j.cub.2019.05.070. PubMed PMID: 31231050; PubMed Central PMCID: PMCPMC6633915.

141. Yuan Q, Lin F, Zheng X, Sehgal A. Serotonin modulates circadian entrainment in Drosophila. Neuron. 2005;47(1):115-27. doi: 10.1016/j.neuron.2005.05.027. PubMed PMID: 15996552.

142. Nicolai LJ, Ramaekers A, Raemaekers T, Drozdzecki A, Mauss AS, Yan J, et al. Genetically encoded dendritic marker sheds light on neuronal connectivity in Drosophila. Proceedings of the National Academy of Sciences of the United States of America. 2010;107(47):20553-8. doi: 10.1073/pnas.1010198107. PubMed PMID: 21059961; PubMed Central PMCID: PMC2996714.

143. Macpherson LJ, Zaharieva EE, Kearney PJ, Alpert MH, Lin TY, Turan Z, et al. Dynamic labelling of neural connections in multiple colours by trans-synaptic fluorescence complementation. Nat Commun. 2015;6:10024. Epub 2015/12/04. doi: 10.1038/ncomms10024. PubMed PMID: 26635273; PubMed Central PMCID: PMCPMC4686661.

144. Fuxe K, Dahlstrom AB, Jonsson G, Marcellino D, Guescini M, Dam M, et al. The discovery of central monoamine neurons gave volume transmission to the wired brain. Progress in neurobiology. 2010;90(2):82-100. doi: 10.1016/j.pneurobio.2009.10.012. PubMed PMID: 19853007.

145. Vizi ES, Fekete A, Karoly R, Mike A. Non-synaptic receptors and transporters involved in brain functions and targets of drug treatment. British journal of pharmacology. 2010;160(4):785-

809. doi: 10.1111/j.1476-5381.2009.00624.x. PubMed PMID: 20136842; PubMed Central PMCID: PMC2935987.

146. Trueta C, De-Miguel FF. Extrasynaptic exocytosis and its mechanisms: a source of molecules mediating volume transmission in the nervous system. Frontiers in physiology. 2012;3:319. doi: 10.3389/fphys.2012.00319. PubMed PMID: 22969726; PubMed Central PMCID: PMC3432928.

147. Nässel DR, Elekes K. Ultrastructural demonstration of serotonin-immunoreactivity in the nervous system of an insect (Calliphora erythrocephala). Neurosci Lett. 1984;48(2):203-10. PubMed PMID: 6384830.

148. Gordon MD, Scott K. Motor control in a Drosophila taste circuit. Neuron. 2009;61(3):373-84. doi: 10.1016/j.neuron.2008.12.033. PubMed PMID: 19217375; PubMed Central PMCID: PMC2650400.

149. Ansorge MS, Zhou M, Lira A, Hen R, Gingrich JA. Early-life blockade of the 5-HT transporter alters emotional behavior in adult mice. Science. 2004;306(5697):879-81. Epub 2004/10/30. doi: 10.1126/science.1101678. PubMed PMID: 15514160.

150. Bengel D, Murphy DL, Andrews AM, Wichems CH, Feltner D, Heils A, et al. Altered brain serotonin homeostasis and locomotor insensitivity to 3, 4-methylenedioxymethamphetamine ("Ecstasy") in serotonin transporter-deficient mice. Mol Pharmacol. 1998;53(4):649-55. Epub 1998/05/09. doi: 10.1124/mol.53.4.649. PubMed PMID: 9547354.

151. Zhao S, Edwards J, Carroll J, Wiedholz L, Millstein RA, Jaing C, et al. Insertion mutation at the C-terminus of the serotonin transporter disrupts brain serotonin function and emotion-related behaviors in mice. Neuroscience. 2006;140(1):321-34. Epub 2006/03/18. doi: 10.1016/j.neuroscience.2006.01.049. PubMed PMID: 16542782.

152. Gardier AM, Guiard BP, Guilloux JP, Reperant C, Coudore F, David DJ. Interest of using genetically manipulated mice as models of depression to evaluate antidepressant drugs activity: a review. Fundam Clin Pharmacol. 2009;23(1):23-42. Epub 2009/03/10. doi: 10.1111/j.1472-8206.2008.00640.x. PubMed PMID: 19267769.

153. Murphy DL, Lesch KP. Targeting the murine serotonin transporter: insights into human neurobiology. Nature reviews Neuroscience. 2008;9(2):85-96. Epub 2008/01/23. doi: 10.1038/nrn2284. PubMed PMID: 18209729.

154. Hidalgo S, Molina-Mateo D, Escobedo P, Zarate RV, Fritz E, Fierro A, et al. Characterization of a Novel Drosophila SERT Mutant: Insights on the Contribution of the Serotonin Neural System to Behaviors. ACS chemical neuroscience. 2017;8(10):2168-79. Epub 2017/07/01. doi: 10.1021/acschemneuro.7b00089. PubMed PMID: 28665105.

155. Araujo SM, Poetini MR, Bortolotto VC, de Freitas Couto S, Pinheiro FC, Meichtry LB, et al. Chronic unpredictable mild stress-induced depressive-like behavior and dysregulation of brain levels of biogenic amines in Drosophila melanogaster. Behav Brain Res. 2018;351:104-13. Epub 2018/05/29. doi: 10.1016/j.bbr.2018.05.016. PubMed PMID: 29803654.

156. Borue X, Cooper S, Hirsh J, Condron B, Venton BJ. Quantitative evaluation of serotonin release and clearance in Drosophila. J Neurosci Methods. 2009;179(2):300-8. Epub

2009/05/12. doi: 10.1016/j.jneumeth.2009.02.013. PubMed PMID: 19428541; PubMed Central PMCID: PMCPMC2691387.

157. Daubert EA, Heffron DS, Mandell JW, Condron BG. Serotonergic dystrophy induced by excess serotonin. Molecular and cellular neurosciences. 2010;44(3):297-306. Epub 2010/04/17. doi: 10.1016/j.mcn.2010.04.001. PubMed PMID: 20394820; PubMed Central PMCID: PMCPMC2878889.

158. Barker EL, Blakely RD. Structural determinants of neurotransmitter transport using cross-species chimeras: studies on serotonin transporter. Methods in enzymology. 1998;296:475-98. PubMed PMID: 9779469.

159. Barker EL, Perlman MA, Adkins EM, Houlihan WJ, Pristupa ZB, Niznik HB, et al. High affinity recognition of serotonin transporter antagonists defined by species-scanning mutagenesis. An aromatic residue in transmembrane domain I dictates species-selective recognition of citalopram and mazindol. The Journal of biological chemistry. 1998;273(31):19459-68. PubMed PMID: 9677366.

160. Demchyshyn LL, Pristupa ZB, Sugamori KS, Barker EL, Blakely RD, Wolfgang WJ, et al. Cloning, expression, and localization of a chloride-facilitated, cocaine-sensitive serotonin transporter from Drosophila melanogaster. Proceedings of the National Academy of Sciences of the United States of America. 1994;91(11):5158-62. PubMed PMID: 8197200; PubMed Central PMCID: PMC43951.

161. Rodriguez GJ, Roman DL, White KJ, Nichols DE, Barker EL. Distinct recognition of substrates by the human and Drosophila serotonin transporters. The Journal of pharmacology and experimental therapeutics. 2003;306(1):338-46. doi: 10.1124/jpet.103.048751. PubMed PMID: 12682215.

162. Sealover NR, Felts B, Kuntz CP, Jarrard RE, Hockerman GH, Barker EL, et al. The external gate of the human and Drosophila serotonin transporters requires a basic/acidic amino acid pair for 3,4-methylenedioxymethamphetamine (MDMA) translocation and the induction of substrate efflux. Biochemical pharmacology. 2016;120:46-55. doi: 10.1016/j.bcp.2016.09.006. PubMed PMID: 27638414.

163. Henry LK, Field JR, Adkins EM, Parnas ML, Vaughan RA, Zou MF, et al. Tyr-95 and Ile-172 in transmembrane segments 1 and 3 of human serotonin transporters interact to establish high affinity recognition of antidepressants. The Journal of biological chemistry. 2006;281(4):2012-23. doi: 10.1074/jbc.M505055200. PubMed PMID: 16272152.

164. Giang T, Ritze Y, Rauchfuss S, Ogueta M, Scholz H. The serotonin transporter expression in Drosophila melanogaster. Journal of neurogenetics. 2011;25(1-2):17-26. Epub 2011/02/15. doi: 10.3109/01677063.2011.553002. PubMed PMID: 21314480.

165. Romero-Calderon R, Shome RM, Simon AF, Daniels RW, DiAntonio A, Krantz DE. A screen for neurotransmitter transporters expressed in the visual system of Drosophila melanogaster identifies three novel genes. Developmental neurobiology. 2007;67(5):550-69. doi: 10.1002/dneu.20342. PubMed PMID: 17443808.

166. Corey JL, Quick MW, Davidson N, Lester HA, Guastella J. A cocaine-sensitive Drosophila serotonin transporter: cloning, expression, and electrophysiological characterization.

Proceedings of the National Academy of Sciences of the United States of America. 1994;91(3):1188-92. PubMed PMID: 8302852; PubMed Central PMCID: PMC521479.

167. Becnel J, Johnson O, Luo J, Nassel DR, Nichols CD. The serotonin 5-HT7Dro receptor is expressed in the brain of Drosophila, and is essential for normal courtship and mating. PloS one. 2011;6(6):e20800. doi: 10.1371/journal.pone.0020800. PubMed PMID: 21674056; PubMed Central PMCID: PMC3107233.

168. Nichols CD. 5-HT2 receptors in Drosophila are expressed in the brain and modulate aspects of circadian behaviors. Developmental neurobiology. 2007;67(6):752-63. doi: 10.1002/dneu.20370. PubMed PMID: 17443822.

169. Yuan Q, Joiner WJ, Sehgal A. A sleep-promoting role for the Drosophila serotonin receptor 1A. Current biology : CB. 2006;16(11):1051-62. Epub 2006/06/07. doi: 10.1016/j.cub.2006.04.032. PubMed PMID: 16753559.

170. Sitaraman D, LaFerriere H, Birman S, Zars T. Serotonin is critical for rewarded olfactory short-term memory in Drosophila. Journal of neurogenetics. 2012;26(2):238-44. doi: 10.3109/01677063.2012.666298. PubMed PMID: 22436011.

171. Liu Y, Luo J, Carlsson MA, Nassel DR. Serotonin and insulin-like peptides modulate leucokinin-producing neurons that affect feeding and water homeostasis in Drosophila. The Journal of comparative neurology. 2015;523(12):1840-63. doi: 10.1002/cne.23768. PubMed PMID: 25732325.

172. Alekseyenko OV, Chan YB, Fernandez MP, Bulow T, Pankratz MJ, Kravitz EA. Single serotonergic neurons that modulate aggression in Drosophila. Current biology : CB. 2014;24(22):2700-7. doi: 10.1016/j.cub.2014.09.051. PubMed PMID: 25447998; PubMed Central PMCID: PMC4254562.

173. Dierick HA, Greenspan RJ. Serotonin and neuropeptide F have opposite modulatory effects on fly aggression. Nature genetics. 2007;39(5):678-82. doi: 10.1038/ng2029. PubMed PMID: 17450142.

174. Haynes PR, Christmann BL, Griffith LC. A single pair of neurons links sleep to memory consolidation in Drosophila melanogaster. eLife. 2015;4. Epub 2015/01/08. doi: 10.7554/eLife.03868. PubMed PMID: 25564731; PubMed Central PMCID: PMCPMC4305081.

175. Wisor JP, Wurts SW, Hall FS, Lesch KP, Murphy DL, Uhl GR, et al. Altered rapid eye movement sleep timing in serotonin transporter knockout mice. Neuroreport. 2003;14(2):233-8. Epub 2003/02/25. doi: 10.1097/00001756-200302100-00015. PubMed PMID: 12598736.

176. Shaw PJ, Tononi G, Greenspan RJ, Robinson DF. Stress response genes protect against lethal effects of sleep deprivation in Drosophila. Nature. 2002;417(6886):287-91. Epub 2002/05/17. doi: 10.1038/417287a. PubMed PMID: 12015603.

177. Singh P, Donlea JM. Bidirectional Regulation of Sleep and Synapse Pruning after Neural Injury. Current biology : CB. 2020;30(6):1063-76 e3. Epub 2020/03/07. doi: 10.1016/j.cub.2019.12.065. PubMed PMID: 32142703; PubMed Central PMCID: PMCPMC7199647.